

From the:
Comprehensive Pneumology Center (CPC)
München of the Ludwig-Maximilians-Universität München
Directors: Dr. Ali Önder Yildirim



Dissertation
zum Erwerb des Doctor of Philosophy (Ph.D.) an der
Medizinischen Fakultät der
Ludwig-Maximilians-Universität zu München

***Validation and application of human in vitro models for
investigating bronchial response to cigarette smoke***

vorgelegt von:

Michal Mastalerz

aus:

Wroclaw, Poland

Jahr:

2022

Mit Genehmigung der Medizinischen Fakultät der
Ludwig-Maximilians-Universität zu München

First evaluator (1. TAC member): *PD Dr. Claudia Staab-Weijnitz*

Second evaluator (2. TAC member): *Prof. Dr. Thomas Gudermann*

Third evaluator: *Prof. Dr. med. Hermann Fromme*

Dean: **Prof. Dr. Thomas Gudermann**

Datum der Verteidigung:

2.11.2022

Title of the thesis:
Prepared in: Comprehensive Pneumology Center
Max-Lebsche-Platz 31
81377 München

First PhD supervisor:
(Helmholtz Zentrum München) PD Dr. Claudia Staab-Weijnitz
Spokesperson CPC Research School
Vice-Speaker RTG "Targets in Toxicology"
Principal Investigator "Collagen biosynthesis and maturation in lung fibrosis" in Comprehensive Pneumology Center (CPC)
phone: +49 (0) 89 3187-4681
mail: staab-weijnitz@helmholtz-muenchen.de

Second PhD supervisor:
(LMU) Prof. Dr. med. Thomas Gudermann
Chair and Head of the Walther-Straub-Institut of Pharmacology and Toxicology
Ludwig-Maximilians-Universitaet Muenchen
Walther Straub Institute of Pharmacology and Toxicology
Goethestrasse 33
80336 Muenchen
Germany
Phone: +49 (0) 89 2180-75702
Email: thomas.gudermann@lrz.uni-muenchen.de

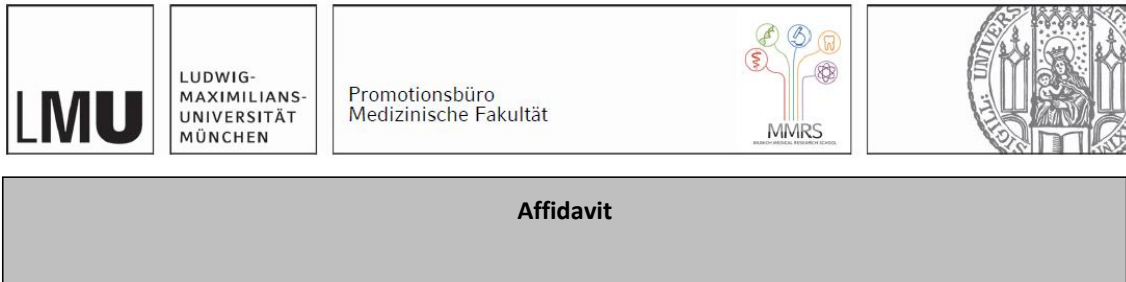
Third PhD Supervisor Prof. Dr. med., Dr. rer. nat. Robert Bals
Direktor der Klinik
Universitätsklinikum des Saarlandes und Medizinische Fakultät der Universität des Saarlandes
Klinik für Innere Medizin V
Gebäude 41
66421-Homburg
Phone: +49 (0) 6841 - 16 - 1 50 51
Email: m5.sekr@uks.eu

Fourth PhD Supervisor Dr Otmar Schmid
Comprehensive Pneumology Center (CPC)

phone: +49 (0) 89 3187-4681
mail: staab-weijnitz@helmholtz-muenchen.de

Director of Institute Dr. Ali Önder Yildirim
Comprehensive Pneumology Center / Phone: +49 (0) 89 3187-4037
Institute of Lung Biology and Email: oender.yildirim@helmholtz-muenchen.de
Disease

"What matters most is how well you walk through fire"
-Charles Bukowski

**Affidavit**

Mastalerz Michal

Surname, first name

I hereby declare, that the submitted thesis entitled:

Validation and application of human in vitro models for investigating bronchial response to cigarette smoke

is my own work. I have only used the sources indicated and have not made unauthorised use of services of a third party. Where the work of others has been quoted or reproduced, the source is always given.




I further declare that the submitted thesis or parts thereof have not been presented as part of an examination degree to any other university.

Munich, 20.01.2023

place, date

Michal Mastalerz

Signature doctoral candidate

	LUDWIG- MAXIMILIANS- UNIVERSITÄT MÜNCHEN	Promotionsbüro Medizinische Fakultät		
---	---	---	---	---

**Confirmation of congruency between printed and electronic version of
the doctoral thesis**

Mastalerz Michal

Surname, first name

I hereby declare, that the submitted thesis entitled:

Validation and application of human in vitro models for investigating bronchial response to cigarette smoke

is congruent with the printed version both in content and format.

Munich, 20.01.2023

place, date

Michal Mastalerz

Signature doctoral candidate

Table of content

Table of content.....	1
Summary	3
1. Introduction	5
1.1 Bronchial epithelium.....	5
1.1.1 Anatomy.....	5
1.1.2 Airway cell types and cell compositions.....	5
1.2 Cigarette smoke – major inhalative insult	7
1.2.1 CS constituents	8
1.2.2 Lung deposition of CS particles	10
1.3 Effects of chronic smoking on bronchial epithelium: lung diseases associated with smoking.....	10
1.3.1 Lung cancers.....	11
1.3.2 Chronic obstructive pulmonary disease	11
1.3.3 Idiopathic pulmonary fibrosis	12
1.3.4 Other lung diseases	14
1.4 Cigarette smoke models	14
1.4.1 <i>In vivo</i> models	14
1.4.2 <i>In vitro</i> models.....	15
1.5 <i>In vitro</i> cultures in molecular biology of CS response.....	16
2. Addressed hypotheses and specific aims	18
3. Chapter A – validation of <i>in vitro</i> CS exposure models.....	19
3.1 Introduction	19
3.2 Results	20
3.2.1 Cell-delivered dose applied in different experimental models can be directly compared by gravimetric assessment of absolute mass of CS.....	20
3.2.2 Basal cells successfully differentiate to bronchial epithelium featuring cell composition observed <i>in vivo</i>	26
3.2.3 Doses of cigarette smoke used in experiment were not cytotoxic.....	28
3.2.4 PhBECs exposure models differ substantially in their response to CS.	30
3.2.5 SERGs are expressed by basal and luminal cell types	46
3.2.6 CYP1A1 has lower basal expression in comparison to other aryl hydrocarbon receptor (AhR) responsive genes, which is unaffected by smoking history	49
4. Chapter B – unbiased proteomic approach reveals regulators behind the response to CS.....	51
4.1 Introduction	51
4.2 Results	51
4.2.1 The proteome data reveals a number of significantly changed genes, prominently including a number of SERGs.....	51
4.2.2 Ingenuity Pathway Analysis confirms SERGs activating xenobiotic metabolism pathways, and indicates novel targets regulated by CS exposure	52

5. Chapter C – How smoking and disease status affects CS response – <i>in vivo</i> and <i>in vitro</i> comparison	57
5.1 Introduction	57
5.2 Results	59
5.2.1 Persistent and transient changes in smoke-induced proteins upregulations are not recapitulated in differentiated primary bronchial epithelial cells	59
6. Discussion	61
7. Conclusions	68
8. Final remarks	69
8.1 Applications	69
8.2 Limitations	69
8.3 Follow up studies	69
9. Materials and Methods	71
9.1 Materials	71
9.1.1 Antibodies list	71
9.1.2 Primers	72
9.1.3 Patient material	73
9.1.4 Cell culture media	74
9.1.5 Reagents and chemicals	75
9.1.6 Buffer formulations	76
9.1.7 Consumables	77
9.1.8 Laboratory equipment	79
9.1.9 Software	80
9.1.10 Assay kits and standards	81
9.2 Methods	81
9.2.1 Dose determination by gravimetric analysis	81
9.2.2 Preparation of CSE	81
9.2.3 Cell culture methods	82
9.2.4 RNA analysis	86
9.2.5 Protein analysis	89
9.2.6 Immunofluorescence staining	91
9.2.7 <i>In silico</i> analysis	91
References	94
Appendix A:	115
List of abbreviations	116
List of figures	118
List of tables	120
List of publications	121
Acknowledgements	122

Summary

Cigarette smoke (CS) is the single most deadly and preventable cause of death. It profoundly affects smokers' lungs, by altering genes expression profiles, epigenetic modifications, causes DNA damage and changes cell function and morphology [1]. The respiratory tract is the main lung compartment exposed to CS. The bronchial epithelium lining the airway tracts subjected to chronic smoking often leads to incurable diseases such as lung cancers or chronic obstructive pulmonary disease (COPD).

Due to its complicated nature and profound impact on human health, the response to CS has been extensively studied in both *in vivo* and *in vitro* settings. While CS effects can be investigated in numerous distinct experimental set-ups, little has been done in terms of standardization or validation of these methods. Here, a comprehensive direct comparison between different *in vitro* CS exposures has been established and analyzed. The cell-delivered dose and the expression profile of genes typically upregulated among smokers were assessed between models, also in relation to expression profile in human lungs. Three surprisingly dissimilar models, namely acute submerged basal cells exposure to cigarette smoke extract (CSE), chronic basolateral CSE exposure and acute whole cigarette smoke exposure, yielded responses that were substantially better than any other investigated experimental set-up. Despite the cell-delivered doses varying substantially between these three models, each of them significantly upregulated at least six of out 10 analyzed genes in the primary human bronchial epithelial cells (phBECs).

Conclusions from validation study helped choosing the right model, which was later used in the next study, in the proteomic differential expression analysis. Chronic basolateral CSE exposure was the only model that successfully upregulated seven out of 10 genes typically upregulated in smokers. Results of the proteomic analysis further validated the physiological relevance of the model by identifying activation of the molecular pathways characteristic for the CS exposure, such as activation of xenobiotic metabolism pathways and inhibited sirtuin 1 pathway [2]. Interestingly, by using advanced pathway analysis software, a new potential ferroptotic regulator was found, namely nuclear factor 1 (NUPR1). Overall, this study reported a first evidence of critical ferroptosis repressor being aberrantly changed by the CS in phBECs derived from healthy donors.

The final topic of this study addressed the question whether the differentiated phBECs from ex- and current smokers exhibit transient and persistent changes caused by smoking that can be seen *in vivo*. Here, the advantage was taken from proteomic study performed on bronchoalveolar lavage samples, which were derived from never-, ex- and current smokers. After identifying several genes which expression changes were either transient or persistent after smoking cessation, the basal expression levels of these genes was analyzed on transcript level in differentiated phBECs *in vitro*, derived also from never-, ex- and current smokers. Surprisingly, the *in vitro* analysis revealed lower constitutive expression of analyzed genes in phBECs from patients from history of smoking, which did not reflect changes seen in BALF study.

Taken together, this thesis presents a successful validation of the several CS exposure models on phBECs. One of them, namely chronic basolateral CSE exposure, was further validated by the proteomic analysis, which, for the first time, revealed NUPR1, a crucial ferroptosis regulator [3], as a CS-regulated gene. This study establishes practical technique of validating CS exposure models, which can be used in *in vitro* studies, despite possibly different basal genes expressions of CS-regulated genes.

1. Introduction

1.1 Bronchial epithelium

1.1.1 Anatomy

One of the main roles of the airways is to allow an efficient air circulation between the external environment and respiratory surfaces. The epithelium lining the respiratory tract plays a critical role in maintaining this function. Additionally, once the air has passed the nasal cavities, the pharynx, the larynx and the trachea, all constituents of the upper airways, the air enters bronchi layered with bronchial epithelium, which serves as the main line of defense in the lower airways [4-6]. Although the trachea functionally is included in the upper airways [5], anatomically however belongs to lower airways as it is also layered with cells characteristic for bronchi [4]. Supported by the tracheal cartilage rings, the trachea terminates on the first main bifurcation, called bronchi. While similar in structure, it differs from trachea by circular cartilage rings. Further branching of bronchial tree goes on for 23 airway generations [7]. The proximal bronchi divide into smaller bronchi and, more distally, into bronchioles. The main anatomical difference between the proximal bronchi and the bronchioles is the lack of cartilage at the level of bronchioles and a smaller diameter of around 1 mm or lower. Further branching down leads to the terminal bronchioles directly leading into the respiratory bronchioles [4]. The latter are directly connected to some alveoli allowing for limited gas exchange in that region, but, most importantly, lead into alveolar ducts which supply numerous alveoli with air and correspond to the main area of gas exchange [8]. The number of alveoli in the adult lung averages around 480 million, which correlates with human total lung volume [9] and translates to approximately 70-140 m² lung surface [10]. Sex differences in lung anatomy have been reported, with the trachea showing the largest size discrepancy, being 35% smaller in women. This difference becomes less apparent in the lower airways (26%) [11].

1.1.2 Airway cell types and cell compositions

The lower airways are lined by a tubular pseudostratified epithelium that comprises a range of different cell types and cellular structures which differ along the airway tract. The four main cell types are the ciliated, club, goblet and basal cells. Submucosal glands rich with mucus-producing goblet cells are observed more abundantly in trachea, upper airways or in the first to fifth division of bronchial tree [12, 13]. The proximal airways are also characterized by a lower presence of club and ciliated cells when compared to the distal and terminal bronchioles (between sixth and 23rd division in an adult human) [14, 15]. (Figure 1.1). Throughout the respiratory tract, also basal and undifferentiated columnar cells are present, which give rise to more specialized cell types [13]. After the 23rd branching, the airway epithelium starts to merge with alveoli and creates bronchoalveolar duct junctions (BADJ), the main regeneration source of distal epithelia [13, 16].

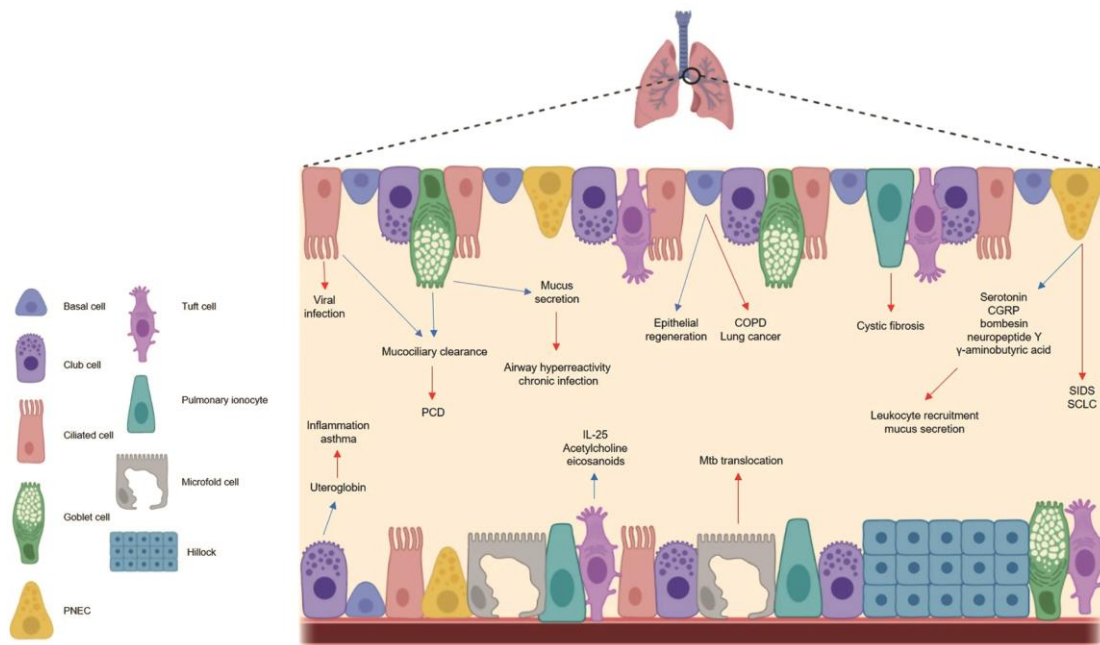


Figure 1.1. Cell types residing in bronchial epithelium. Modified from [17]

Each of these cell types are attributed distinct roles. Mucin secreted by the goblet cells is a major constituent of mucus and has an essential role in creating and maintaining the protective mucus barrier [18]. Club cells secrete other mucus components and regulate the contents of mucus lining, especially in distal airways, but also take part in a xenobiotic metabolism [19]. Club cells pertain some of the progenitor cell capabilities, as they can differentiate into goblet or ciliated cells [20]. Interestingly, they hold an ability of dedifferentiation to basal cells when needed (e.g. upon injury) [21]. Another important player in cleansing airways from particles and noxious agents are ciliated cells, characterized by specialized organelles on the luminal surface termed cilia [22]. On average, cilia length ranges between 4-7 μm , with longer cilia appearing on ciliated cells occupying smaller airways [23]. Additionally, they produce defense-related proteins [13] and contain microvilli, which fulfill roles in transepithelial fluid transport [24]. Through ciliary beating, ciliated cells constitute the mucociliary escalator, which propels all pathogens, particulates or other xenobiotics upwards [23]. They also constitute the most abundant cell type within the airway epithelium, ranging from $47\pm 2\%$ in the trachea to $73\pm 1\%$ in the distal bronchial epithelium [25]. The main airway progenitor cells are basal cells, cuboidal in shape and located close to the basement membrane [26]. Their presence is inversely correlated with ciliated cells, constituting one third of the whole epithelial cell population in trachea, down to only 10% in distal airways [27].

1.1.2.1 Rare airway cell types

The first identified cell type that is substantially rarer than main four cell types explained earlier are pulmonary neuroendocrine cells (PNECs). Early studies suggested they function as a part of the innate immune response [13]. Recently however, Mou and colleagues reported three subtypes within PNECs population, all exhibiting expression of similar neuropeptides and neurotransmitters, in the response to environmental stimuli [28]. Tuft cells, another rare cell type, was only recently characterized as chemosensing cells which mediate immune- and neuromodulatory re-

response [29]. Additionally, tuft cells are responsible for acetylcholine, IL-25 and eicosanoid synthesis [17]. Once secreted, acetylcholine partakes in variety of functions such as maintaining epithelial homeostasis and airway remodeling [30, 31]. Furthermore, serous cells reside in distal parts of the submucosal glands and are responsible for secretion of glandular fluid components involved in airway defense, such as lactoferrin, defensin or mucin 7 [32]. Another cell type rarely seen in the airways is the microfold cell, known also as M cell [17]. Similarly to tuft cells, M cells are involved in immunoresponse, most likely by transporting bacterial antigens to antigen presenting cells [33, 34].

With recent breakthroughs in the single-cell RNA-seq (scRNA-seq) technology, one more cell type has been discovered, the pulmonary ionocyte [20, 35]. Interestingly, while all the described main cell types express the cystic fibrosis transmembrane conductance regulator (CFTR), ionocytes, the least abundant cell population, express the majority of CFTR, implying that this cell type may represent a new target for cystic fibrosis (CF) therapy [20]. The same scRNA-seq study has led to the discovery of hillock cells. These cuboidal structures comprise keratin 13-expressing basal cells and have been shown to express squamous differentiation markers. Hillock cells are thought to have a higher turnover rate than other cell types, however, more investigations are needed to fully understand their role and function [20].

1.2 Cigarette smoke – major inhalative insult

The first signs of tobacco smoke exposure have been reported to take place in the Pleistocene, approximately 12.300 years ago around Peru and Ecuador [36, 37]. Ever since then, through long-term social exposure to tobacco, it has found its use in rituals, medicine, and social environments, resulting in a profound impact on earlier civilizations that has been retained in oral traditions [36, 38]. Tobacco was first brought to Europe by Christopher Columbus in the XV century. Even though smoking was initially repressed, it found its foothold in European society ironically through claims of its medicinal properties [37]. Cigarette consumption drastically increased in the XX century [39]. Despite recent decrease in developed countries, average rates of smoking globally are still on the rise through rapidly increasing numbers of smokers in underdeveloped countries [40].

Nowadays, cigarette smoke (CS) is used by over 1 billion people around the world, and has been associated with over 40 diseases [41]. Notably, it is considered a major causal factor for eight out of 10 most diseases causing most deaths worldwide, ultimately contributing to 7 million deaths each year. It is therefore considered a leading preventable cause of death [42]. CS is a main contributor to squamous-cell carcinoma lung cancer, one of the most prevalent non-small cell lung cancers (NSCLC) [43-45], but also associated with prevalence of adenocarcinoma [45, 46] and small cell lung carcinomas (SCLCs) [47] or a number of cancers targeting other organs [48]. It is well known that cigarette smoking is involved in development of chronic obstructive pulmonary disease (COPD) [49-51], an incurable illness for which the most effective intervention treatment to-date is still smoking cessation [52, 53]. Smoking was tied to higher incidence of ischemic heart disease [54-56], stroke [57, 58] and puts smokers at a disadvantage against lower respiratory infections, when compared to never smokers [59, 60]. It is an independent risk factor for type I and type II diabetes [61-63], chronic kidney disease [64, 65] and increases prevalence of Alzheimer's disease [66, 67]. Passive or environmental smoking has also detrimental effects on health [68, 69] especially when individuals are exposed to tobacco smoke in early life [70].

1.2.1 CS constituents

Modern cigarette smoking varies significantly from dried tobacco leaves used in ancient times. Nowadays, smoking exposure comes in many different forms, as cigarettes, smokeless tobacco (e.g. snus), or roll-your-own cigarettes with filters, all of which vary considerably in the list of chemical compounds they comprise (Table 1.1).

Table 1.1. Abbreviated list of CS constituents considered as harmful by the Food and Drug Administration (FDA).

Cigarette Smoke	Smokeless tobacco	Roll-your-own cigarette smoke
Acetaldehyde	Acetaldehyde	Ammonia
Acrolein	Arsenic	Arsenic
Acrylonitrile	Benzo[a]pyrene	Cadmium
4-Aminobiphenyl	Cadmium	Nicotine (total)
1-Aminonaphthalene	Crotonaldehyde	NNK
2-Aminonaphthalene	Formaldehyde	NNN
Ammonia	Nicotine (total and free)	
Benzene	NNK	
Benzo[a]pyrene	NNN	
Carbon monoxide		
Crotonaldehyde		
Formaldehyde		
Isoprene		
Nicotine (total)		
NNK		
NNN		
Toluene		

NNK = 4-(methylnitrosamino)-1-(3-pyridyl)-1-butanone. NNN = N-nitrosornicotine. **Adapted from** www.fda.gov/downloads/TobaccoProducts/Labeling/RulesRegulationsGuidance/UCM297828.pdf (accessed 13.11.2021)

Importantly, not all smoke constituents originate from tobacco, paper and additives, as some of them are created during pyrolysis. That prompted researchers to analyze not only compounds found in cigarette but also in the cigarette smoke itself, which totals more than 4000 different compounds [71, 72]. Additionally, the quantities of compounds identified in cigarettes significantly vary between brands [73]. In order to introduce more reproducibility between different exposure

methods used in experimentations, standardized research cigarettes were created, namely standard reference cigarette (3R4F, or more recently 1R6F, Kentucky Tobacco Research & Development Center, USA). Based on their known health effects, smoke constituents can be categorized as respiratory, cardiovascular or carcinogenic toxicants [74].

1.2.1.1 Respiratory toxicants

Acrolein, an unsaturated aldehyde considered as the most powerful irritant [75], causes cilia and DNA damage by depleting intracellular antioxidants, and is reported to increase the risk of COPD [76]. Other aldehydes, namely acetaldehyde and formaldehyde, are also substantial lung and throat irritants [77], can cause acute bronchospasm while impairing the intracellular self-repair system [78]. Exposure to acetaldehyde, the most abundant constituent of CS, causes coughing and burning in the upper respiratory tract [77]. Another strong irritant in CS is ammonia, similarly impairing breathing through coughing [79].

1.2.1.2 Cardiovascular toxicants

As mentioned previously, cardiac arrest is one of the most common causes of death. CS toxicants affecting the cardiovascular system include carbon monoxide, hydrogen cyanide, various oxidants such as free radicals, or nicotine [80]. Through damaging arteries, interfering with blood vessel flow, and reducing erythrocytes' capacity to bind oxygen they pose a great risk for stroke or ischemic attack [81].

1.2.1.3 Carcinogenic toxicants

First reports providing evidence for a causal link between smoking and cancer were published already in the 1950s [82]. Later, an interdisciplinary research on tobacco, aerosol chemistry and biological activity of isolated compounds of CS revealed a wide range of substances that can act as carcinogens. Possibly most important are tobacco smoke-specific N-nitrosamines, which are created during plant processing from tobacco-specific alkaloids [83, 84]. NNN (N'-nitrosonornicotine) and NNK (4-(methylnitrosamino)-1-(3-pyridyl)-1-butanone) are present only in CS and are reported to cause various upper airway cancers, among others [85, 86]. Another substantial compound group of carcinogens are polycyclic aromatic hydrocarbons (PAHs), also greatly contributing to lung cancer development [87, 88]. To most abundant PAHs in CS, according to the International Agency for Cancer, are included benzo[a]pyrene, and to lesser extent dibenz[a,h]anthracene, indeno[1,2,3-cd]pyrene, dibenzo[a,e]pyrene and dibenzo[a,i]pyrene [89, 90]. Last, but not least, a number of carcinogenic metals has been reported in cigarette smoke, such as arsenic, cadmium or lead. Their presence in CS is most likely due to plants absorbing them from soil. Consequently, they cause lung and oral cancers [91] but also cancers of other organs, such as bladder, kidney or head [91, 92].

1.2.1.4 E-cigarettes constituents

In recent years, in parallel to a general decrease of tobacco smoking in developed countries increasingly more people have started using electronic cigarettes (e-cigarettes), propagated as a cigarette smoking alternative. An e-cigarette is a device with heating elements which aerosolize e-liquid, usually a nicotine solution with added flavors [93]. Although it is seen as a far healthier alternative to smoking traditional cigarettes [94] it raises concerns that it has been popularized

mostly among youth and that it effectively targets also younger people who would not reach for tobacco cigarettes otherwise. Besides, adults who quit smoking by using e-cigarettes, become dependent to “vaping” instead, therefore calls for more balanced consideration of e-cigarettes in public health have been made [95].

1.2.2 Lung deposition of CS particles

As previously described, apart from smokeless tobacco, other tobacco products have a profound impact on the lungs. It has been established that smoke toxicity is dose dependent [96] and that smoke particles deposition is not uniform throughout the bronchial tree [97]. According to particle size, most particles of 5-20 μm size are deposited in the upper airways, whereas smaller particles (0.5-5 μm) reach the lung periphery [98]. It is worth noting, that smokers differ in individual smoking topography, which is influenced by bronchial tree anatomy and type of cigarette consumed, as mentioned earlier, but also by smoking behavior (Table 1.2) [99], and final deposition is often much greater than of any other environmental pollutants [100].

Table 1.2. Reviewed factors influencing smoking behavior, modified from [99]

Puffs/cigarette	8–16.
Interpuff interval	18–64 s.
Cigarette duration	232–414 s.
Puff duration	1.6–2.4 s.
Puff volume	21–66 ml.
Peak flow	28–40 ml/s.
Inhalation volume	413–918 ml.

State-of-the-art computer models based on high-resolution computer tomography (CT) images of bronchial tree of lung particle deposition have allowed for precise simulation of transient particle flow through the airways up to the sixth bronchial generation. In accordance with previous reports, most cigarette smoke particles deposit in oral cavities and on carinas of bifurcations in the bronchial tree. It has also been shown that very fine particles (0.1 – 1 μm) go through 6 generations of bronchi, leading to higher deposition in distal airways [101].

1.3 Effects of chronic smoking on bronchial epithelium: lung diseases associated with smoking

Due to its complex nature, CS affects lungs in numerous ways. As mentioned previously, CS contributes to COPD and lung carcinogenesis but also to a range of other lung pathologies, which occur less frequently.

1.3.1 Lung cancers

The carcinogenic potential of a wide range of CS constituents has already been well documented [102], making CS a strong risk factor for a plethora of cancers, particularly lung cancers. Up to 95% of lung cancers patients have a history of smoking, either active or involuntary [103, 104], with poor prognosis and a 5-year survival rate between 8-15% [105]. Importantly, epidemiological studies have reported clear correlations between cigarettes smoked per day [106] or smoking cessation time [107] and cumulative risk of lung cancer. In fact, until today stopping smoking is the most effective intervention. CS constituents increase the DNA mutation burden, by creating DNA adducts, gene fusions on epigenetic aberrant changes, which decrease over time after cessation, but not completely [108]. Interestingly, reports also showed that the mutation burden does not persist after smoking cessation within epithelial airways, suggesting that other pathomechanisms trigger lung cancer in ex-smokers [109]. Evidence based on DNA microarrays established involvement of bronchial epithelial cells in carcinogenic activity [110]. Since the response to CS is so heterogeneous between smokers, researchers postulated an inter-individual variation in gene expression profiles in airway epithelium affecting susceptibility to cancer and other diseases [111]. Transcriptomic studies performed on bronchial biopsies from smokers and never smokers have shown increased activation of PAHs-metabolizing pathways, oxidant response and down-regulation of tumor suppressor pathways [112, 113]. The relationship between airway epithelial gene expression and cancer pathologies implied it could be leveraged in cancer diagnostics. Spira and his colleagues [114] reported cancer-specific response to CS in cytologically normal epithelial cells of larger airways collected by flexible bronchoscopies, suggesting a transcriptomic profile that could serve as a biomarker of early cancer onset detection.

1.3.2 Chronic obstructive pulmonary disease

According to the WHO, chronic obstructive pulmonary disease (COPD) is globally the fourth most common cause of death [115]. If environmental risk factors, such as CS, pollution and combustible products of biomass, COPD is predicted to become third by 2030 [116]. In 2010, 384 million people were suffering worldwide because of this devastating and so far incurable disease [117]. COPD is regarded as one of the biggest dangers to public health, because of its prevalence, therapy costs, and impact on the patient and patient's family. One of the major risk factors for COPD is cigarette smoke. Every third woman and tenth man who develops COPD has no history of smoking [51].

It is now well known that smoking contributes to airway remodeling, promotes squamous cell metaplasia and decreases the number of ciliated cells [118]. Moreover, there is evidence of CS shortening length of cilia through smoke-induced autophagy i.e. 'ciliophagy' [119]. Impairment of mucociliary clearance leads to goblet cell hyperplasia and thus increased mucus production [118, 120], which has been linked to higher incidence of COPD exacerbations [121]. Furthermore, CS has been shown to disrupt epithelial cell junctions via epidermal growth factor-regulated mechanism [122] and increased reactive oxygen species (ROS) production leading to reduced e-cadherin expression [123]. Excessive ROS is also thought to be a culprit behind increased cell senescence through cell cycle arrest, interfering with repair mechanisms, and ultimately depleting airway stem cells and reducing airway multipotentiality capabilities [124].

Another aspect in smoke-related COPD pathogenesis is alterations in targeted cell death mechanisms. Reports have shown that inhibiting mTOR1 pathways induces selective autophagy in

epithelial cells [125]. The key regulation of ROS production in COPD is PINK-PARK2 pathway, reported to be altered by CS exposure, that in turn induced mitophagy (autophagy selectively targeting mitochondria) [126]. There is also evidence for CS promoting excessive NF- κ B and AP-1 pathways activation that causes necroptosis [127]. *In vivo* experimental models also indicate involvement of CS in NCOA4-mediated ferritinophagy, process of autophagic ferritin degradation [128], which increases labile iron pool and promotes ferroptosis in epithelial cells [129].

As mentioned before, CS fine particles can reach terminal bronchioles and alveoli. Reports have shown CS causing emphysematous lesions, through the senescence of alveolar type I cells [130] or the deranged Nrf2 pathway, as shown in Nrf2-deficient mice developing emphysema, exacerbated by CS exposure [131]. Together with macrophages, alveolar epithelial cells exhibit pattern recognition receptors (PPRs) on their surface, activated via smoke-induced damage-associated molecular patterns [132], which in turn activates the expression of a range of inflammatory cytokines and interleukins, namely IL-1 α , IL-1 β , IL-33, and IL-18. This results in the recruitment of neutrophils, macrophages, helper T cells, key components of autoinflammatory response, crucial for COPD development [133, 134]. Overall, COPD is a complex disease, and effect of CS embodies various altered cellular mechanisms that promote its development.

1.3.3 Idiopathic pulmonary fibrosis

Although not so prevalent as COPD, idiopathic pulmonary fibrosis (IPF) is another complex and incurable lung disease, which pathomorphologically drastically differs from COPD, despite CS being a major risk factor (over 60% of IPF patients has a history of smoking) [135, 136]. The main hallmarks of the disease are the progressive fibrosis of lung parenchyma, creating characteristic honey comb cyst formations, in parallel with continuous damage of alveolar epithelium triggering deranged repair processes [137] leading to declining lung functions and respiratory failure. The median survival is approximately 3 years after the diagnosis [138], although updated clinical data in more recent studies suggest patients to live longer [139].

Since the IPF pathogenesis concentrates around alveoli and lung-resident fibroblasts, the bronchial epithelium was not taken into consideration as much, until genome-wide association studies (GWAS) have revealed genetic risk variants of genes specific or overexpressed in airway epithelial cells, which were linked to poorer prognosis in both sporadic and familial pulmonary fibrosis [140-142]. Single polynucleotide polymorphism (SNP) linked with increased susceptibility to IPF that are expressed in airway epithelium are listed in Table 1.3. Among the first identified SNPs located in the promoter of mucin 5B (MUC5B) were a goblet cell-specific protein, on chromosome 11 [143]. Clinical studies indicate an increased mortality, the overexpression of MUC5B and an increasing risk of developing IPF up to 35% [144, 145]. Single cell RNA sequencing data points towards overexpression of MUC5B with the promoter variant rs35705950 in goblet cells, in the terminal bronchiole, close to honeycomb cysts. Additionally, Adjacent to the MUC5B promoter is toll interactive protein (TOLLIP) with 3 variants, namely rs111521887, rs5743894, rs574389, which show a positive association with the risk of higher IPF incidence and mortality [142]. In IPF lungs TOLLIP is downregulated [146] while being primarily expressed in distal epithelial cells [147] and in lung macrophages [148]. Kaminiski and Rosas identified in their single cell RNA sequencing datasets transcriptionally different cells termed basaloid cells, which exhibits highest TOLLIP expression [149]. Of note, total TOLLIP expression decreases by 40-50% whenever variants rs111521887 and rs5743894 are present, however with rs5743890 the TOLLIP expression is

lowered by 20% and was associated with less frequent IPF development. Interestingly, these patients who developed IPF with this risk variant had a higher mortality rate [142]. Another gene highly expressed by bronchial epithelial cells, desmoplakin (*DSP*), had one functional and noncoding variant, rs2076295, associated with development of IPF by deregulation of cell-cell adhesion complexes [150, 151]. By silencing rs2076295 in *in vitro* experiments on immortalized bronchial cell line 16HBE cell migration was increased, along with expression of metalloproteinases MMP7 and MMP9, responsible for extracellular matrix (ECM) degradation, which is overproduced in IPF and considered a driver in fibrosis propagation [152]. Interestingly, one of the FDA-approved drugs that slows down IPF progression, nintedanib, showed better results in patients who carried rs35705950 and rs2076295 in *MUC5B* and *DSP*, respectively, which indicates therapy personalization strategies [153]. Several other GWAS showed correlation between rs2609255 variant in family with sequence similarity 13 A (*FAM13A*) with increased susceptibility to COPD [154] and IPF [141, 154]. Similarly to *MUC5B* or *TOLLIP*, one of *FAM13A* risk variants, namely rs2609255*T, has shown protective against IPF, but again patients who developed IPF had poorer outcomes [155]. *In vivo* knockout of *FAM13A* revealed an exacerbation of bleomycin-induced pulmonary fibrosis, while *in vitro* knockdown of *FAM13A* resulted in an epithelial to mesenchymal transition (EMT) of the epithelial cell line A549, therefore suggesting importance of *FAM13A* expression in IPF development [156]. A kinase anchor protein 13 (*AKAP13*) was found to have a risk variant, rs62025270, which has been associated with increased risk. Epithelial regions aberrantly changed by fibrosis exhibited 1.42-fold higher expression than lungs from healthy patients [157]. *AKAP13* acts as a regulator of TGF- β -RhoA pathway activation, known to be involved in profibrotic pathways [158].

Table 1.3. Genes associated with risk variants, which are predominantly expressed in bronchial epithelial cells.

Gene	Gene function	Risk allele	References
MUC5B	Airway defense by mucus production and mucociliary transport	rs35705950	[144, 145]
TOLLIP	Innate immune response regulation, through toll-like receptor and the transforming growth factor β signaling pathways	rs111521887, rs5743894, rs2743890	[142]
DSP	Cell-cell adhesion	rs2076295	[150, 151]
FAM13A	Signal transduction	rs2609255	[154]
AKAP13	Intracellular signal transduction, cell growth, nuclear transport	rs62025270	[157]

Since the first GWAS discoveries on risk variants, more evidence on involvement of bronchial airways in IPF pathogenicity has emerged. Prasse and colleagues reported association of bronchoalveolar lavage fluid (BALF) containing basal cells-specific proteomic signature from with

poorer prognosis of IPF [159]. Elsewhere, reports have shown increased expression of proapoptotic proteins, namely p53, p21, caspase-3 and bax, and downregulated bcl-2, antiapoptotic marker, in bronchial and alveolar epithelial cells from biopsies of IPF patients, suggesting increased apoptosis in the airway epithelium, resulting in the delayed re-epithelialization [160, 161]. Other reported pathomechanisms involving bronchial epithelial cells include also long non coding RNA (lncRNA) [162, 163] or developmental pathways crucial for IPF, such as transforming growth factor β 1 (TGF- β 1) promoting cell senescence [164], sonic hedgehog signaling (SHH) stimulating ECM production [165] and Wnt signaling involved in pathological tissue remodeling [166].

1.3.4 Other lung diseases

Chapter 1.2 highlighted diseases which are the most common causes of death, where CS is a major risk factor. In fact, there are many other pathologies, which one can develop after chronic CS exposure. Interstitial lung diseases (ILDs) are a large group of over 200 diseases [167], including aforementioned IPF. Among there, CS has been causally linked also to development of bronchiolitis-interstitial lung disease (RB-ILD), desquamative interstitial pneumonitis (DIP) and adult pulmonary Langerhans' cell histiocytosis (PLCH), which are collectively termed 'smoking-related interstitial lung diseases' [168]. Smoking is referred to as precipitating factor (triggering the onset of the disease) to acute eosinophilic pneumonia (AEP) and pulmonary hemorrhage syndrome [169]. Combined pulmonary fibrosis and emphysema (CPFE) encompasses features characteristic for both COPD and IPF, which occurs predominantly in smokers [170]. Interestingly, patients with CPFE have an increased risk of developing lung cancer as compared to the patients suffering from COPD [171]. It is suggested that an environmental smoking, especially during childhood, increases chances of developing asthma [172, 173] and that smoking history increases asthma severity [173].

1.4 Cigarette smoke models

1.4.1 *In vivo* models

Even though much progress has been made in *in vitro* research to increase the physiological relevance [174-176], *in vivo* models are still the most relevant and accurate tools for testing hypotheses generated in human studies, and stand in between *in vitro* basic science and clinical applications. Naturally, the *in vivo* experimentations are the most useful when the biological and physiological features of these models are directly relevant to humans. Animal models allow for confirming *in vitro* data findings, which otherwise would not be possible without going directly into human trials [177]. Different animals' species have been successfully used in the cigarette smoke exposure research, including guinea pigs, rats, hamsters, dogs or primates [178-180]. The most predominantly used animals in lung research are mice, mainly because they are time- and cost-efficient and have already been proven successful multiple times in predicting dosage and treatment efficiency in humans [177]. The most common methods are whole-body smoking chambers, where mice are exposed by inhalation to mainstream and side stream cigarette smoke, generated from the research grade cigarettes, for several hours a day, 4-7 days per week, and for the duration of several weeks up to one year [181-183]. In the acute lung injury research were also reported successful exposures, that lasted only several hours, but were still physiologically relevant

[184]. Since CS exposure often are performed *in vitro* with cigarette smoke extract (CSE). A comparative study between whole CS and CSE exposures *in vivo* has shown the lower physiological relevance of CSE exposure, and inconsistency with whole CS results [181]. Importantly, mouse CS exposure models COPD-like morphological and physiological emphysematous changes [185] and it serves well to model first stages of the disease. The main limitations of whole body exposures are CS particles deposited on the fur of the animal, which, when ingested, can influence the results. Also, the emphysematous inflammatory changes discontinue when CS exposure is stopped [186].

1.4.2 *In vitro* models

1.4.2.1 Cigarette smoke extract and cigarette smoke condensate

In *In vitro*, CS can be also administered in different ways. The cigarette smoke extract (CSE) exposure is a straightforward method, which is probably the most used modality for *in vitro* experimentations. Extract is created by generating mainstream smoke from cigarettes and bubbling it through the medium. After filtration, this medium is considered as the 100% CSE and then diluted for experimentations accordingly [187-190]. In an acute exposure, incubation with CSE varied between 30 min [191] to 72 h [192]. For a chronic exposures, CSE was used with the medium, administered with every media change over longer periods of time, up to 28 days [118] and in some reports the cells were starved prior to exposure [193].

Bronchial epithelial cells can be cultured in either submerged conditions or at the air-liquid-interface (ALI) on a collagen-coated membrane, where they undergo differentiation into an epithelium resembling physiological conditions. These distinct cell culture modalities allow researchers to perform various exposures, depending on the tested hypotheses. With that being said, cells can be exposed to CSE in under submerged conditions [193] or in air-liquid interface (ALI). As described in chapter 1.1, the bronchial epithelium is pseudostratified [12] and the bronchial epithelial cells are cultured on transwell inserts which gives the unique opportunity of exposing cells to CSE from either the basolateral [118] or the apical side [194, 195]. Furthermore, cells can be CSE-exposed in chronic fashion throughout differentiation [118, 196, 197] or acutely, once differentiation is finished [198].

Cells can be exposed also to cigarette smoke condensate (CSC). The main difference from CSE is that smoke is first deposited on fiber filters (retains 99.9% of CS particulate matter bigger than 0.1 μm) and subsequently dissolved in dimethyl sulfoxide (DMSO). Once diluted to nontoxic concentrations, CSC can be used in settings as described above for CSE [199, 200].

1.4.2.2 Whole cigarette smoke

There are important advantages of whole cigarette smoke exposure (wCS) over the other experimental set-ups. It is considered to be mimicking best the physiological delivery of CS [201], also it contains all CS components that other exposure types lack [202] and can be administered in doses close to the highest theoretical cell-delivered doses in the lungs [197] and finally, it is used primarily on cells cultured in ALI. Similarly to CSE, wCS has already been frequently applied in *in vitro* experimentations [176, 201, 203-206]. With state-of-the art automated smoking machines, it is possible to design repeated exposures, with certain smoking regimes (e.g. puffing duration and

volume or flow speed), which can be set up in accordance with standardized protocols for smoking conditions and regimen ISO 3308:2012 [204].

1.4.2.3 Models comparison and main limitations

All mentioned CS exposure types have their advantages and disadvantages. When CS is bubbled through the medium, in final CSE is retained only the water soluble phase, making this solution incomplete in comparison to CSC or wCS. Additionally, the exact constituents of CSE are unknown [207]. Together with CSC, the exposure of cells happens in the liquid phase, which does not precisely resemble *in vivo* setting. High oxidizing capabilities are an important factor of CS gaseous phase. CSE on the other hand has been proven to be more reductive, similarly to particulate phase of CS. According to estimations made by Church and his colleagues, only 5% of all oxidizing compounds are retained during generation of CSC and CSE, as compared to wCS [208]. During generation of 100% CSE, it is usually only compared with other batches of CSE within the same laboratory and the final concentration or constituents of CSE can vary between research groups. In comparison to CSC and CSE, wCS comes with fewer limitations. Bronchial epithelial cells in *in vitro* wCS exposures interact with wider size range of particulate matter, as in human lungs much of particulates greater than 3 μm are deposited in upper airways and wCS exposure dose has reportedly more variation than liquid phase exposures [206]. Other limitation of wCS set-ups is the necessity of creating more sophisticated, in-house built exposure equipment [197], or purchasing smoking machines, such as VitroCell [209].

A common limitation between all the mentioned *in vitro* models is that no effort has been done in terms of standardization or validation of experimental models using CS. wCS exposures have indeed ISO and Canada health standardized protocols for smoking conditions and regimen ISO 3308:2012 [201, 204]. However, a standardization of physiological epithelial response has not been extensively investigated, a point, which will be addressed in Chapter A of this thesis.

1.5 *In vitro* cultures in molecular biology of CS response

Apart from different CS models, many approaches modeling the epithelium have been developed and investigated in the literature. One of the first models used were immortalized cell lines, originated from tumor, such as A549 [210], BEAS-2B [187, 211] or NCI-H292 [191]. Even lacking in physiological relevance, cell lines can still serve as good economic and fast solution for preliminary studies. Differentiated primary human bronchial epithelial cells however, are probably the most physiologically relevant models among monocultures [118, 212]. To study interplay between different cell types more in-depth, co-cultures with fibroblasts [205] or endothelial cells [213] layered on the bottom part of membrane on which bronchial epithelial cells are cultured, or macrophages cultured on top of epithelial layer [214] have been developed. Notably, more recent advancements in lung biology have allowed to study complex epithelial structures also in three dimensional (3D) models called lung organoids [215-217]. They are generated from induced pluripotent stem cells (iPSCs) or lung-specific progenitor cells in a process called self-organization. Since organoids have remarkably high physiological relevance with the process of development of human lungs, which cannot be so accurately recapitulated in animal models, holding therefore promise of cutting down on animal experiments in the future [218]. To date, researchers have been able to successfully differentiate iPSCs into tracheospheres, bronchospheres of distal and proximal airways and alveolospheres, thus covering the most critical parts of human airways

[217]. Since spheroid structure does not allow direct exposure in the *lumen*, CSE exposures has been used, similar to basolateral exposure of differentiated 2D primary human bronchial epithelial cells (phBECs) [219]. As far as ALI exposure is concerned, crucial for more physiologically relevant CS-exposures, new systems of ALI-3D models are being investigated [220]. After differentiation of epithelial progenitor cell spheroids, they are disassociated from matrigel and then replated in 2D culture, where Konishi and colleagues identified ciliated, club, goblet, neuroendocrine and basal cells.

Other, more complex *in vitro* lung models for CS exposure, are lung-on-a-chip concepts [175]. In efforts to come as close to physiological relevance as possible, Nossa and colleagues compiled necessary systems characteristics based on *in vivo* lung microenvironments. Apart from ALI of bronchial and alveolar epithelia for *lumen* exposures, the ideal experimental system should have other cell types present, such as endothelial cells on the bottom part of the membrane, macrophages and pneumocytes. Instead of statically added medium, a lung-on-a-chip has a microfluidic system recapitulating the blood lung circulation system and the mechanical stretching design mimicking movements of lung respiratory areas (Figure 1.2).

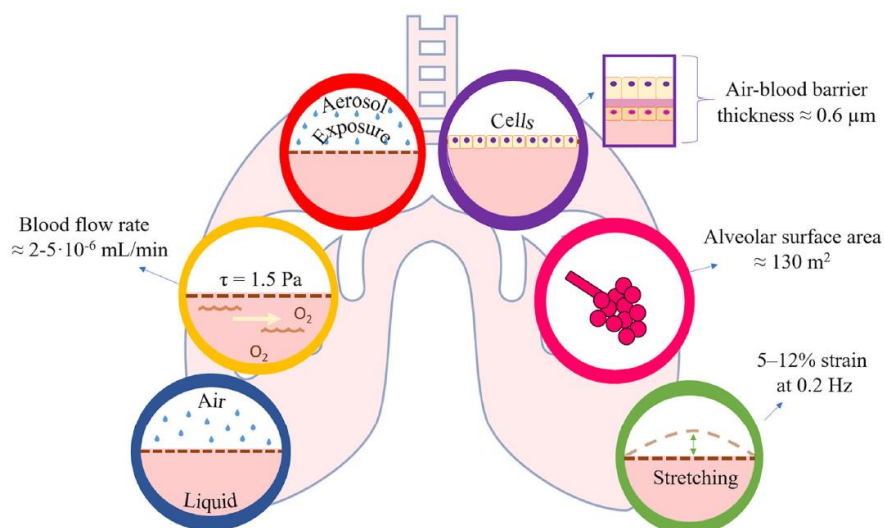


Figure 1.2. Main characteristics of lung microenvironments required in ideal physiologically relevant *in vitro* models. Modified from [175].

Lung-on-a-chip systems have already been successfully used in CS exposures, identifying ciliary pathologies, COPD-like signatures, and epithelial response similar to *in vivo* CS exposure. One limitation of such exposures is the lack of fibroblast attached to bottom-side of the membrane, and immune cells flowing through microfluidic system, addition of which could lead to increased cytokine cascades upon injurious stimuli. Additionally, the thickness of the membrane serving as a support for alveolar cells is much thicker than alveoli septa, and volume of media is much higher when compared with blood-tissue ratios in the lungs [221].

2. Addressed hypotheses and specific aims

Chapter A – Primary human bronchial epithelial cells exposure models vary in their response to CS.

When designing *in vitro* cigarette smoke exposure set-ups, a number of model variables have to be characterized, such as form of CS (wCS, CSE or CSC), route of CS administration (submerged, apical, basolateral), CS cell-delivered dose or concentration, the stage of phBECs differentiation, and the exposure time frame (acute, chronic). Surprisingly, the scientific literature provides little evidence on why certain variables were used and not others, with the exception of *CYP1A1* expression measurements [118], nicotine concentration [192] or measuring the cell-delivered dose [222, 223]. Moreover, the information regarding the physiological relevance is often insufficient, usually only showing cytotoxicity measurements when establishing the concentration or the dose used in experimentations [224, 225], not showing, however, how this relates to *in vivo* conditions. The main rationale why a certain experimental set-up was employed is frequently missing. In efforts to address this issue, in Chapter A a thorough, multifactorial validation study was performed, aiming to elucidate the physiological relevance of several CS exposure models by comparing their ability to alter expression of genes typically upregulated in smokers. Furthermore, calculations of cell-delivered doses allowed for direct dose comparison between models and *in vivo* conditions. Finally, the study shows also if the selected gene expression patterns are captured on protein level and analyzes which cell types are the main driver of the CS-induced response.

Chapter B – Proteomic study on chronic basolateral CSE exposure of bronchial epithelial cells reveals novel molecular targets altered by cigarette smoke.

It is well established that the cigarette smoke profoundly alters molecular signaling pathways and expression patterns [114, 226-230]. The study presented in Chapter A revealed the chronic basolateral CSE exposure *in vitro* model to resemble best the expression patterns shown *in vivo* [114, 231-233]. Chapter B leveraged proteomics together with an advanced pathway enrichment analysis software to unravel what pathways are differentially activated upon a physiologically relevant CS exposure. Its main aims were to further validate the exposure model by comparing altered signaling pathways with the literature evidence, as well as to find novel targets that could be employed in future studies on therapeutic approaches.

Chapter C – In vitro study of baseline gene expression in bronchial epithelial cells derived from never-, ex- and current smokers recapitulates persistently altered proteins levels found in vivo.

As previously explained, cigarette smoke exposure studies show changes caused by CS constituents within the whole lung tissue [234-237], which can develop into incurable chronic diseases. This effect can be attributed by some of the gene expressions which are irreversibly changed due to a CS exposure [238]. The last study in this thesis, aimed to elucidate whether the changes found in *in vivo* proteomic study based on the bronchoalveolar lavage samples derived from never-, ex- and current smokers could be recapitulated in fully differentiated bronchial epithelium *in vitro* from patients also stratified by their smoking history.

3. Chapter A – validation of *in vitro* CS exposure models.

Parts of this chapter have previously been published as: Michal Mastalerz, Elisabeth Dick, Ashesh Anjankumar Chakraborty, Elisabeth Hennen, Andrea C Schamberger, Andreas Schröppel, Michael Lindner, Rudolf Hatz, Jürgen Behr, Anne Hilgendorff, Otmar Schmid, and Claudia A Staab-Weijnitz, Validation of *in vitro* models for smoke exposure of primary human bronchial epithelial cells, *American Journal of Physiology-Lung Cellular and Molecular Physiology*, 2021.

3.1 Introduction

Primary human bronchial epithelial cells are the most physiologically relevant 2D monocultures available, in *in vitro* research on bronchial epithelium. Chapter 1.4 described a wide range of CS exposure modalities, ranging from cell lines to advanced airway-on-a-chip models, with various approaches on how CS is administered to the cells. Little is known, however, about why certain concentrations or cell-delivered doses are chosen. Usually, studies present cytotoxicity assessments only, and physiological relevance was rarely assessed, e.g. through analyzing *CYP1A1* expression [118], or by measuring blood levels of nicotine or other CS components found in smokers' tissues [192]. Notably, several studies have provided an assessment of whether delivered dose of CS and/or type of exposure leads to CS-induced changes typically observed *in vivo*. Several studies have addressed gene expression changes in bronchial epithelium of healthy smokers [114, 226-230]. Single-cell RNA sequencing or microarray analyzes from never- or active smokers resulted in distinct transcriptomic signatures developed in smokers. Few differences set apart experimental approaches in transcriptomic studies. Four out of five studies included patients with no respiratory symptoms and non-pathological lung function characteristics, namely in GSE994 [114], GSE4498 [231], GSE20257 [232], GSE52237 [233]. Beane and colleagues in dataset GSE7895 excluded only lung cancer patients who had a history of smoking. These studies were used for establishing consistently and differentially expressed list of genes in patients with smoking history across all the transcriptomic datasets, collectively termed smoke exposure regulated genes (SERGs, Table 3.2). Importantly, ten selected SERGs were deliberately not only the highest upregulated targets, but also chosen within a variety of ranges: very high (> 10; AKR1B10, CYP1A1, CYP1B1), high (> 5 and ≤ 10; ADH7, ALDH3A1, UCHL1) and moderate fold changes (<5; AKR1C1, MUC5AC, NQO1, PIR, Table 3.2). Differently expressed genes belong to various metabolic pathways, such as cytochrome P450-driven metabolism of xenobiotics (e.g., CYP1A1, CYP1B1, ALDH3A1) or redox balance (e.g., AKR1B10, AKR1C1).

CS exposure models can be characterized by the CS type (wCS, CSE or CSC), the route of administration (apical, basolateral, submerged), duration or timeframe of exposure, but also by the cell-delivered dose. Surprisingly, the dose is rarely mentioned when CSE is generated; typically only the concentration relative to 100% freshly generated CSE is given. Hence, the cell-delivered dose direct comparison between experimental models is rendered difficult if not impossible and has never been assessed before. Variables contributing to increased variability between different CSE batches are number of cigarettes used for CSE generation, flow speed or amount of medium used, to name a few.

In order to comprehensively compare different CS exposure models, SERGs were utilized for standardization models' response in relation to physiological resemblance. To increase experimental relevance of the study, exposure model set-ups were based on designs found most frequently in the literature and, through measurements cell-delivered dose in each set-up, directly compared to wCS exposure by employing comparable doses. Among the most commonly used models are:

- acute basal submerged exposure [190, 239, 240],
- acute basolateral exposure [198]
- chronic basolateral exposure [118, 196]
- acute apical exposure on differentiated pHBEs [212, 241],
- acute apical exposure on differentiated pHBEs with starvation preceding the experiments [193, 242, 243]

Cell-delivered CS doses were quantified in gravimetric assessments and compared between models and with the CS dose deposited in bronchial airways *in vivo*. Overall, both physiological and gravimetric assessments were used to standardize the comparison of six different CS exposure models of primary human bronchial epithelial cells in time- and cost-efficient manner.

3.2 Results

3.2.1 Cell-delivered dose applied in different experimental models can be directly compared by gravimetric assessment of absolute mass of CS

In efforts to compare the cell-delivered dose between all the exposure models, a mass of the cigarette smoke contained in CSE and wCS had to be assessed. For CSE, gravimetric analysis resulted in very similar CSE concentrations (PneumaCult™-ALI medium: 1.40 mg/ml; BEGM medium: 1.25 mg/ml) (Figure 3.1). The dose was then calculated for each exposure scenario (Table 3.1) based on the known CSE dilution and the volume of cell culture medium used for each experiment.

For wCS exposure, the dose of cell-delivered smoke particulates on each insert in the Air Liquid Interface Cigarette smoke Exposure (ALICE-Smoke) was determined by the alcohol spectrofluorometry performed on the metal inserts placed in the occupied inserts on the plate and of the quartz filter located downstream from the ALICE incubation chamber after each experiment did not show significant variability between experiments or between wells within one experiment. Therefore, the average dose of $12 \pm 1.5 \mu\text{g}/\text{cm}^2$ from wCS could be compared to each CSE exposure model (Table 3.1).

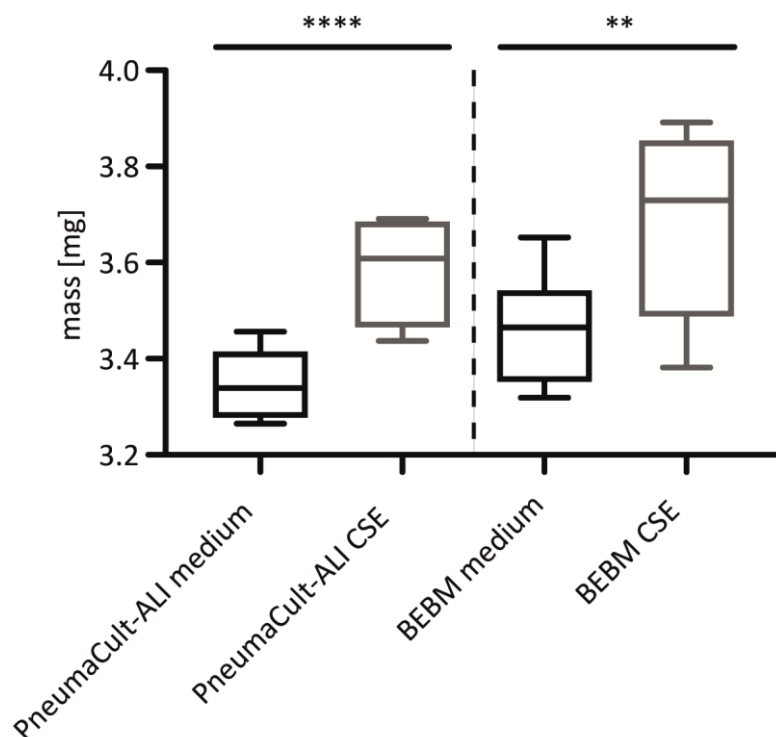


Figure 3.1. Dose of CSE was successfully determined by gravimetric measurement of cigarette smoke particulates in cigarette smoke extract (CSE).

To assess the cell-delivered dose, the vessels for medium (Whatman® quartz filters) were first weighed 3 times each on the analytical scale and then placed in dessicatoros. Next, 200 μ l of PneumaCult™ ALI (n=7 technical replicates) or BEBM (n=5 technical replicates) medium without any supplements and CSE in the exact same medium were carefully pipetted on the quartz filters and left until dried completely. Afterwards, the filters were again weighed on the same scale, giving the absolute weights of the media with and without dissolved cigarette smoke particulates. Finally, through simple subtraction, the calculated difference between 200 μ l media and 200 μ l CSE-media was 0.28 mg and 0.25 mg for ALI and BEGM, respectively. Finally, these differences were multiplied by 5 to yield CSE concentrations: 1.40 mg/ml for PneumaCult™ ALI and 1.25 mg/ml for BEGM media. For statistical analysis, two tailed unpaired student *t*-test was used (*; $p < 0.05$). **Note: This figure and figure legend have been published in Mastalerz et al., 2021.**

Table 3.1. List of evaluated cigarette smoke extract (CSE) and whole cigarette smoke (wCS) models. For details on the respective models, please refer to the relevant figures and text passages in the Material and Methods section. **Note: This table and table description have been published in Mastalerz et al., AJP Lung, 2021.**

#	Model	CSE concentrations	CS dose [$\mu\text{g}/\text{cm}^2$]	Volume delivered [$\mu\text{l}/\text{cm}^2$]	(Exposure) and Incubation time	Starvation	Refers to	Graphical outline
1	Acute submerged CSE exposures (n=4)	2.5%, 5%, 10%, 20%	6.6, 13, 26, 53	210	24 h	No	Figure 3.4	<p>Submerged Basal cells CSE 2.5 - 20% Expansion phase 24h</p>
2	Chronic basolateral CSE exposure (n=5)	5%	62	890	28 days	No	Figure 3.6	<p>Air-liquid interface Basal cells CSE Pseudostratified epithelium Continuous treatment (d0-d28), 5.0 % CSE</p>
3	Short acute apical CSE exposure (n=5)	40%	100	180	(5 min) 24 h	No	Figure 3.8	<p>Air-liquid interface Pseudostratified epithelium 40 % CSE Differentiation phase 5' 24h</p>
4	ALICE-Smoke (n=5)	N/A	12±1.5	N/A	(5 min) 24 h	No	Figure 3.8	<p>Air-liquid interface Pseudostratified epithelium wCS Differentiation phase 5' 24h</p>
5	Acute apical exposure (n=4)	3%, 6%, 12%	7.5, 15, 30	180	24 h	Yes/No	Figure 3.10 Figure 3.11	<p>Air-liquid interface Pseudostratified epithelium CSE 3.0 - 12 % Differentiation phase 24h</p>
6	Acute basolateral CSE exposure (n=5)	5%	62	890	24 h	No	Figure 3.12	<p>Air-liquid interface Pseudostratified epithelium 5.0 % CSE Differentiation phase 24h</p>

3.2.2 Basal cells successfully differentiate to bronchial epithelium featuring cell composition observed *in vivo*

The differentiation started upon reaching confluency on transwell membranes and changing expanding medium PneumaCult™ – ALI and was maintained until day 28 (Figure 3.2 A). Starting from day 0, membranes were collected for immunofluorescent stainings every week at day 0, 7, 14, 21 and 28. Analysis of specific cell-type markers, namely p63, acetylated tubulin, CC10 and MUC5AC revealed successful differentiation of basal cells into the other cell types, achieving the cell composition resembling *in vivo* airway cell populations (Figure 3.2B, C) [27, 244, 245].

For assessing epithelial cell junctions' integrity, transepithelial electrical resistance (TEER) measurements were carried out at days 7, 14, 21, 28. Considerable intra- and interdonor variability diminished at later time points, achieving high consistency at week four. All collected resistance measurements were within 200-800 Ohm range, indicating epithelial barrier integrity was maintained at all times (Figure 3.2D). Taken together, performed analyses show successful differentiation of primary human basal cells into a fully blown bronchial epithelium consisting of all main cell types with the physiologically relevant compositions.

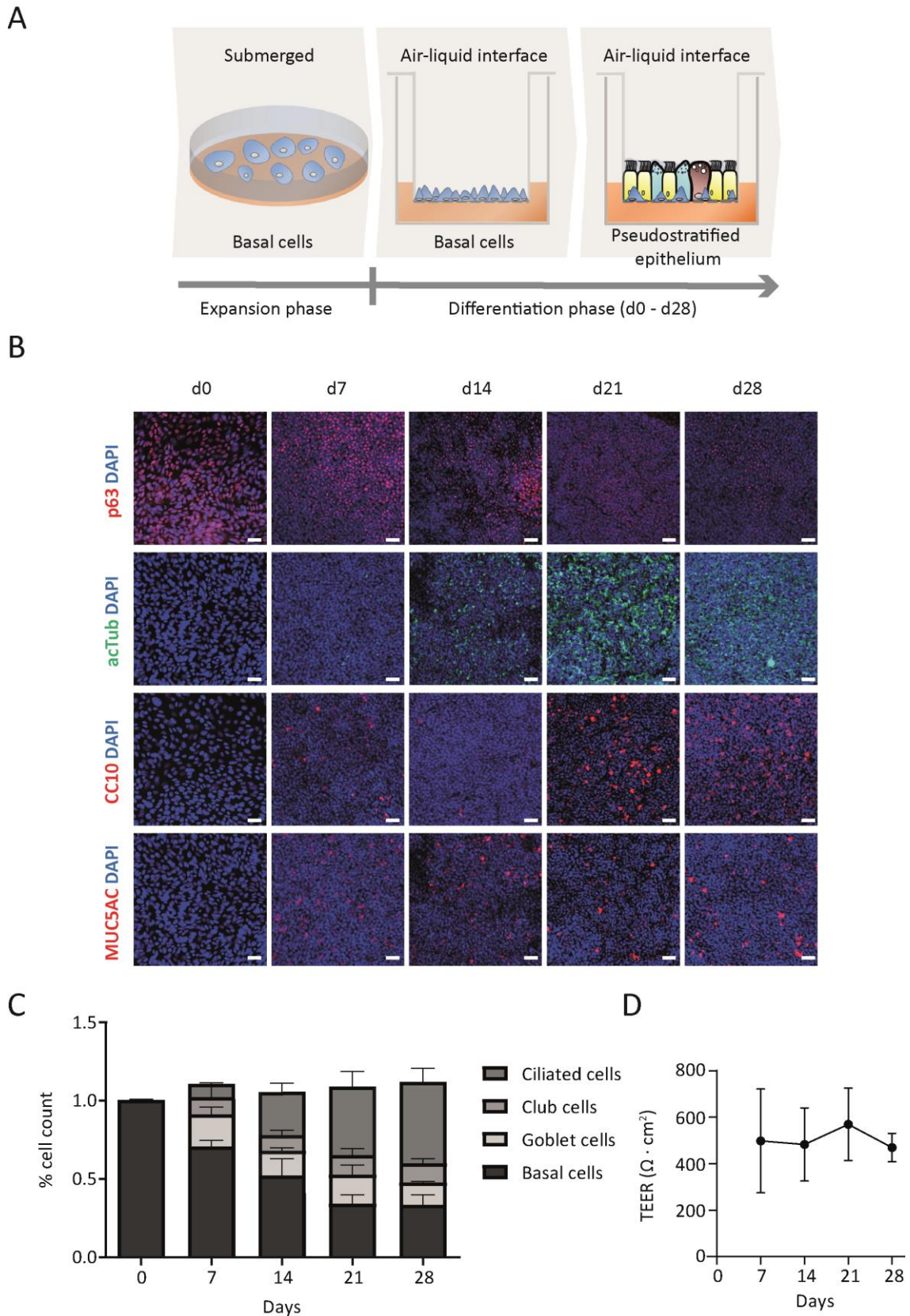


Figure 3.2. Differentiation analyses proved the differentiations of primary bronchial epithelial cells were successful.

(A) Graphical representation of expansion and differentiation of bronchial epithelial cells. On the day 0 cells were placed on the collagen I-precoated 100 mm plates. When the cells reached 80% confluency

after culturing for 4-7 days, cells were then transferred on the collagen IV-precoated membrane inserts on transwells. The PneumaCult™ Ex-Plus medium was then added in the basolateral and apical compartments and removed from the latter once cells reached confluency, creating air-liquid interface (ALI) resembling physiological conditions, which also was considered as the day 0 of differentiation. Of note, ALI was maintained throughout 28 days of differentiation while using PneumaCult™ ALI medium, and thereafter considered as fully differentiated bronchial epithelium, according to the medium's manufacturer protocols. **(B)** Correct differentiation was confirmed by immunofluorescent (IF) stainings performed on samples collected every week starting from day 0 to day 28 (biological replicates n=4) of specific markers for four main cell types: tumor protein 63 (p63), acetylated tubulin (acTub), club cells 10 kDa secretory protein (CC10), and mucin 5AC (MUC5AC) for basal, ciliated, club, and goblet cells, respectively. **(C)** Cell quantification based on IF imaging shows increase of ciliated, club and goblet cells populations until day 21, which remained stable in the last week of differentiation. Results shown are representative for n=4 biological replicates. **(D)** Data collected from transepithelial electrical resistance measurements (n=5 biological replicates) reveals that the epithelial barrier integrity stabilized after first week and was maintained throughout the rest of differentiation within the range of 200-800 $\Omega \cdot \text{cm}^2$ which is recommended by differentiating medium manufacturers. Results are given as mean \pm SD. Scale bar, 40 μm . **Note: This figure and figure legends have been published in Mastalerz et al., 2021. Immunofluorescent pictures were carried out by Elisabeth Dick and cell quantification was done by Elisabeth Dick and Ashesh Chakraborty.**

3.2.3 Doses of cigarette smoke used in experiment were not cytotoxic.

Upon cell death, LDH test shows increased release of lactate dehydrogenase [246]. Furthermore, dead cells detach from the surface, which eventually compromises cell junction, detectable by TEER measurement [247]. Post-exposure LDH and TEER measurements were not significantly altered in comparison to the mock controls for wCS (ALICE-Smoke), and CSE acute exposures (Figure 3.3). The basolateral chronic 5% CSE exposure has been established as non-toxic in basal phBECs and fully differentiated phBECs [118, 190, 248]. In summary, TEER and LDH data revealed all used CSE and wCS cell-delivered doses yielded no cytotoxicity.

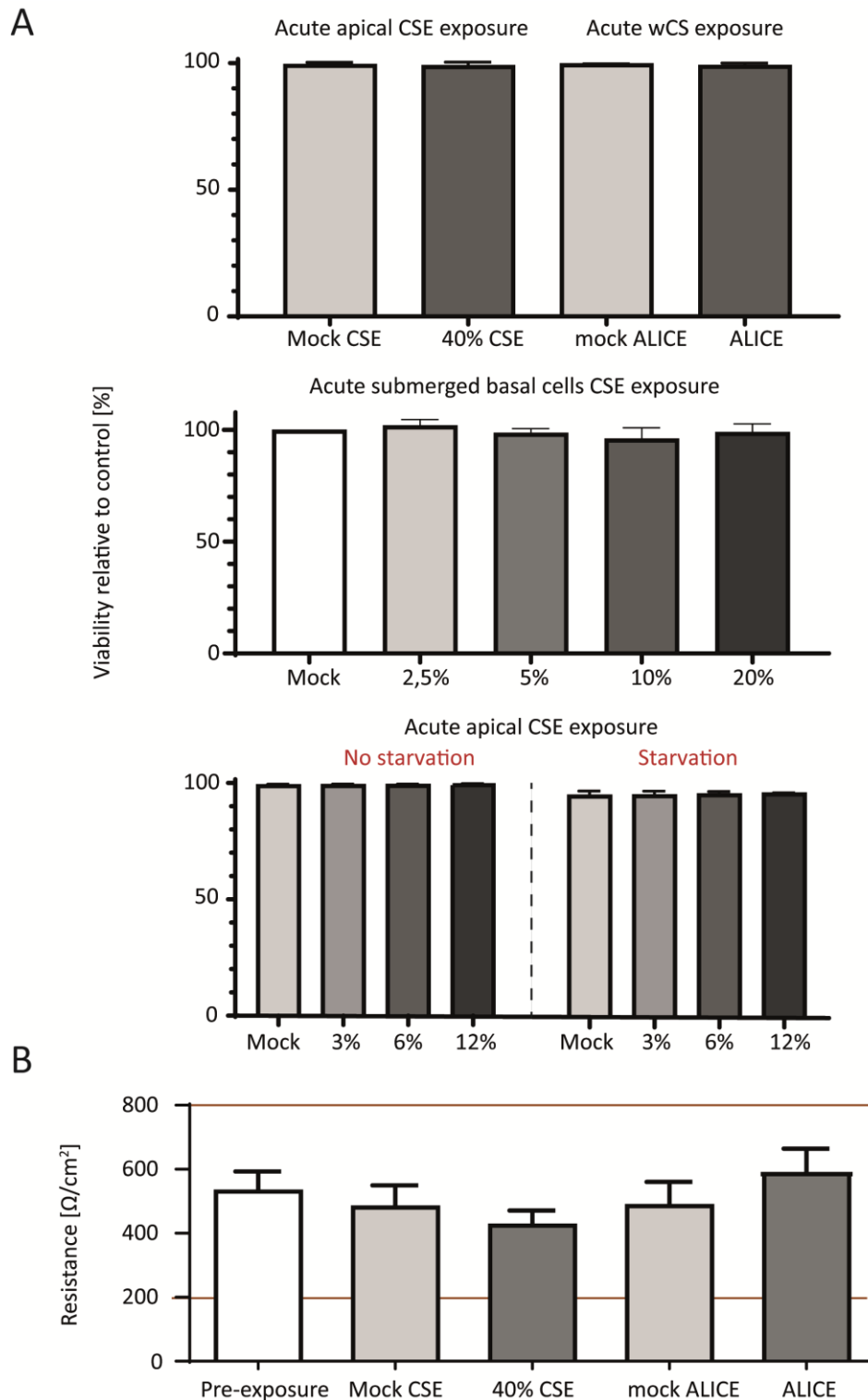


Figure 3.3. TEER and LDH assessments show no non-toxic doses were used in CS exposures.

(A) Lactate dehydrogenase (LDH) released during Air Liquid Interface Cigarette smoke Exposure (ALICE-Smoke) and short apical CSE exposure in a direct comparison, acute submerged basal cells CSE and acute apical CSE exposure, with or without prior starvation (PneumaCult™-ALI medium with no supplements) ($n=3$ biological replicates in each exposure setting). All tests were carried out in technical triplicates. **(B)** Measurement of the transepithelial electrical resistance (TEER) pre- and post-exposure for ALICE-Smoke directly compared with short acute apical CSE (both $n=5$ biological replicates). All tests were carried out in technical triplicates, on at least 3 inserts per donor. Additionally, TEER was measured

3 times for each insert. As mentioned previously, basolateral exposure with 5% CSE has been already reported previously as non-toxic [118, 248], with identical protocol of CSE generation. TEER measurements recorded during basolateral exposure are disclosed in Figure 3.7A. **Note: This figure and figure legends have been published in Mastalerz et al., AJP Lung, 2021.**

3.2.4 PhBECs exposure models differ substantially in their response to CS.

Overall, the expression of 10 smoke exposure regulated genes (SERGs) in primary bronchial epithelial cells was assessed in five CSE exposure settings and one wCS exposure setting (Table 3.2).

Of note, at least four donors were used in all the exposures from the same source, while in some

Table 3.2. List of smoke exposure regulated genes (SERGs).

List of genes chosen as smoke exposure reference genes. Selection was based on upregulated expressions found in current smokers relative to non-smokers in publicly available datasets: GSE994, GSE4498, GSE7895, GSE20257 and GSE52237. Results are presented as fold changes are and given as +/- SD.

Note: This table and table description has been published in Mastalerz et al., AJP Lung, 2021.

#	Gene name	Protein	Fold change ± SD
1	CYP1B1	Cytochrome P450 1B1	33 ± 30
2	AKR1B10	Aldo-keto reductase 1B10	22 ± 3.6
3	CYP1A1	Cytochrome P450 1A1	13 ± 11
4	UCHL1	Ubiquitin carboxyl-terminal hydro- lase isozyme L1	10 ± 7.2
5	ALDH3A1	Aldehyde dehydrogenase 3A1	7.2 ± 1.4
6	ADH7	Alcohol dehydrogenase class 4	5.7 ± 2.5
7	MUC5AC	Mucin 5AC	3.9 ± 1.3
8	AKR1C1	Aldo-keto reductase family 1 mem- ber C1	4.0 ± 0.7
9	NQO1	NAD(P)H dehydrogenase [quinone] 1	3.9 ± 0.4
10	PIR	Pirin	3.3 ± 0.7

exposures with a higher result variability one more donor was used (Table 3.3). This study revealed three settings standing out as capable of upregulating six to seven SERGs on transcript

level. Following two settings showed significant upregulation of six genes on transcript level: submerged basal acute CSE exposure (2.5%, 5%, 10% and 20% CSE) (*AKR1B10*, *AKR1C1*, *CYP1A1*, *NQO1*, *PIR*, *UCHL1*); and ALICE-Smoke wCS exposure (*AKR1B10*, *AKR1C1*, *CYP1A1*, *CYP1B1*, *NQO1*, *UCHL1*). When 5% CSE was added basolaterally throughout differentiation, seven SERGs were significantly upregulated, namely *AKR1B10*, *ALDH3A1*, *CYP1A1*, *CYP1B1*, *NQO1*, *PIR*; In a sharp contrast to these findings, various CSE concentrations added in acute manner, either apically or basolaterally, did not significantly change the expression of more than one gene (*CYP1A1*) from all SERGs (Table 3.4).

Table 3.3. Basic metrics and smoking status of donors used in cigarette smoke exposures.
Note: This table and table description have been published in Mastalerz et al., AJP Lung, 2021.

Donor No.	Age	Gender	Smoking status	Smoking cessation period	Pack years	Experiment
1	73	M	Ex-smoker	>20 years	21-40	1, 2, 3, 4, 5, 6
2	80	W	Ex-smoker	>20 years	21-40	1, 2, 3, 4, 5, 6
3	66	W	Ex-smoker	10-20 years	21-40	1, 2, 3, 6
4	72	W	Never-smoker	n/a	n/a	4, 5, 6
5	80	M	Never-smoker	n/a	n/a	2, 3
6	74	W	Never-smoker	n/a	n/a	1, 2, 3, 4, 5, 6

List of experiments:

- 1 – Exposure of basal phBECs under submerged conditions
- 2 – Chronic basolateral exposure of differentiated phBECs
- 3 – Acute basolateral exposure of differentiated phBECs
- 4 – Acute apical exposure of differentiated phBECs with CSE
- 5 – Acute apical exposure of differentiated phBECs with CSE with 24h starvation
- 6 – Acute apical exposure of differentiated phBECs with wCS

Table 3.4. Overview of smoke exposure-regulated genes (SERGs) mRNA fold changes in the evaluated models, in comparison to upregulation by CS in current smokers (top row).

Statistically significant results ($p < 0.05$) number of significantly upregulated genes is given in bold in the last column. **Note: This table and table description has been published in Mastalerz et al., AJP Lung, 2021.**

	Dose per area [$\mu\text{g}/\text{cm}^2$]	CYP1B1	AKR1B10	CYP1A1	UCHL1	ALDH3A1	ADH7	MUC5AC	AKR1C1	NQO1	PIR	No.
Healthy smokers ^a	N/A	33	22	13	10	7.2	5.7	3.9	4.0	3.9	3.3	10
Chronic basolateral CSE exposure ^b	62	4.9	2.6	56	1.8	1.8	1.4	1.7	1.8	1.5	1.6	7
ALICE-Smoke exposure	12	74	6.6	42215	32	2.4	0.8	0.6	8.0	3.3	2.0	6
Acute submerged basal cells CSE exposure ^c	56	2.0	4.0	6.4	4.2	3.1	0.4	N/A	7.1	4.2	2.7	6
Acute basolateral CSE exposure	62	2.1	2.2	5.4	0.9	1.1	1.2	0.7	1.1	0.9	1.1	1
Acute apical CSE exposure w/starvation ^d	30	1.5	1.1	11	1.0	1.5	1.3	1.3	1.2	1.0	1.4	1
Acute apical CSE exposure w/o starvation ^d	30	2.3	1.4	12	1.6	1.7	1.2	1.7	1.5	1.2	1.3	1
Short acute apical CSE exposure	100	0.8	0.9	1.8	1.1	1.2	0.9	1.8	1.2	1.0	1.0	0

^a mRNA fold changes in bronchial cells brushed from healthy active smokers, obtained from transcriptomic data, references in Table 3.2

^b Fold changes shown for day 28. For *CYP1A1* significance was obtained at days 7 and 21, for *AKR1C1* at days 7 and 14, and for *PIR* at day 21 (see Fig. 3.6)

^c Fold changes shown for 20% CSE

^d Fold changes shown for 12% CSE

3.2.4.1 Submerged exposure of basal cells with CSE upregulates six out of nine possible SERGs

Undifferentiated basal cells were exposed acutely to CSE under submerged conditions (Fig. 4A). One of the SERGs, *MUC5AC*, is a protein solely expressed by goblet cells, therefore not expressed by basal cells [249]. RT-qPCR analysis revealed significant upregulation of six (*AKR1B10*, *AKR1C1*, *CYP1A1*, *NQO1*, *PIR*, *UCLH1*) out of nine remaining reference genes; (Fig. 4B). Furthermore, the submerged basal cell treatment with 2.5, 5, 10, and 20% of CSE showed dose-dependent upregulation, visible for *AKR1B10*, *UCLH1*, *NQO1*, *AKR1C1* and *PIR*. Interestingly, levels of *ADH7* were significantly lowered with increasing CSE concentrations. Apart from using cells originated from CPC BioArchive, identical CSE treatment was performed on commercially available primary bronchial epithelial cells from Lonza, on which significant upregulations of all the SERGs were observed, with the exception of *ADH7* and *MUC5AC*, the latter for aforementioned reasons (Figure 3.5). These findings were not pooled deliberately to demonstrate that substantial changes in gene expression of analyzed smoke-induced genes occur unrelated to the source of the cells. In an agreement with results on the transcript level, trends for dose-dependent upregulation were qualitatively confirmed for three genes, namely *AKR1B10*, *AKR1C1*, and *NQO1*, on protein level by Western blot analysis. Interestingly, *ADLH3A1* protein levels were increased, as opposed to unchanged transcript levels (Figure 3.4B and C), whereas in commercially available primary cells protein levels of *ADLH3A1* were not visibly changed, despite significant upregulation of mRNA expression (Figure 3.5B and C).

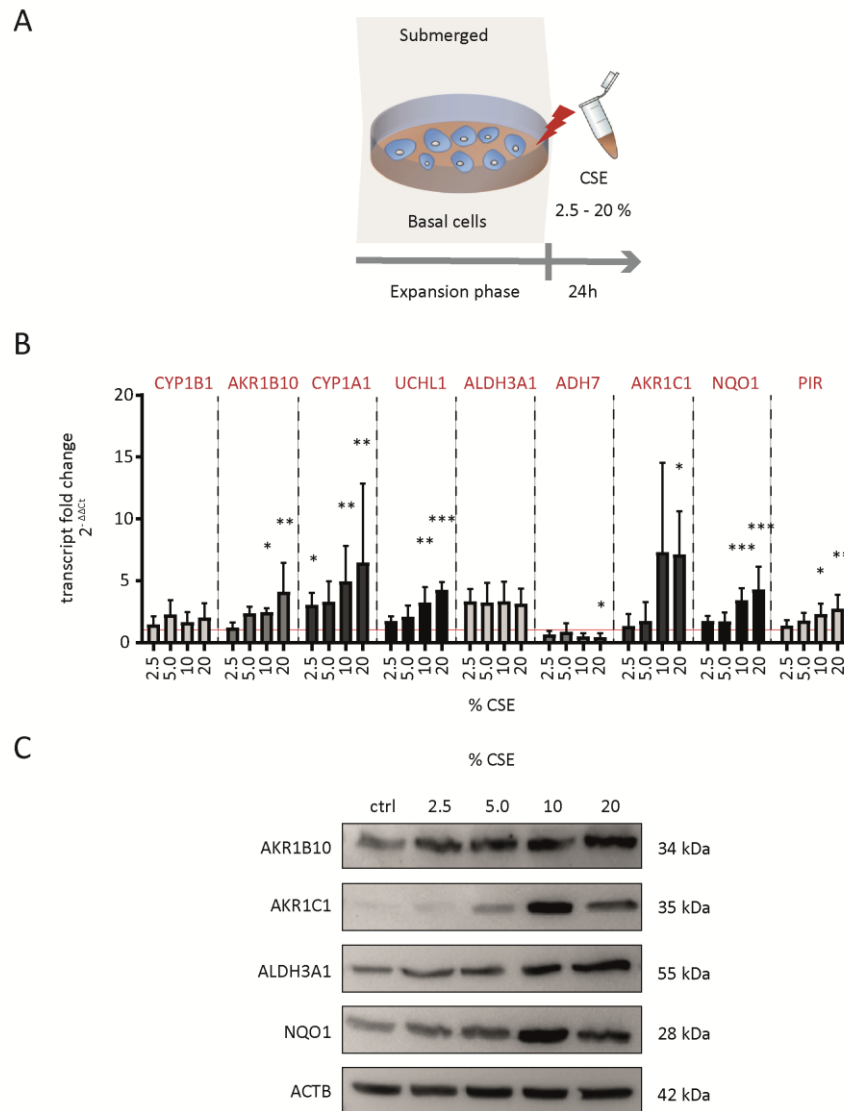


Figure 3.4. Acute submerged basal cell exposure to various concentrations of cigarette smoke extract (CSE) resulted in upregulation of six out of nine smoke exposure regulated genes (SERGs).

(A) Experimental set-up. Primary human bronchial epithelial basal cells were exposed to 0, 2.5, 5.0, 10 and 20% CSE for 24 h. After incubation RNA and protein were collected for the analysis. **(B)** Results of RT-qPCR are shown as a fold change of nine SERGs, relative to the control normalized to 1 (red line). Mucin 5AC (MUC5AC), a marker of goblet cells was not included since it is not expressed in the basal cells. Genes are ordered by the regulation strength in healthy smokers from highest (left) to lowest (right) fold change (see Table 3.2) and show a dose-dependent increase of the expression upregulation. Hydroxymethylbilane synthase transcript (HMBS) was used as an internal reference gene. Statistical analysis was assessed by a one-way ANOVA with Bonferroni correction for multiple comparisons (*, $p < 0.05$; **, $p < 0.01$; ***, $p < 0.001$). **(C)** Representative Western Blots for ALDH3A1, NQO1, AKR1B10 and AKR1C1 show dose-dependent regulation also on protein level. β -actin (ACTB) was used as loading control. Results shown are based on $n=4$ (independent donors) and given as mean \pm SD. **Note: This figure and figure legends have been published in Mastalerz et al., AJP Lung, 2021.**

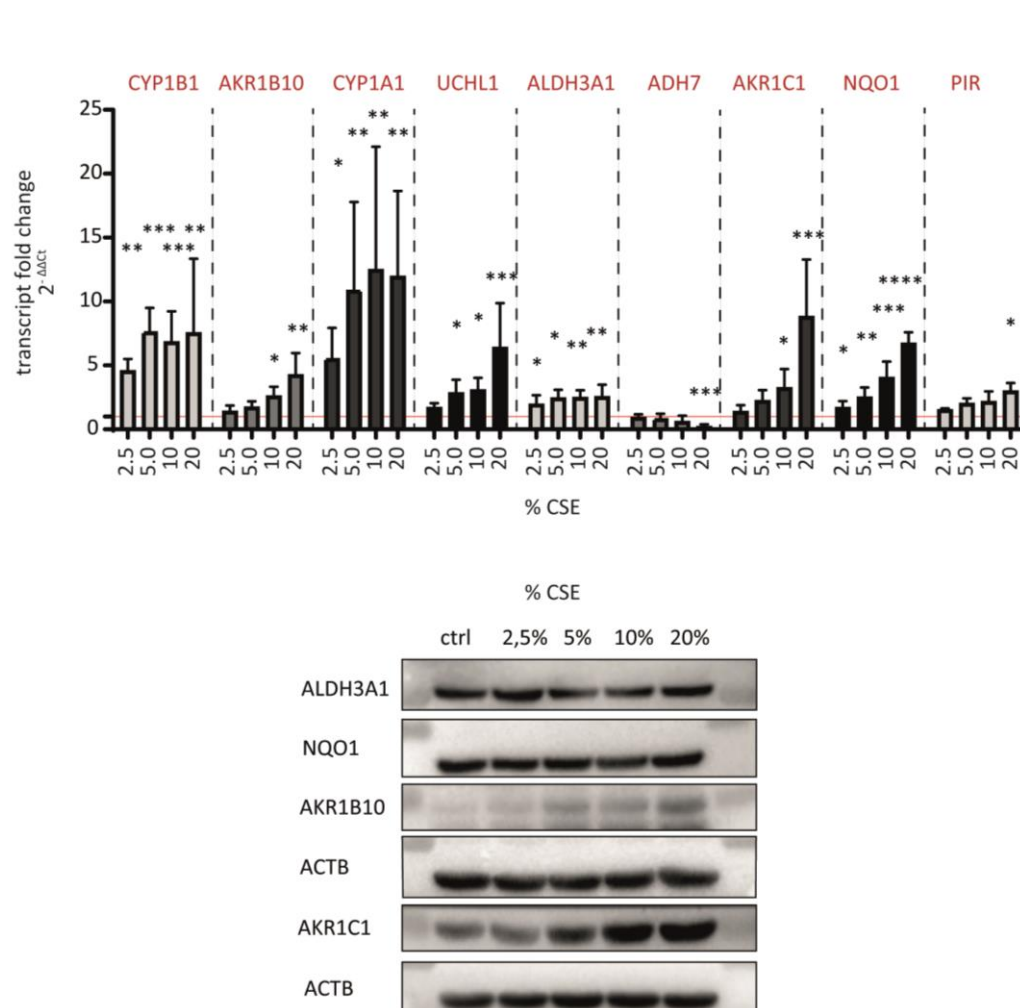


Figure 3.5. Acute submerged exposure with cigarette smoke extract (CSE) of primary human bronchial epithelial basal cells.

Here, cells of healthy donors were purchased from Lonza. Results of the RT-qPCR are presented as a fold change of 9 SERG genes. Mucin 5AC (MUC5AC), a cell-type specific goblet cell marker, is not expressed by the basal cells, therefore was excluded from the set. Results are presented relative to the control normalized to 1 (dotted line). Porphobilinogen deaminase (HMBS) was used as a housekeeping gene. Statistical analysis was assessed by 1-way ANOVA followed by Dunnet correction for multiple comparisons ($p < 0.05$). (C) Representative Western Blots are shown for ALDH3A1, NQO1, AKR1B10 and AKR1C1, where dose dependent upregulation can be seen only for AKR1C1. β -actin (ACTB) was used as loading control. **Note: This figure and figure legends have been published in Mastalerz et al., AJP Lung, 2021.**

3.2.4.2 Chronic basolateral exposure with CSE during differentiation upregulates seven out of ten SERGs

In the only chronic setting assessed in this study, pHBEs were treated with 5% CSE from basolateral compartment, continuously throughout entire differentiation (28 days) (Figure 3.6A). The RT-qPCR analysis of transcript collected at days 7, 14, 21, 28 revealed significant upregulation of seven out of 10 SERGs, namely *AKR1B10*, *AKR1C1*, *ALDH3A1*, *CYP1A1*, *CYP1B1*, *NQO1*, *PIR* (Figure 3.6B). Among these, the most dramatic upregulation was observed for *CYP1B1* and

CYP1A1, where expressions were increased more than 10-fold. Other significantly increased SERGs were increased in a more moderate manner, with 2-fold change increase. Trends for upregulation were also observed on protein level for AKR1B10, NQO1 and ALDH3A1 (Figure 3.6C). In addition to transcript and protein assessments, basolateral exposure TEER and cell population quantification was compared with results reported by Schamberger and her colleagues [118]. Interestingly, in contrast with previous findings, the continuous treatment yielded lower TEER values (Figure 3.7A). Furthermore, similarly to the work of Schamberger and her colleagues, an increase of basal cell population as well as a decreased number of ciliated cells were observed, however both results failed to reach significance (Figure 3.7B).

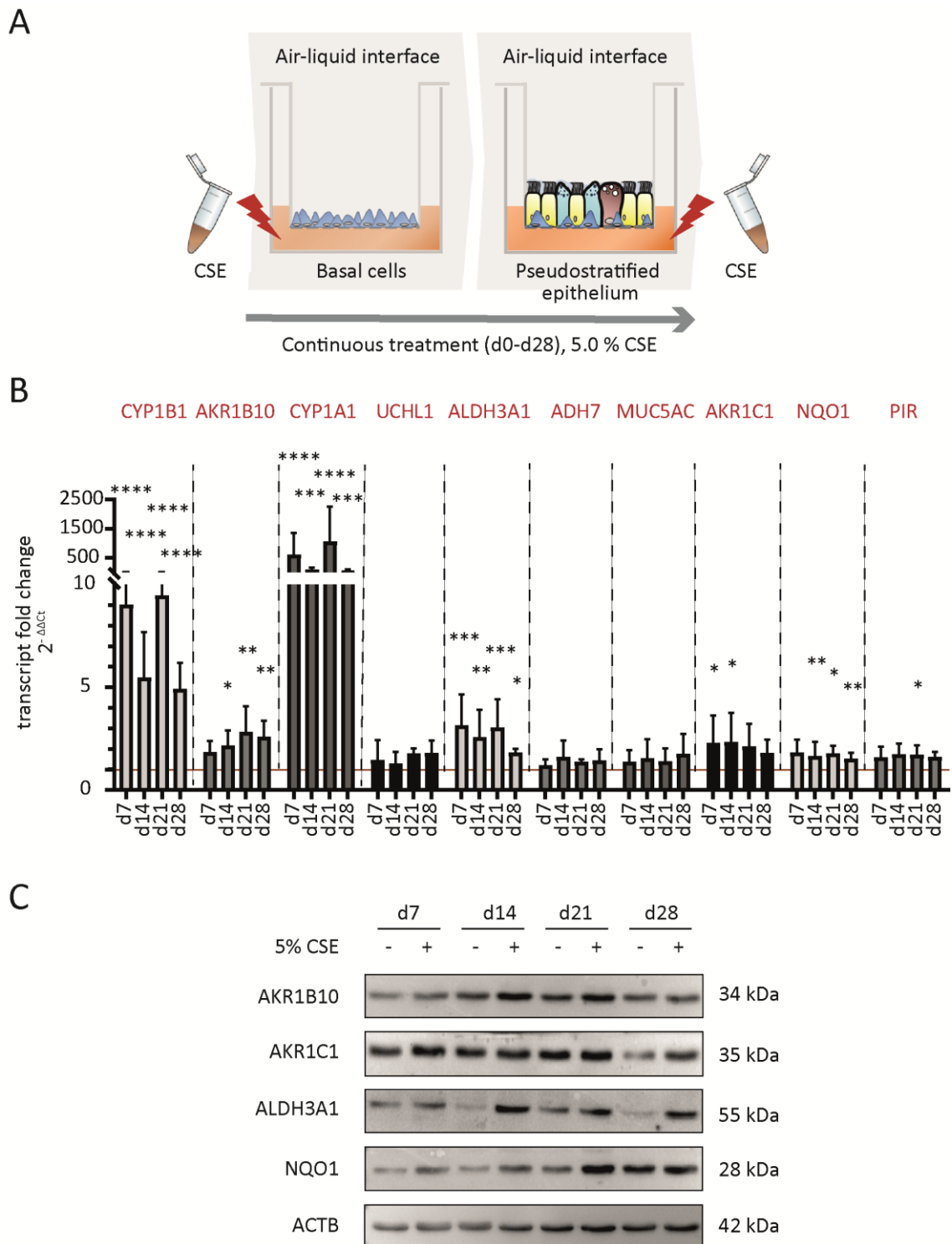


Figure 3.6. Chronic basolateral exposure to 5% cigarette smoke extract (CSE) of primary human bronchial epithelial cells during the complete course of differentiation revealed CSE significantly upregulates seven out of 10 smoke exposure regulated genes (SERGs).

(A) Experimental set-up. PhBECs were chronically exposed to 5% CSE in the basolateral compartment from day 0 to day 28 of differentiation and with the mock exposures were collected every week for mRNA and protein analysis. **(B)** Results of RT-qPCR are presented as a fold change relative to the control normalized to 1 (red line). SERGs are shown in order of the regulation strength in healthy smokers from

highest (left) to lowest (right) fold change (see Table 3.2). WD repeat-containing protein 89 (WDR89) transcript was used as internal reference gene. Statistical analysis was assessed by 1-way ANOVA followed by Bonferroni correction for multiple comparisons ($p < 0.05$; *, $p < 0.05$; **, $p < 0.01$; ***, $p < 0.001$). **(C)** In an agreement with the transcript data, representative Western Blots for four selected SERGs show a regulation on protein level for ALDH3A1 and NQO1, but less prominently for AKR1B10 and AKR1C1. β -actin (ACTB) was used as a loading control. Results shown are based on $n = 5$ (independent donors) and given as mean \pm SD. **Note: This figure and figure legends have been published in Mastalerz et al., 2021.**

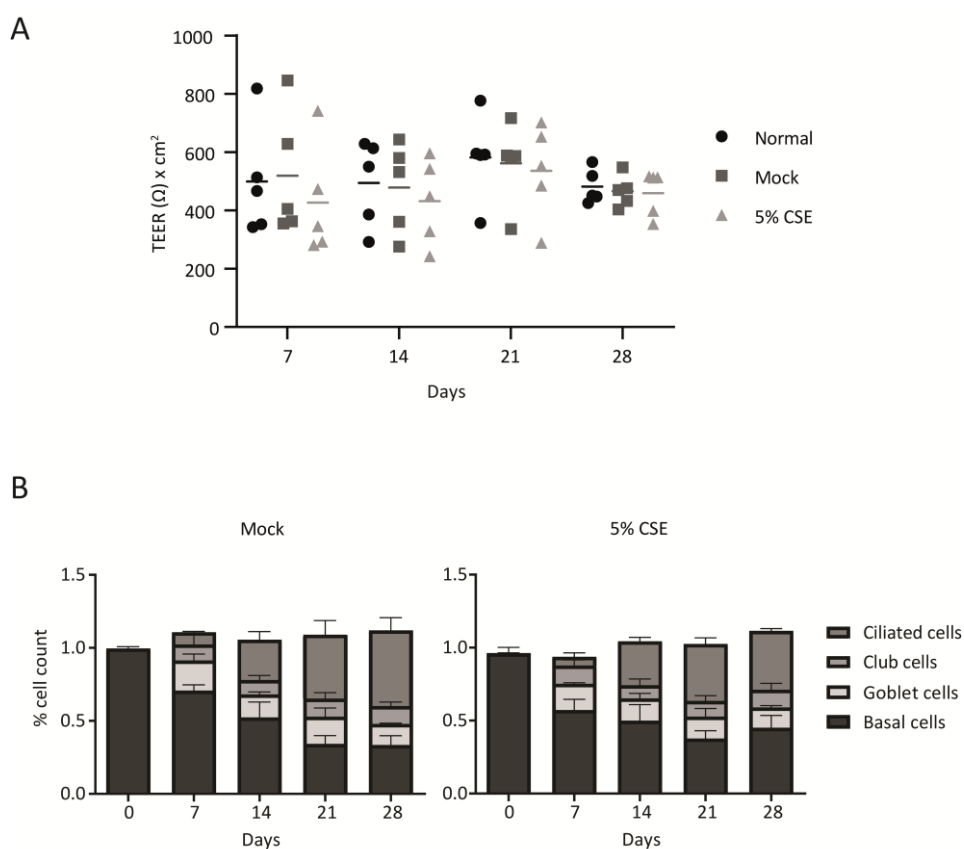


Figure 3.7. Quantitative immunofluorescence of major cell types and transepithelial electrical resistance (TEER) during chronic basolateral treatment with cigarette smoke extract (CSE) during differentiation shows no cytotoxicity incurred by CSE, relative to mock.

(A) Epithelial barrier integrity assessed on a weekly basis by TEER was not significantly altered by CSE. Results shown are from $n = 5$ (independent donors) and presented as mean \pm SD. **(B)** The immunofluorescent quantification of all main bronchial epithelial cell types. Results presented as stacked columns representing the cell composition based on the cell count performed on cells collected every week, starting from day 0. Measurements based on $n = 4$ (independent donors) and given as mean \pm SD. Due to a non-normal sample distribution, for statistical analyses Friedman test with Dunn's correction for multiple comparisons was used. **Note: This figure and figure legends have been published in Mastalerz et al., 2021.**

3.2.4.3 Whole cigarette smoke exhibits most substantial upregulations of SERGs expressions

Fully differentiated pHBEs were transferred to the ALICE-Smoke incubation chamber (Figure 3.8A, Figure 3.9) and exposed to the continuous flow of cigarette smoke generated from 3 cm of a filtered research cigarette, therefore mimicking best the physiological exposure environment. In the transcript analysis, expressions of six out of 10 SERGs were significantly increased, namely *AKR1B10*, *AKR1C1*, *CYP1A1*, *CYP1B1*, *NQO1*, *UCLH1* (Figure 3.8B). Markedly, wCS yielded the most drastic upregulations observed among all assessed models, for *CYP1B1*, *UCLH1* and most notably for *CYP1A1*, which increase was magnitudes higher than in any other exposure model. Higher upregulations of more than 5-fold were also observed for *AKR1B10* and *AKR1C1* and *NQO1* showed similar upregulation as in the previously described models. Interestingly, the transcript of *MUC5AC* was significantly reduced upon the wCS exposure. On a protein level, *AKR1C1*, *AKR1B10* and *NQO1*, *UCLH1* and *PIR* showed trends for upregulation, while *ALDH3A1* was not consistently upregulated, in an agreement with no significance reached on the transcript level (Figure 3.8C and D).

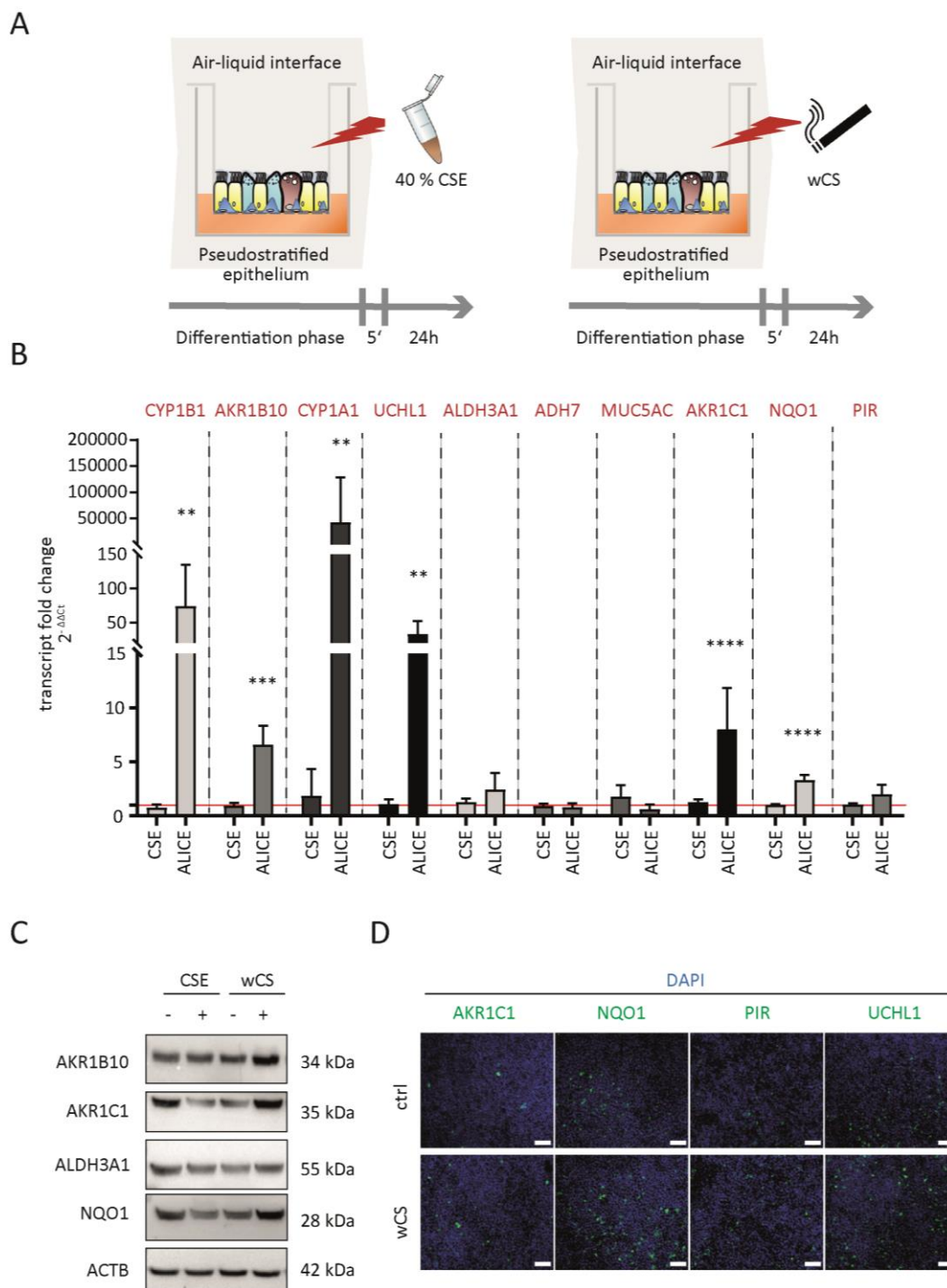


Figure 3.8. Short acute apical exposure of differentiated primary human bronchial epithelial cells with whole cigarette smoke (wCS) and cigarette smoke extract (CSE) using comparable CS particulate doses resulted in significant upregulation of six out of 10 smoke exposure regulated genes (SERGs) for wCS, but none for CSE.

(A) Experimental set-up. Fully differentiated phBECs were either exposed apically to 200 μ l of 40% CSE for 5 min or to 5 min exposure to wCS generated by 3 cm of a research grade cigarette followed by incubation for 24 h and sample collection for mRNA and protein analysis. **(B)** Results of RT-qPCR are

presented as a fold change of 10 genes relative to the control normalized to 1 (red line). WDR89 transcript was used as an internal reference gene. Statistical analyses were performed using two-tailed student's t-test (*, $p < 0.05$; **, $p < 0.01$; ***, $p < 0.001$). **(C)** Representative western blots for 4 selected SERGs show no upregulation on a protein level for CSE, but a moderate upregulation for all 4 for wCS. β -actin (ACTB) was used as a loading control. **(D)** Representative immunofluorescent stainings demonstrate moderate increases in the number of the AKR1C1⁺, NQO1⁺, PIR⁺, and UCHL1⁺ cells. Scale bar 40 μ m. Results shown are based on $n = 5$ (independent donors) and given as mean \pm SD. **Note: This figure and figure legends have been published in Mastalerz et al., AJP Lung, 2021.**

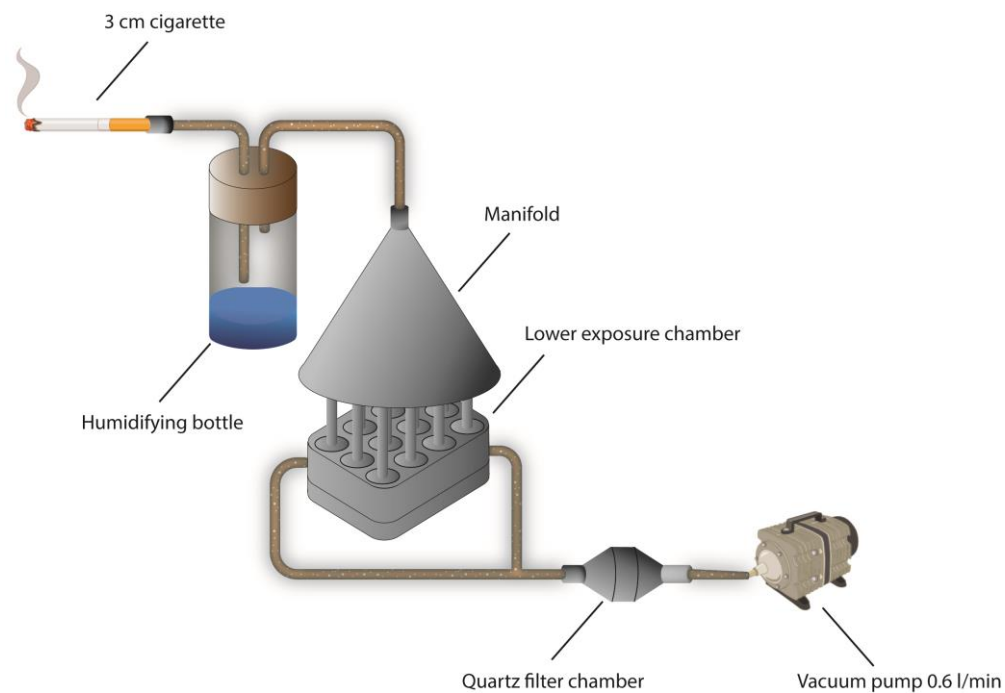


Figure 3.9. Air-Liquid Interface Cigarette Smoke Exposure (ALICE-Smoke) system allows for continuous exposure to cigarette smoke.

After the end of each differentiation, inserts containing phBECs were washed once with the pre-warmed HBSS and transferred to the lower exposure chamber. After tightly assembling the lower exposure chamber with the Manifold, ALICE-Smoke was placed into incubation chamber on the heating plate set to temperature of 37°C. Along with ALICE-Smoke, a Humidifying bottle was placed inside the Incubation chamber. After connecting all the tubing and putting the quartz filter in a Quartz filter chamber, a 3 cm of research grade cigarette was installed into the cigarette holder and lit up with a lighter. Immediately, the Vacuum pump set to flow rate of 0.6 L/min was turned on and the smoke generated from the cigarette passed subsequently through the Humidifying bottle, Manifold, Lower exposure chamber and Quartz filter chamber, where approximately 95% of all smoke was deposited. Flow rate was maintained at 0.6 L/min, controlled by flow-meter located between Quartz filter chamber and Vacuum pump. Some parts of the Figure were created using BioRender.com. **Note: This figure and figure legends have been published in Mastalerz et al., AJP Lung, 2021.**

3.2.4.4 Acute CSE exposures on differentiated phBECs upregulates only *CYP1A1* expression, a robust responder to CS

Leveraging the opportunity to quantify and thence compare the cell-delivered doses in wCS and CSE exposures, the experiment aiming to compare both CS exposure modalities was performed (Figure 3.8A). In parallel, fully differentiated phBECs were exposed to the aforementioned wCS set-up and apically added 40% CSE, chosen as a high non-toxic dose of CS particulates. With gravimetric measurement results described previously (Figure 3.1), 40% CSE corresponded to 100 $\mu\text{g}/\text{cm}^2$ of cell-delivered CS dose, which is markedly 8 times higher than average CS cell-delivered dose determined for the wCS exposures by spectrophotometry ($12 \pm 1.5 \mu\text{g}/\text{cm}^2$). In detail, CSE was applied for 5 min and then aspirated (without apical washing), in efforts to resemble the time of total continuous flow time during wCS exposure. Most strikingly, the former exposure failed to upregulate any of SERGs, as compared to six genes expressions increased by wCS, sometimes in a drastic fashion (Figure 3.8B). In accordance with the transcript results, a high non-toxic exposure was also unable to alter the protein levels of chosen SERGs (AKR1C1, AKR1B10, NQO1 and ALDH3A1, Figure 3.8C).

Elsewhere, acute CSE exposures of the differentiated phBECs were assessed in other settings such as: 24 h exposure of 3%, 6% and 12% of CSE (Figure 3.10A), also including prior starvation of the differentiated phBECs (Figure 3.11A), as well as basolateral 5% CSE 24 h exposure (Figure 3.12A). Importantly, a direct dose comparison based on the gravimetric results (Figure 3.1) revealed that 3%, 6% and 12% CSE corresponded to 7.5, 15 and 30 $\mu\text{g}/\text{cm}^2$, a range within which is also wCS dose of 12 $\mu\text{g}/\text{cm}^2$. For acute apical exposures, RT-qPCR revealed that only one SERG was significantly upregulated, *CYP1A1*, in 12% CSE, which corresponded to 30 $\mu\text{g}/\text{cm}^2$, dose 2.5-fold higher than in wCS exposure (Figure 3.10B). Similar level of upregulation of *CYP1A1* was observed when a starvation prior to the exposure was used (Figure 3.11B). Failure in SERGs upregulation in both set-ups was also confirmed on protein level for AKR1C1, AKR1B10, NQO1 and ALDH3A1 (Figure 3.12C and Figure 3.12C).

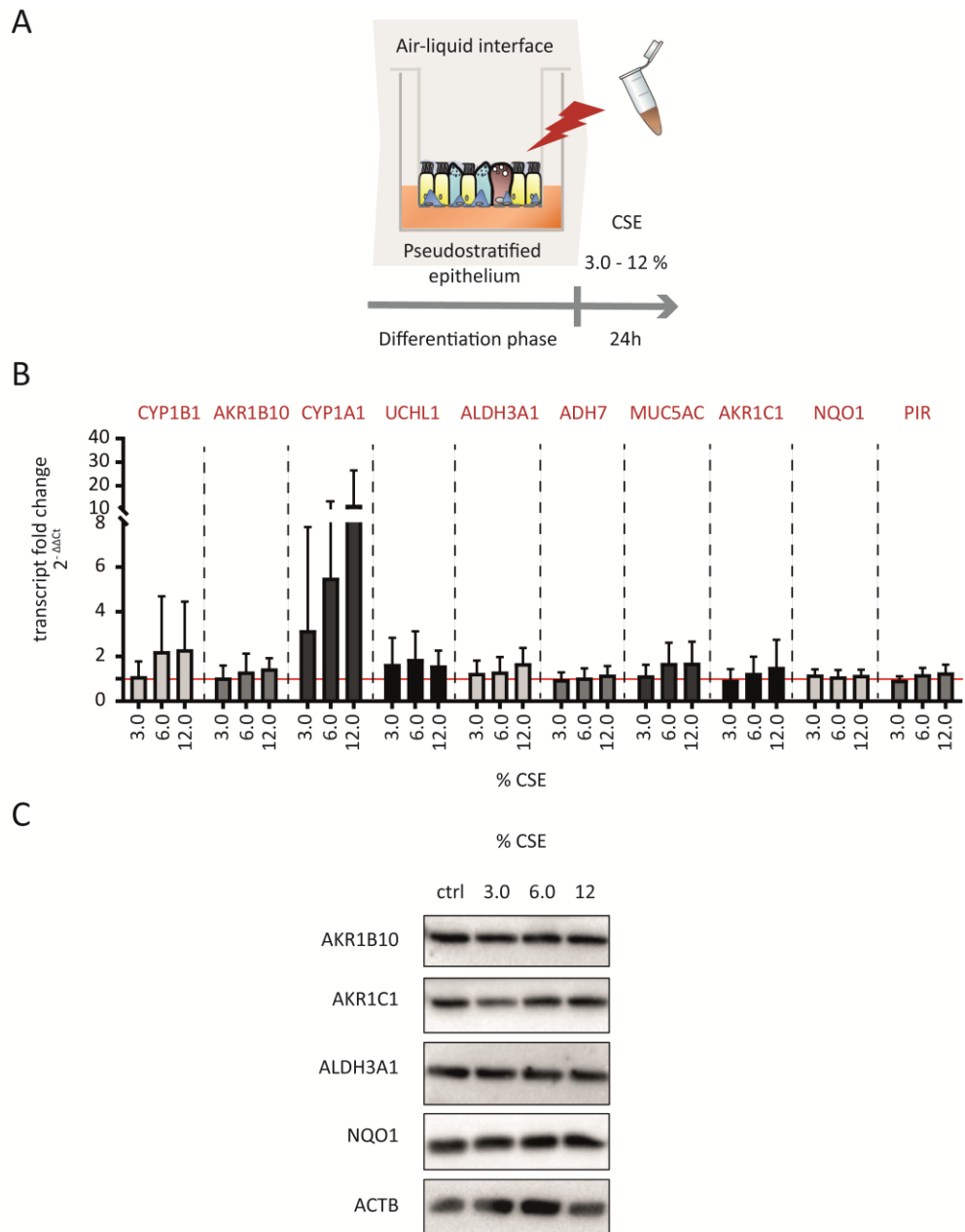


Figure 3.10. Acute apical exposure of differentiated primary human epithelial cells with various concentrations of cigarette smoke extract (CSE) revealed only one significant upregulation at highest used CSE concentration.

(A) Experimental set-up. Fully differentiated phBECs were exposed apically to 200 μ l of 0% 3%, 6%, 12% CSE for 24 h followed by collection of the treated membranes with cells for mRNA and the protein analysis. **(B)** Results of RT-qPCR are presented as a fold change of 10 genes relative to the control normalized to 1 (red line). SERGs are presented in order of regulation strength in healthy smokers from highest (left) to lowest (right) fold change (see **Table 3.2**). Hypoxanthine-guanine phosphoribosyltransferase (*HPRT*) was used as an internal reference gene. Statistical analysis was assessed by the one-way ANOVA with Bonferroni correction for multiple comparisons (*, $p < 0.05$). **(C)** Representative western blots for ALDH3A1, NQO1, AKR1B10 and AKR1C1 show no regulation on the protein level. β -actin (ACTB) was

used as a loading control. Results shown are based on n= 4 (independent donors) and given as mean ± SD. **Note: This figure and figure legends have been published in Mastalerz et al., AJP Lung, 2021.**

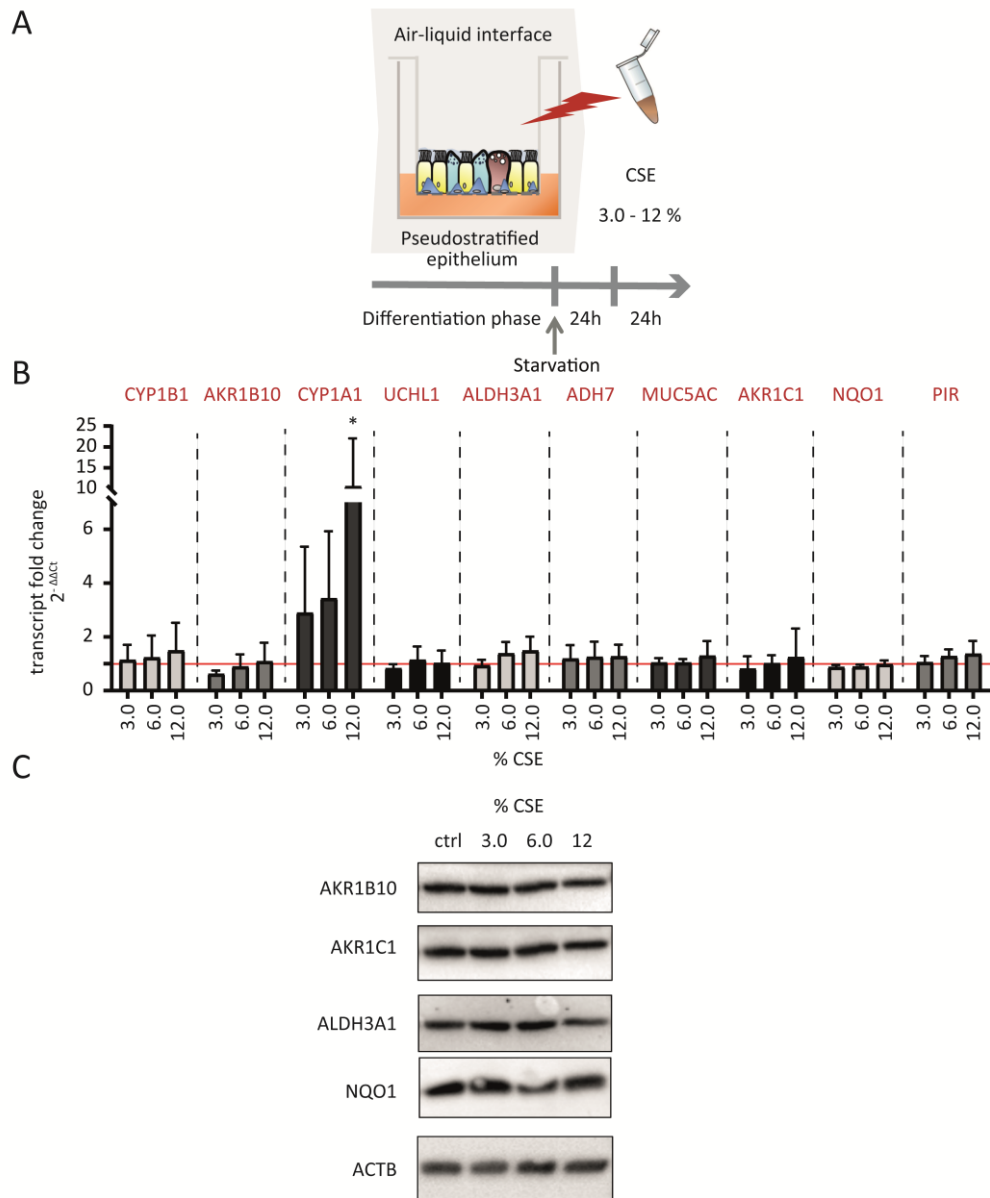


Figure 3.11. Acute apical exposure to various concentrations of cigarette smoke extract (CSE) including prior starvation reveals another treatment upregulating only in SERG.

(A) Experimental set-up. Fully differentiated phBECs (n=4 independent donors) were exposed apically to 200 μ l of 0% 3%, 6%, 12% CSE for 24 h and then the cells were collected for mRNA and protein analysis. (B) Results of the RT-qPCR are presented as a fold change of 10 SERGs relative to the control normalized to 1 (dotted line). Hypoxanthine-guanine phosphoribosyltransferase (*HPRT*) was used as a reference gene. Statistical analysis was assessed by the one-way ANOVA with Bonferroni correction for multiple comparisons ($p < 0.05$). (C) Representative Western Blots are shown for ALDH3A1, NQO1, AKR1B10 and AKR1C1, which revealed no visible upregulation. β -actin (ACTB) was used as a loading control. Results

shown are based on n= 4 (independent donors) and given as mean ± SD. **Note: This figure and figure legends have been published in Mastalerz et al., AJP Lung, 2021.**

In a sharp contrast with chronic treatment, 24 h basolateral exposures of 5% CSE (Figure 3.12A) showed no significant upregulation of SERGs on mRNA level except for *CYP1A1* (Figure 3.12B). Similarly to other models, RT-qPCR of *ALDH3A1*, *AKR1B10*, *AKR1C1* and *NQO1* were later confirmed on protein level, where all targets remained unchanged upon treatment (Figure 3.12C).

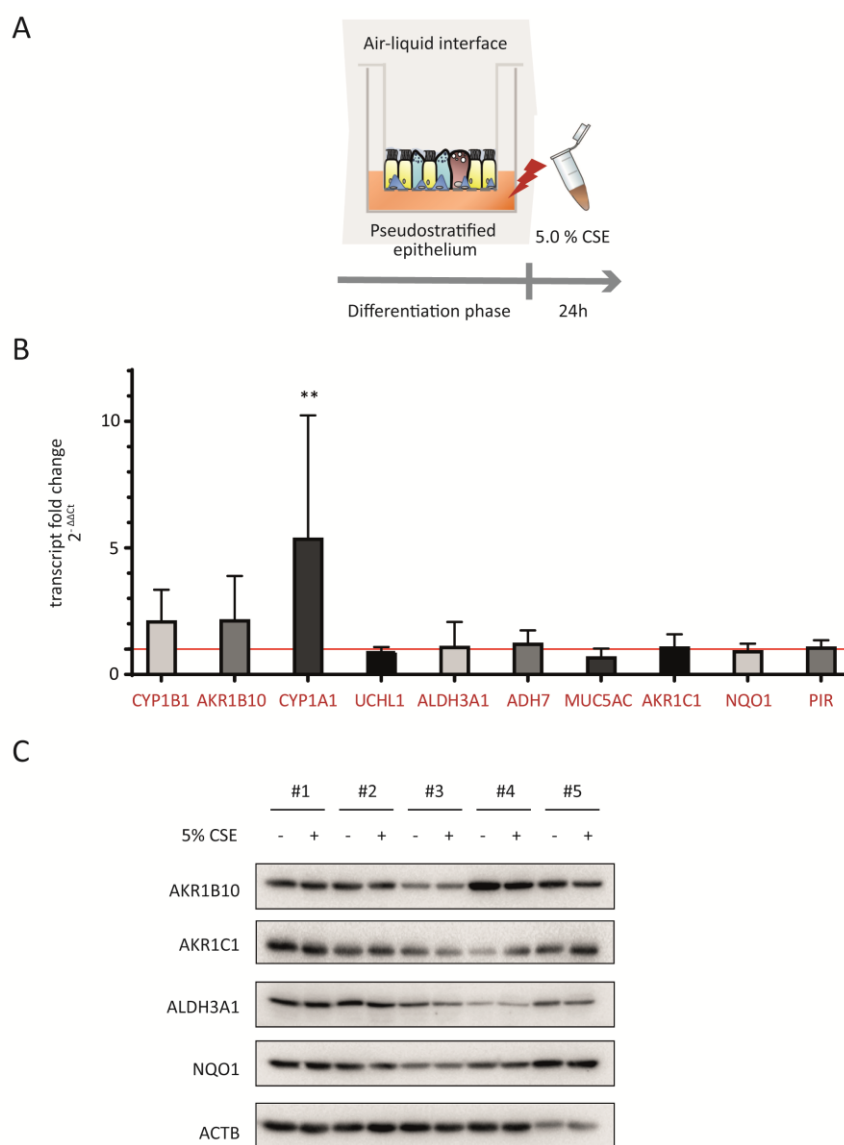


Figure 3.12. Acute basolateral exposure of fully differentiated primary human bronchial epithelial cells to 5% cigarette smoke extract (CSE) resulted in significant upregulation of 1 smoke exposure regulated gene (SERGs).

(A) Experimental setup. Fully differentiated phBECs were exposed basolaterally to 5 % cigarette smoke extract (CSE) for 24 h, which was followed by the collection of cells for mRNA and protein analysis. (B) Results of RT-qPCR (n=5 independent donors) are presented as a fold change of 10 genes relative to

the control normalized to 1 (dotted line). SERGs results are shown in an order of regulation strength in healthy smokers from highest (left) to lowest (right) fold change (see Table 3.2). Polyubiquitin-C (*UBC*) was used as a housekeeper gene. Statistical analyses were performed using paired two tailed *t*-test ($p < 0.05$). (C) Western Blots ($n=5$) are shown for ALDH3A1, NQO1, AKR1B10 and AKR1C1, which revealed no visible upregulation. β -actin (*ACTB*) was used as a loading control. Results shown are based on $n=5$ (independent donors) and given as mean \pm SD. **Note: This figure and figure legends have been published in Mastalerz et al., AJP Lung, 2021**

3.2.5 SERGs are expressed by basal and luminal cell types

In the chronic basolateral exposure, basal cells are in a direct contact with CSE. Since this exposure type has resulted in upregulation of most of the SERGs, the new hypothesis was investigated, whether basal cells are main responders to cigarette smoke. wCS was chosen because of its most dramatic SERGs response, physiological relevance and because it contains all main cell types, featured in *in vivo* bronchial epithelium. Upon exposure to wCS particles the colocalization stainings of 4 selected proteins has been performed, namely AKR1C1, NQO1, PIR and UCHL1. In agreement with previous findings, immunofluorescence analysis revealed upregulation of protein in SERG-positive cells in ALICE-Smoke exposed cells of all selected proteins (Figure 3.8D). Moreover, all SERGs proteins co-localized with p63, the specific marker for basal cells. Although it has showed some colocalisation with NQO1 and UCHL1, the strongest signal of NQO1, PIR and UCHL1 was observed in the ciliated cells, judged from the colocalisation with acetylated tubulin. In contrast, no co-stainings were observed with MUC5AC, the marker for goblet cells, with the exception of club cells specific marker CC10, which colocalized with AKR1C1 and, to some degree with UCHL1 (Figure 3.13, 3.14).

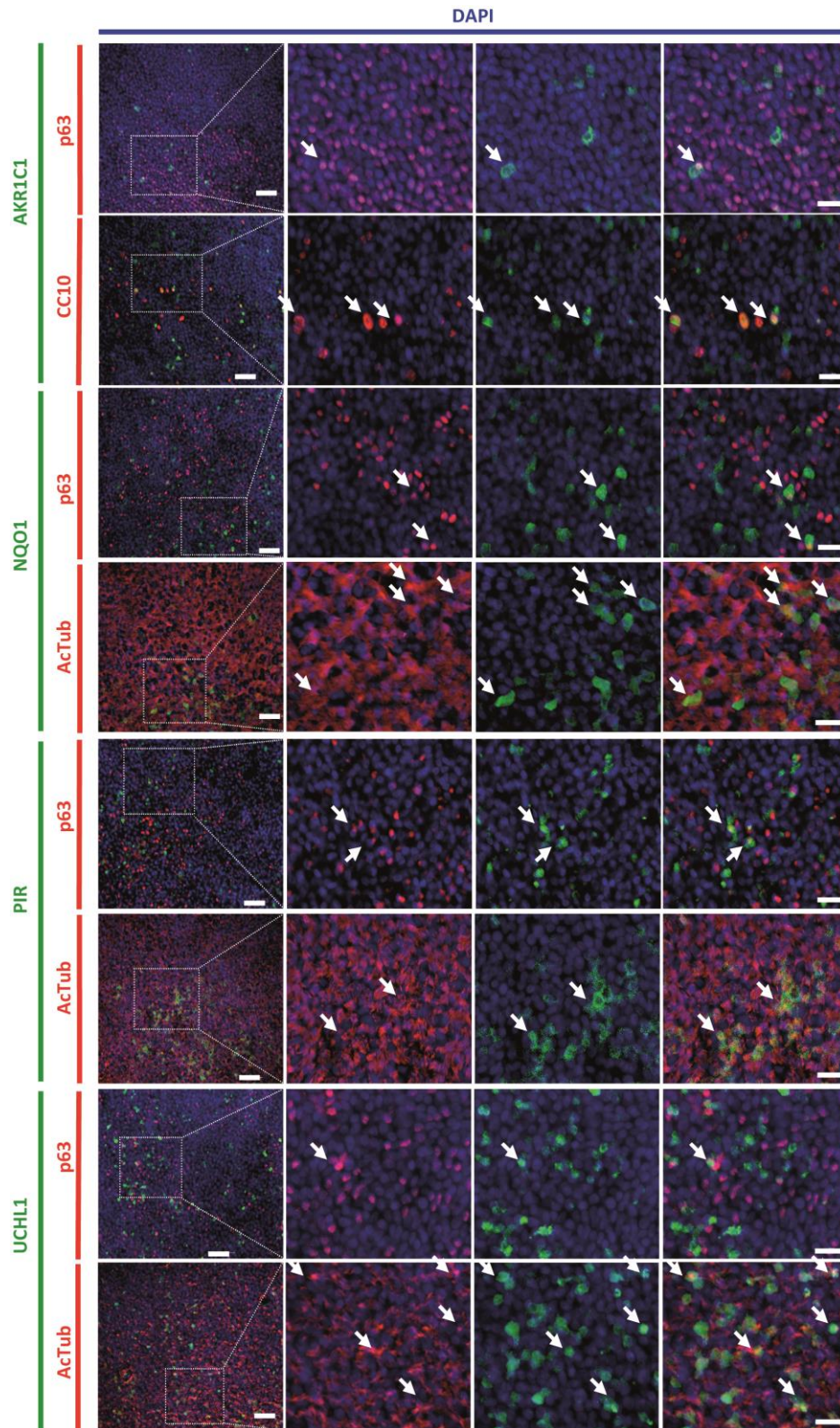


Figure 3.13. Analysis of immunofluorescent stainings revealed ciliated cells as strongest expressers of NQO1, PIR and UCHL1.

Representative immunofluorescent stainings (n=3 independent donors) of primary human bronchial epithelial cells (phBECs) which were exposed to whole cigarette smoke (wCS) demonstrate a low to moderate expression of all selected SERGs in basal cells (p63⁺ cells). In addition, NQO1, PIR, and UCHL1 revealed a strong co-expression in acTub⁺ cells, cell-type specific marker for ciliated cells. AKR1C1 was mainly expressed by CC10⁺ club cells. Scale bars, 50µm and 20µm. For co-stainings with cell-type-specific markers that showed no co-localization, the reader is referred to **Figure 3.14**. Results shown are based on n=3 independent donors. **Note: This figure and figure legends have been published in Mastalerz et al., AJP Lung, 2021.**

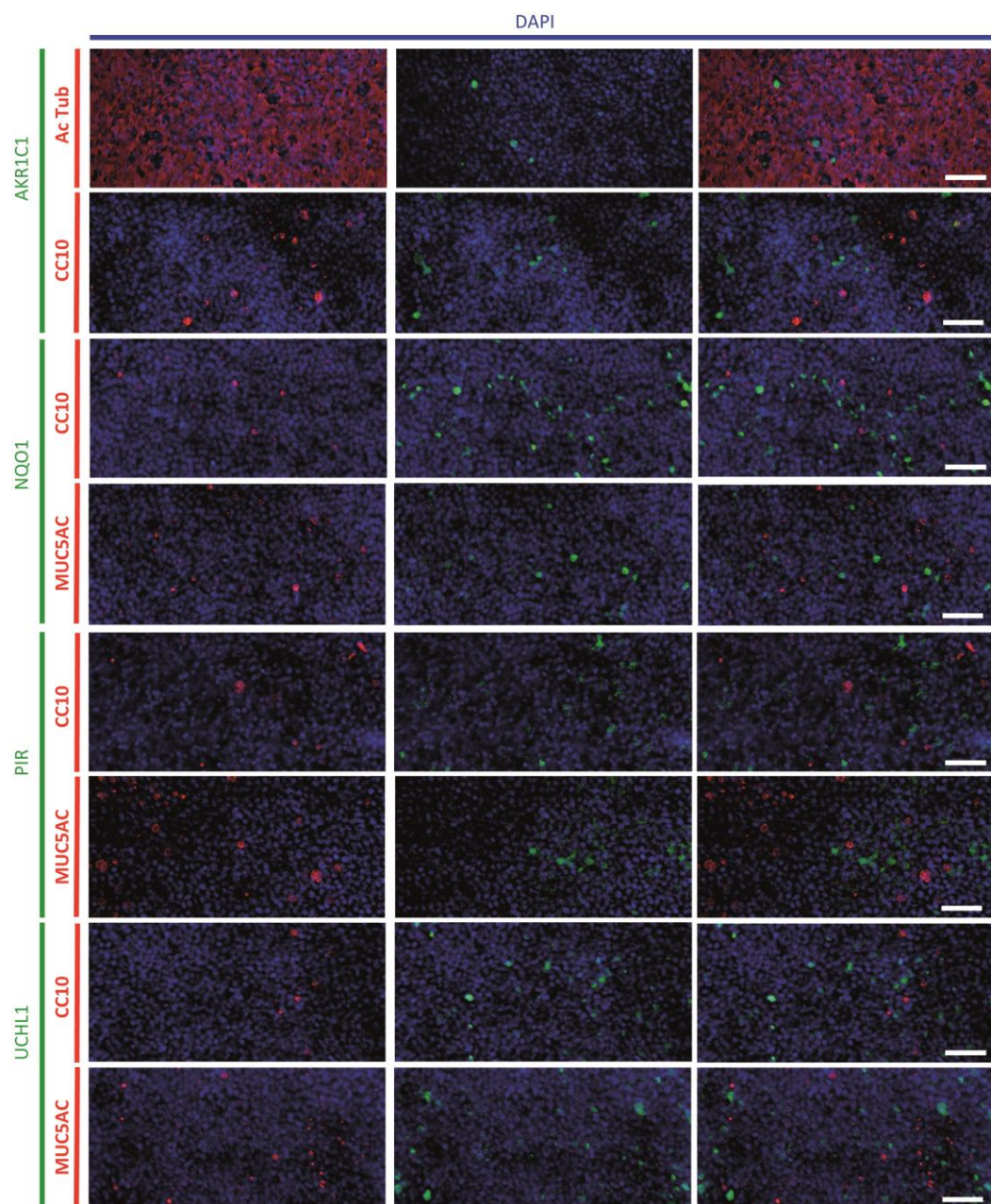


Figure 3.14. Immunofluorescent stainings club cell protein (CC10) revealed no co-expression with NQO1, PIR and UCHL1, while mucin 5AC (MUC5AC) did not co-expressed with all 4 assessed proteins.

Representative immunofluorescent stainings (n=3) of primary human bronchial epithelial cells (phBECs) that were exposed to the whole cigarette smoke (wCS), revealed that Ac Tub⁺ cells do not express of AKR1C1, only SERG among selected proteins. Club cell protein (CC10), a club cell-specific marker, did not colocalized with NQO1, PIR and UCHL1. Interestingly, no co-expression was observed in the goblet cells, demonstrated by co-stainings with mucin 5AC (MUC5AC). To provide a better overview of the stainings, pictures were enlarged by 25%. Scale bars, 50µm. **Note: This figure and figure legends have been published in Mastalerz et al., AJP Lung, 2021.**

3.2.6 CYP1A1 has lower basal expression in comparison to other aryl hydrocarbon receptor (AhR) responsive genes, which is unaffected by smoking history

Several donors used in the experiments had smoking history (Table 3.3), which prompted a question whether that affects baseline exposure of SERGs. According to cycle threshold values, there were no significant differences between ex- and never-smokers (Figure 3.15).

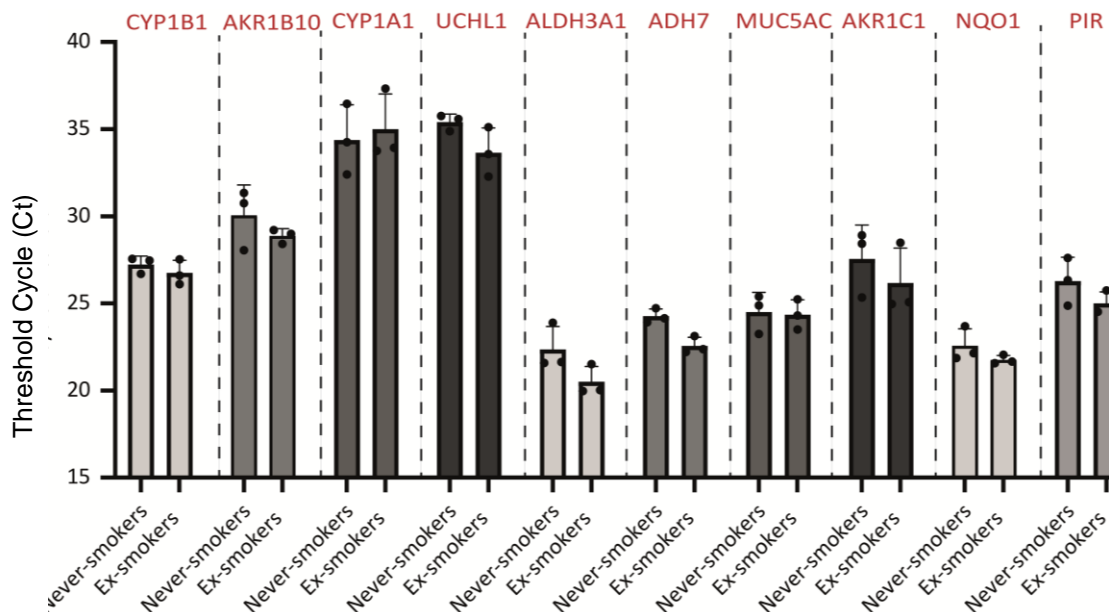


Figure 3.15. Threshold Cycles (Ct) comparison of basal expression of smoke exposure regulated genes (SERGs) between never-smokers and ex-smokers.

Ct values of all SERGs were pooled together from every donor (values from mock-treated fully differentiated phBECs only; n=6, 3 ex-smokers, 3 never-smokers, see also Table 3.3). For statistical analysis, Friedman test with Dunn’s correction for multiple comparisons was used. Results are shown as mean ± SD.

Note: This figure and figure legends have been published in Mastalerz et al., AJP Lung, 2021.

Additionally, *ALDH3A1*, *NQO1*, *CYP1A1* and *CYP1B1* are SERGs activated by AhR. Since *CYP1A1* was significantly upregulated in most of the models, the baseline expressions from all mock experiments were investigated. Interestingly, the constitutive expression of *CYP1A1* was significantly lower than other AhR-responsive genes (Figure 3.16).

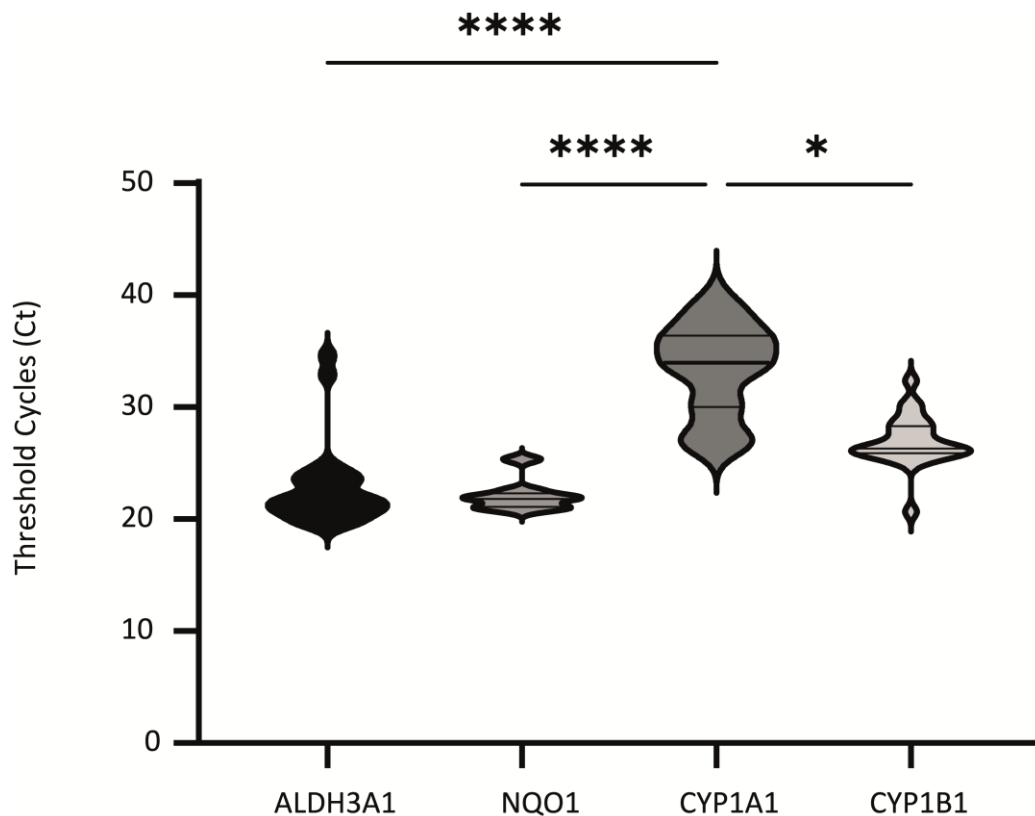


Figure 3.16. Threshold Cycles (Ct) comparison between AhR-responsive SERGs.

Ct values of appropriate genes were pooled together from all experiments (n=25). For statistical analysis Friedman test with Dunn's correction for multiple comparisons was used.

Note: This figure and figure legends have been published in Mastalerz et al., AJP Lung, 2021.

4. Chapter B – unbiased proteomic approach reveals regulators behind the response to CS

Parts of this study were done in collaboration with:

Elisabeth Dick from Claudia Staab-Weijnitz lab, who performed chronic basolateral differentiations with CSE exposure and sample collection.

Juliane Merl-Pham from Research Unit Protein Science at Helmholtz Center Munich, who carried out proteomic analysis, namely sample preparation, mass spectrometry measurements and label-free quantification.

Ronan le Gleut and Hannah Marchi from Core Facility Statistical Consulting at Helmholtz Zentrum, who performed statistical analysis.

4.1 Introduction

In the previous chapter, comparison of models based on mRNA expression levels showed drastic *in vitro* differences in terms of how smoke-induced phBECs gene expression is dependent on variables such as route of administration, concentration and duration of exposure, to name the few. Finding the model which exhibits physiologically relevant phBECs response to CS allowed for more in-depth *in vitro* studies, namely non-biased approaches such as proteomics. It is one of the most established methods for finding diagnostic markers, ligand candidates for new drugs or biological pathways to understand pathogenic or response mechanisms [250]. Chronic basolateral chronic exposure upregulated seven out of 10 SERGs. Other two models, namely acute wCS exposure and acute submerged basal cell CSE exposure, were successful in upregulation of expressions of only one target gene less. Chronic basolateral CSE exposure was chosen because it overall displayed most upregulation at more physiological fold changes of most SERGs than wCS and reflects fully differentiated epithelium, as opposed to submerged basal cells (Table 3.4) [197]. With this in mind, the chronic, basolateral CSE exposure was chosen for performing proteomic analysis on phBECs. Finally, for downstream analysis Ingenuity Pathway Analysis (IPA) was used, a suite of algorithms which infer casual molecular network and predict upstream regulators, biological functions, possible disease outcomes, and molecular networks [251].

4.2 Results

4.2.1 The proteome data reveals a number of significantly changed genes, prominently including a number of SERGs

Due to the unique set-up of the several time points collected during differentiation of the epithelium with or without treatment, additional statistical tests had to be performed. In collaboration with Ronan le Gleut and Hannah Marchi from Core Facility Statistical Consulting the most suitable strategy was employed. After assessing Wald test with Storey correction as most suitable test, data revealed significant differential expression of 186 out of 4861 proteins. Notably, six out of nine SERGs were also identified, namely CYP1B1, ALDH3A1, NQO1, AKR1B10, AKR1C1 and PIR (proteins ordered from highest upregulation of 2.36 fold change for CYP1B1, to PIR showing

only 0.3-fold change increase (Figure 4.1). CYP1A1 was not detected on the protein list. This data corresponds well with results in validation study (see Chapter 3) in two aspects. Firstly, all SERGs significantly upregulated in proteomic analysis were also present in RT-qPCR data (Figure 4.2). Secondly, the upregulation values for NQO1, ALDH3A1, AKR1B10, AKR1C1 were at best moderate, ranging from 0.95 for ALDH3A1 down to 0.65 for NQO1, which correlates to Western blots results, as they depicted only trends of upregulation and no drastic changes for these proteins.

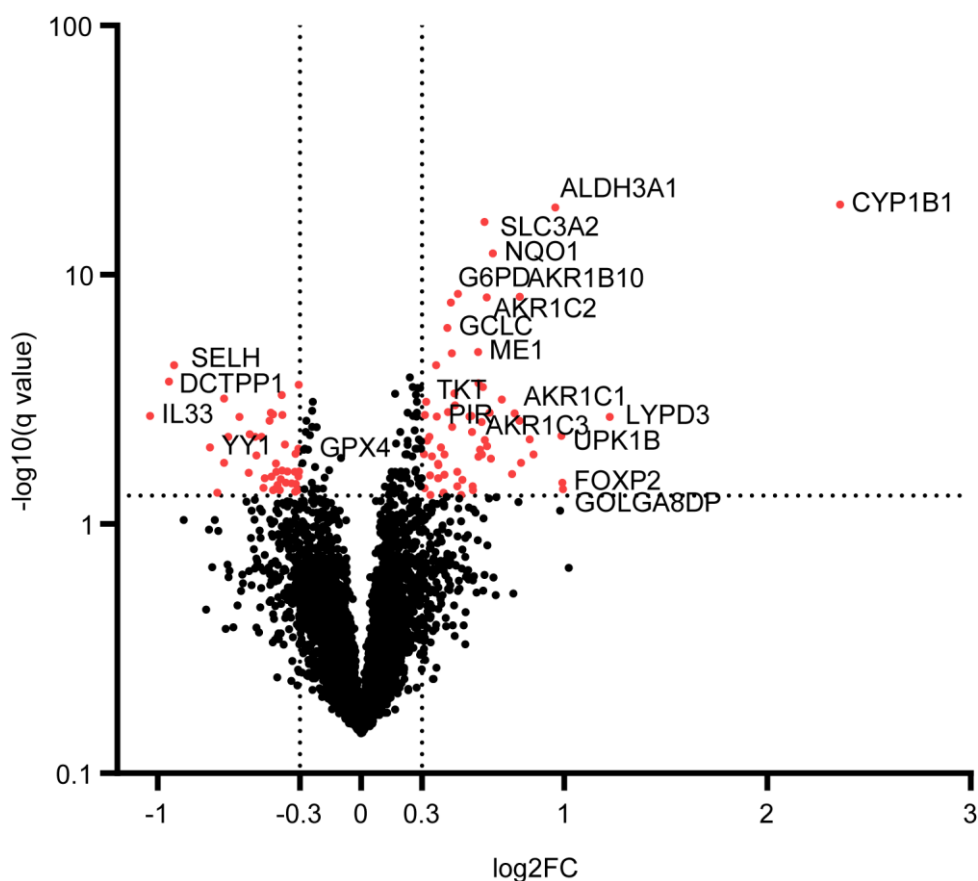


Figure 4.1. Overview of differentially altered proteins expressions in BALF proteomic data. $P < 0.05$, $\log_2FC > 0.3$.

4.2.2 Ingenuity Pathway Analysis confirms SERGs activating xenobiotic metabolism pathways, and indicates novel targets regulated by CS exposure

As described previously, IPA software from Qiagen (version 1.8.02) allows for in-depth bioinformatics analysis of expression datasets. With the consideration of previous biological findings, the interpretation can be greatly facilitated and contextualized. As IPA recommends having at least 300 differentially expressed targets, in order to curate proteomic dataset from chronic basolateral CSE treatment, cut offs used for q-value and fold change values were adjusted following recommendations of IPA and previous findings with less stringent conditions [252-254]. The final cut-offs used were 0.3 for \log_2FC and q value of 0.2. The data was then processed by IPA, looking for links and associations available in the literature. A set of different casual analytics algorithms

scored proteomic dataset and predicted a list of the upstream regulators (URA), the downstream effect analysis (DEA) and the pathway enrichment analysis. In agreement with previous results, the pathways responsible for xenobiotic metabolism, namely xenobiotic metabolism signaling pathways of AhR/PXR/CAR (aryl hydrocarbon receptor, pregnane X receptor and constitutive androstane receptor, respectively) were activated (Figure 4.2A), and downregulation of smoking-related sirtuin pathway activity. In concordance to these findings, among strongly activated predicted upstream regulators was nuclear factor, erythroid 2 like 2 (NFE2L2, also named Nrf2), transcription factor involved in regulation of several SERGs: AKR1C1, AKR1B10, NQO1 [255] and partially Nrf2-dependent CYP1A1 and CYP1B1 [256, 257]. Here, it is visualized with activated protein kinase AKT1, another transcription factor that overlaps with Nrf2 SERGs regulation [154, 258, 259] and phosphoinositide 3-kinases (PI3Ks) [154, 260] (Figure 4.2B).

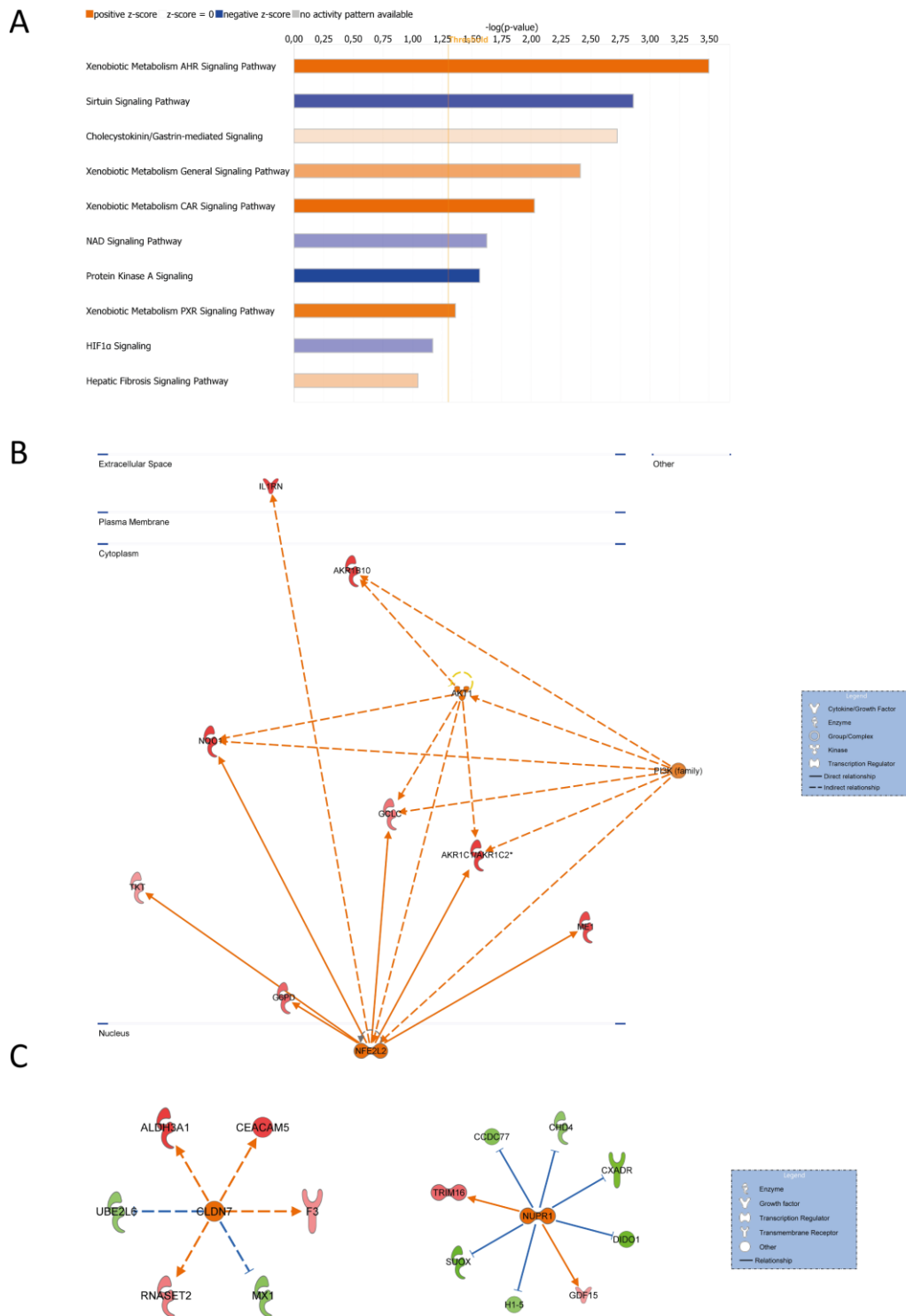


Figure 4.2. Ingenuity Pathway Analysis identified significantly altered pathways and predicted upstream regulators.

(A) Molecular pathways. P-value<0.05 z-score is determined by leveraging information about regulation directionality. It assesses consistency pattern given by fed data and compares against random model. (B) Upstream regulators associated with regulation of xenobiotic metabolic pathways, including SERGs AKR1C1, AKR1B10 and NQO1, segregated by cellular compartments (C) Strongly activated upstream

regulators outside direct xenobiotic response. In each network one node represents a protein and its shape corresponds to its function, as explained in the legend.

Interestingly, among other predictions were also Claudin-7 (CLDN7), and nuclear protein 1 (NUPR1) (Figure 4.2C), which has not been associated with smoking and bronchial epithelial cells in the literature before. Summary of highly activated predicted upstream regulators is visualized in Figure 4.3 and listed in Table 4.1. Downstream effect analysis did not show any substantial predictions.

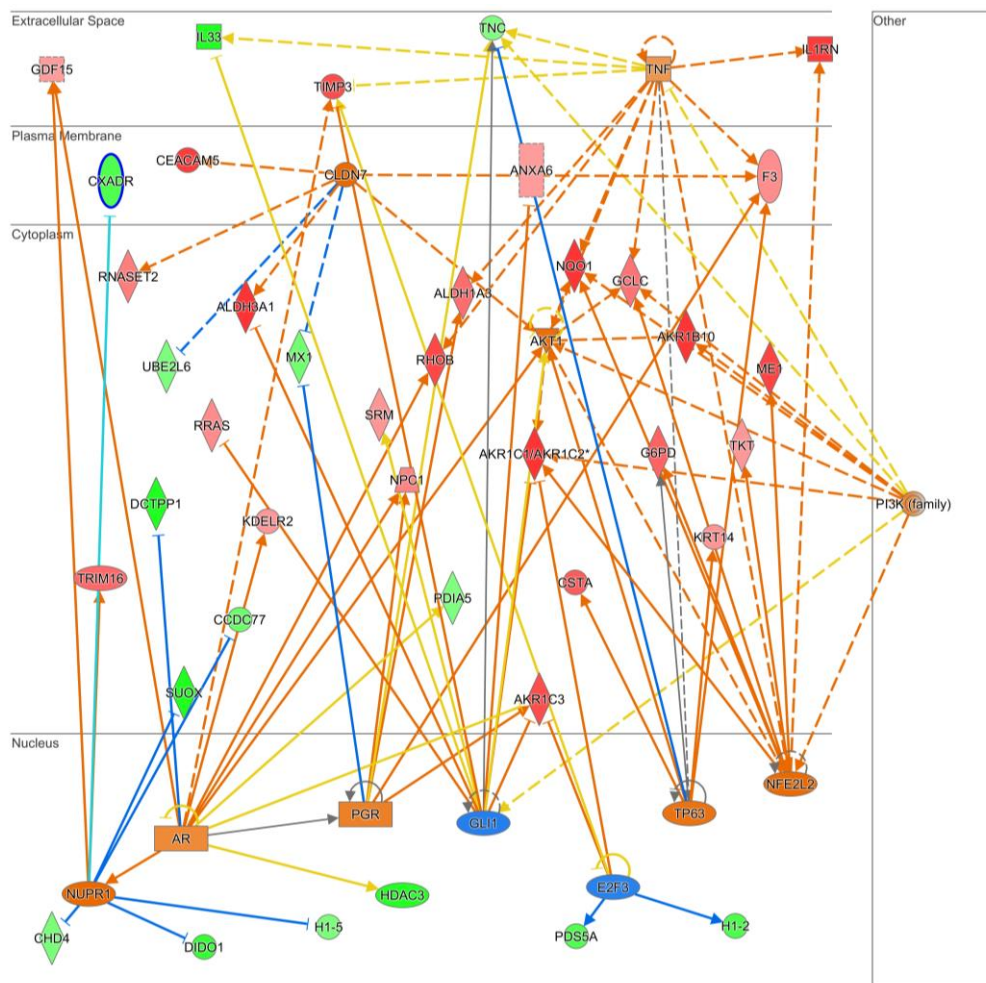


Figure 4.3. Overview of predicted upstream regulators activity.

Table 4.1. Upstream regulators. Z-score>1, p-value<0.05.

Upstream Regulator	Molecule Type	Predicted Activation State	Activation z-score	p-value of overlap	Target Molecules in dataset
NUPR1	transcription regulator	Activated	2,828	3,73E-02	CCDC77,CHD4,CXADR,DIDO1,GDF15,H1-5,SUOX,TRIM16
NFE2L2	transcription regulator	Activated	2,573	4,15E-07	AKR1C1/AKR1C2,G6PD,GCLC,IL1RN,ME1,NQO1,TKT
CLDN7	other	Activated	2,449	3,40E-04	ALDH3A1,CEA-CAM5,F3,MX1,RNASET2,UBE2L6
AKT1	kinase	Activated	2,000	1,61E-04	AKR1B10,AKR1C1/AKR1C2,GCLC, NQO1
TP63	transcription regulator	Activated	1,835	4,92E-02	CSTA,F3,G6PD,KRT14,TNC
PGR	ligand-dependent nuclear receptor	Activated	1,408	1,83E-03	AKR1C3,ALDH1A3,F3,MX1,NPC1,TNC
PI3K (family)	group	Activated	1,342	1,08E-03	AKR1B10,AKR1C1/AKR1C2,GCLC,NQO1,TNC
AR	ligand-dependent nuclear receptor	Activated	1,226	5,87E-05	AKR1C3,DCTPP1,GDF15,HDAC3,KDEL2,NPC1,PDIA5,RHOB,TIMP3
TNF	cytokine	Activated	1,019	1,19E-02	ALDH1A3,F3,GCLC,IL1RN,IL33,NQO1,RHOB,TIMP3,TNC
E2F3	transcription regulator	Inhibited	-1,387	1,58E-03	AKR1C1/AKR1C2,AKR1C3,H1-2,PDS5A,TIMP3
GLI1	transcription regulator	Inhibited	-1,463	6,99E-03	AKR1C1/AKR1C2,AKR1C3,ALDH3A1,ANXA6,IL33,RRAS,SRM,TIMP3,TNC

5. Chapter C – How smoking and disease status affects CS response – *in vivo* and *in vitro* comparison

Parts of the study presented in this chapter were made in collaboration with Herbert Schiller and Christopher Mayr.

5.1 Introduction

CS has a multifactorial, detrimental effect on human lungs. Along with the findings presented in Chapter B, a wide range of transcriptomic and the epigenomic studies already reported distinct smoke-induced gene expression signatures, altered signaling pathways and DNA methylations on systemic level [261-263], within lung tissue [234-237] and when focusing on airways epithelium [110, 201, 228, 229, 264-268]. Interestingly, some of the altered genes exhibited transient nature of the expression changes, while others were persistent and lasted even after individuals stopped smoking [114, 238] (Figure 5.1). Bronchoalveolar lavage (BALF) proteomic findings kindly shared by Herbert Schiller and colleagues indicate some of these changes on protein level. Basic metrics of smoking cohort used in this study are listed in Table 5.1. Four proteins, namely NQO1, TSMB4X, ARPC2 and PSMB2 has shown to have signal retention, even after cessation of smoking.

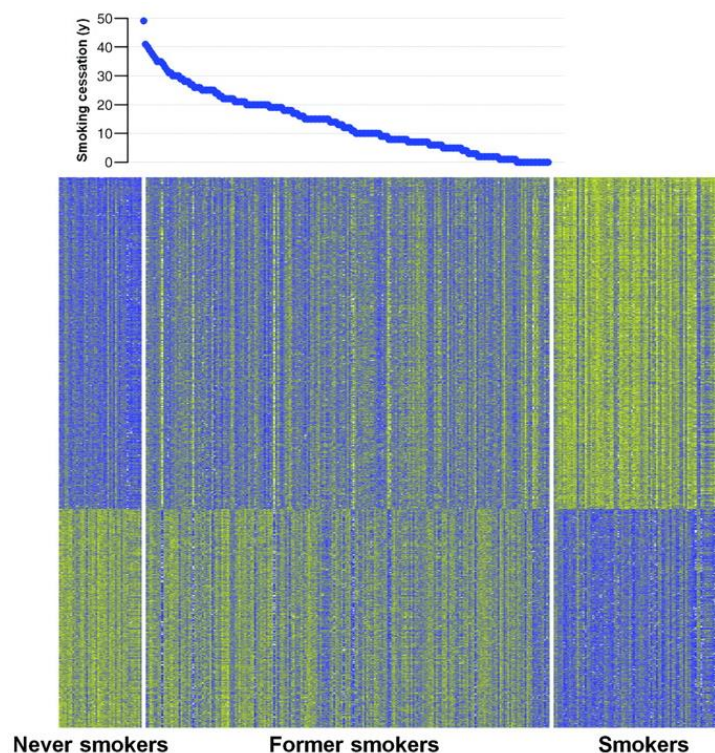


Figure 5.1. Transcriptomic molecular signature comparison between never smokers, former smokers and active smokers.

The heatmap depicts distinct alterations caused by smoking, including signature after smoking cessation. Low expression is shown in blue, while high expression in yellow. Former smokers are ordered by the smoking cessation period as depicted on the top graph. **Figure was adapted from [238].**

Table 5.1. Basic metrics of patients from smoking BALF cohort. FVC – Forced vital capacity, DLCO – diffusing capacity of the lungs for carbon monoxide . Data provided by Herbert Schiller.

Characteristics	Never smokers	Ex-smokers	Active smokers	p-value
Age	58.8 ±13.6	65.9 ±10.9	46.9 ±14.5	<0.0001
Pack years	n/a	30.3 ±23.9	30.3 ±21.4	<0.0001
FVC (%)	79.6 ±18.0	81.1 ±20.7	76.8 ±21.9	0.76
DLCO (%)	63.5 ±21.3	53.6 ±21.3	59.9 ±21.8	0.16

Here, while taking advantage of the access to smoking history of donors from which primary bronchial epithelial cells were collected and differentiated, the indicated changes were further assessed in *in vitro* data. Donors characteristics are presented in Table 5.2.

Table 5.2. Basic metrics and smoking status of donors of phBECs. Note: Parts of this table and table description have been published in Mastalerz et al., AJP Lung, 2021.

Donor No.	Age	Gender	Smoking status	Smoking cessation period	Pack years
1	72	W	Never-smoker	n/a	n/a
2	80	M	Never-smoker	n/a	n/a
3	55	M	Ex-smoker	5-10 years	40-60
4	56	M	Ex-smoker	<5 years	40-60
5	62	M	Ex-smoker	<5 years	40-60
6	61	W	Ex-smoker	5-10 years	

7	73	M	Ex-smoker	>20 years	21-40
8	80	W	Ex-smoker	>20 years	21-40
9	66	W	Ex-smoker	10-20 years	21-40
10	52	M	Current smoker	n/a	40-60
11	53	M	Current smoker	n/a	40-60

5.2 Results

5.2.1 Persistent and transient changes in smoke-induced proteins upregulations are not recapitulated in differentiated primary bronchial epithelial cells

Expression of five out of 10 SERGs that were substantially changed in BALF proteomic dataset, were compared to baseline gene expression of fully differentiated primary bronchial epithelial cells (Figure 5.2A). Label-free quantitation (LFQ) signal intensities analysis shows also-keto reductases AKR1C1 and ARK1B10, and also ALDH3A1 proteins exhibited most significant changes when compared to two other SERGs, PIR and UCHL1. The transient changes were confirmed by identifying no upregulation of these proteins in ex-smokers. Interestingly, same changes were not recapitulated in RT-qPCR analysis of the baseline expression *in vitro*. The analyzed samples consisted of two never smokers, eight ex-smokers and two current smokers. Interestingly, this data suggests downregulation trends in expression of all targets with the exception of *AKR1C1* and *ALDH3A1*. BALF dataset analysis for smoke-induced persistent changes showed four proteins, namely NQO1, TMSB4X, ARPC2 and PSMB2, to have significant or clear trends in expression upregulation retained upon smoking cessation (Figure 5.2B). Of note, a partially reversible upregulation was observed for one of the SERGs, NQO1. In a stark contrast, *in vitro* transcript levels were shown to be largely downregulated in current and ex-smokers when compared to mRNA levels in never smokers.

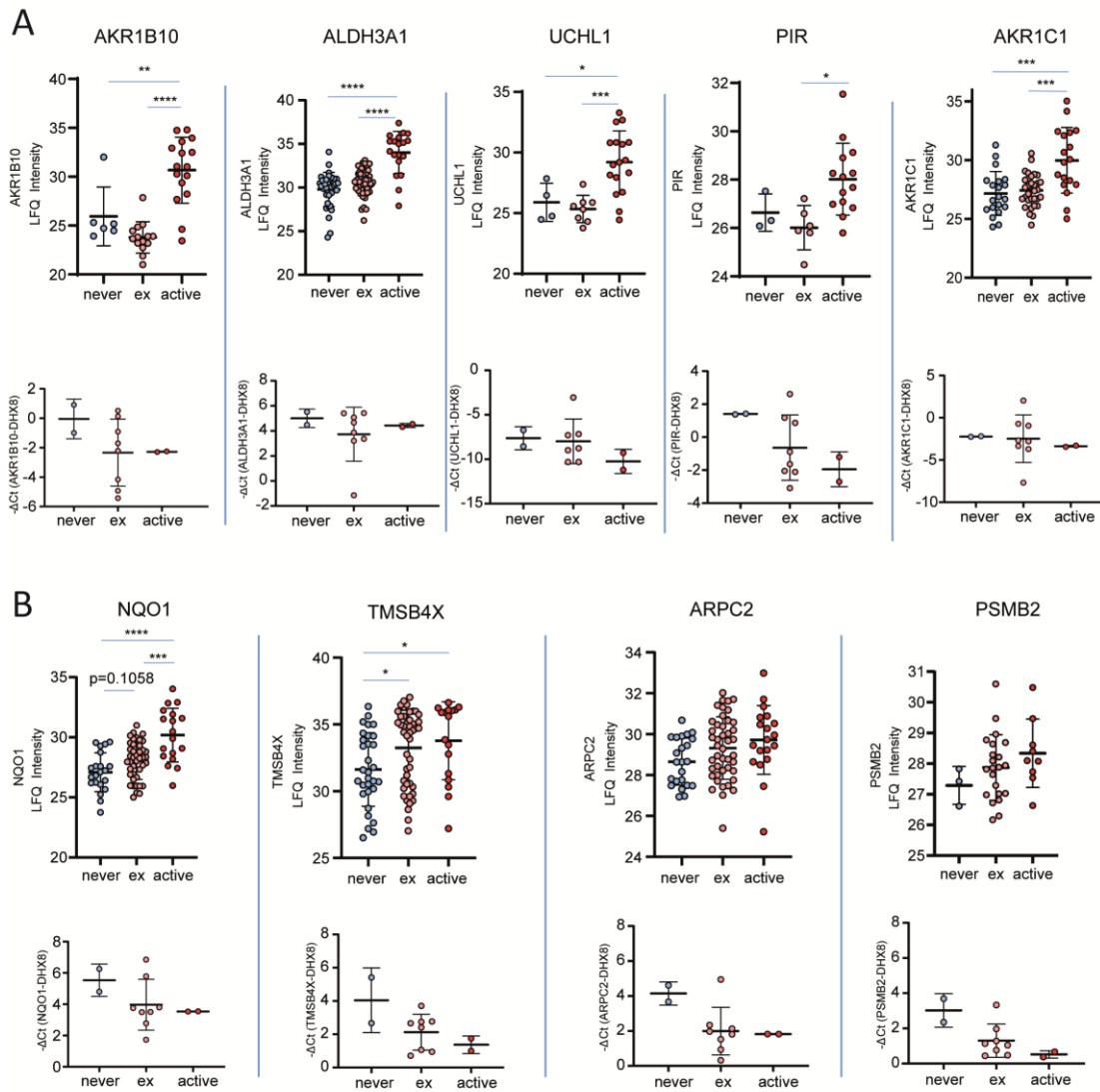


Figure 5.2. *In vitro* experiments indicate neither transience nor persistence reported in *in vivo* bronchoalveolar lavage (BALF) dataset.

(A) According to RT-qPCR data, basolateral expression in differentiated primary human bronchial epithelial cells smoke-induced transiently upregulated genes remain stable or show downregulation trends as compared to BALF dataset. **(B)** Similarly to transient changes, the persistently altered protein expressions or the trends for protein expressions upregulations were not recapitulated in a basal gene expression in pHBEs, showing substantial downregulation trends, similarly *in vitro* data on the transiently changed genes. BALF data is depicted as label-free quantitation (LFQ) intensities. RT-qPCR is depicted as difference of between cycle threshold (ΔC_t) of target gene and ΔC_t of housekeeper gene. As a housekeeper gene DEAH-Box Helicase 8 (DHX8) was used. Never – Never smokers, ex – former smokers, active – current smokers. **BALF dataset was kindly shared by Herbert Schiller and analyzed by Claudia Staab-Wejnitz.**

6. Discussion

Tobacco is arguably the most prevalent intoxicant of a natural origin preferred by humans, that generated a profound social, health and economic impact. The expansion of tobacco was dictated mainly by the Western expansionism, dating back to XV century. Now, tobacco is rooted deeply in traditional practices and hence detrimental to hundreds of people worldwide [269]. *In vitro* research gives a valuable insight into the molecular responses to cigarette smoke in cells populating the airway epithelium.

In chapter A, genes collectively called smoke-related references genes (SERGs, Table 3.2) were carefully selected from the available transcriptomic datasets of differentially expressed genes in smokers versus never smokers, namely GSE994 [114], GSE4498 [231], GSE7895 [270], GSE20257 [232], and GSE52237 [233]. SERGs allowed for the assessment of physiological relevance of the human *in vitro* CS exposure models. Primary human epithelial cells were previously reported to have a physiologically relevant cell composition, and they were used for adequate exposures. Six different CS exposure models were tested (Table 3.1): Acute submerged basal cell CSE exposure (Figure 3.4, Figure 3.5), chronic basolateral exposure of differentiating phBECs with CSE (Figure 3.6), acute apical exposure of differentiated phBECs with CSE (Figure 3.10, Figure 3.11), acute basolateral exposure of differentiated phBECs with CSE (Figure 3.12), and short acute apical exposure of differentiated phBECs with CSE in direct comparison with apical exposure to wCS (Figure 3.8).

The investigation revealed drastic differences between models in response to CS, however none of the models was able to upregulate 10 out of 10 SERGs. Interestingly, three substantially different models were able to significantly upregulate more than six SERGs. Acute basal cells submerged CSE exposure and wCS exposure performed on ALICE-Smoke upregulated expression of six genes, while chronic basolateral CSE exposure of differentiating phBECs significantly increased the expression of seven SERGs. On the other hand, rest of the models does not hold more than two SERGs significantly upregulated, which renders them as not physiologically relevant, as far as *in vivo* transcriptomic expression profile is concerned, despite using comparable cell-delivered doses to other models.

As explained in Chapter 1.3, current state-of-the-art in the CS exposures are wCS, which requires an advanced apparatus available only in few laboratories, while others use primarily liquid-based exposure types e.g. CSE [187-190]. Neither number of cigarettes nor volume of the medium used for the CSE generation are standardized, and usually a final working concentration is based mainly on cytotoxicity results. That makes it challenging to reproduce results and maintain consistency between laboratories [118, 271-273]. On the other hand, in wCS exposures, the cell-delivered dose of smoke particulates is rarely assessed [222, 223] or, similarly to CSE exposures, the selection criteria is based on the cytotoxicity measurements [224, 225]. The study in Chapter A successfully determined the cell-delivered CS dose in gaseous and liquid based exposure settings. That allowed for a direct dose comparison between models and also helped in an assessment of physiological relevance of investigated models, thanks to estimations of theoretical dose of CS *in vivo*. Approximately 82% of a total smoke mass of about 10 mg per cigarette [274] deposits on the lung epithelium (both bronchial and alveolar), which surface area ranges between 70-140 m² [275, 276]. Importantly, as explained in Chapter 1.1, deposition patterns throughout conducting airways are varied and correlate with locations of pathologically changed tissue in diseases such as lung cancers [277-279]. Highest deposition areas have been reported to be

around carinas of bifurcations, where up to 100-fold higher doses of CS particulates can be deposited, thus making them more vulnerable to injurious agents than the other epithelial regions [280]. With simple calculations, a theoretical maximal CS deposition per surface area can be estimated to average between 0.59 – 1.17 $\mu\text{g}/\text{cm}^2$ per cigarette, in areas of higher exposure such as the aforementioned carinas of bifurcations. Comparison between doses used in *in vitro* experimentations (6 – 100 $\mu\text{g}/\text{cm}^2$) and *in vivo* highest theoretical dose deposited in the carinas of bifurcations revealed about 10 to 100-fold higher dose used in *in vitro* settings (Table 3.1). One can assume that this translates to a cumulative dose of 10-100 cigarettes during 24 h exposure, which is not far from *in vivo* conditions among heavy smokers [281]. In direct comparison between wCS and CSE, an incubation of 5 min with CSE was used (Figure 3.8A) in efforts to replicate the duration of wCS exposure time. Importantly, cells were not washed after these exposures, leaving the remained CSE mixture and wCS particles on ALI. Since it is possible that the cells were not affected by the CSE's total dose, an approximately 8-fold higher dose was used, which might still allow for comparing both settings. To address that issue from another angle, in another setting 200 μl of CSE was added apically and left for 24 h incubation, in the dose range comparable with wCS exposure. This scenario may seem more appropriate, due to maintained CSE exposure, however in this case the ALI is compromised for an extended period of time, rendering this scenario as less physiological, which can cause unexpected molecular responses. Interestingly, both CSE exposures had drastically weaker responses when compared to wCS, failing to upregulate most of the SERGs (Figure 3.10B, Figure 3.11B). As mentioned in chapter A, there are drastic discrepancies between expression profiles of smokers, ex- and never-smokers [114, 231-233, 270]. Based on transcriptomic datasets found in the literature, 10 genes upregulated in smokers were selected, in efforts to accurately recapitulate expression change patterns reported *in vivo*, which then can be used for testing *in vitro* CS exposure models. The main selection criteria were consistent and substantial smoke-induced upregulations across all the analyzed datasets (SERGs, Table 3.2). Next, the CSE models used for comparisons were frequently used within the lung research [118, 190, 193, 212, 282, 283]. wCS was also chosen to demonstrate how physiologically relevant models relate to liquid phase exposures. Notably, some of the donors had smoking history (Table 3.3). However, an assessed basal expression of all SERGs yielded no differences between ex- and never-smokers (Figure 3.15).

The cell composition, molecular pathways and gene expression are changed drastically by the exposure to CS in *in vivo* [284, 285] and *in vitro* [118, 190, 282] experiments. However, how different models activate deranged pathways has not been studied extensively. The concentrations or cell-delivered doses were usually based on *CYP1A1* expression levels [118, 286], a xenobiotic enzyme, well known to be induced by PAHs present in CS, such as the before mentioned benzo[a]pyrene and tetrachlorodibenzo-p-dioxin [287]. PAHs cause arylhydrocarbon receptor (AhR) heterodimerization with aryl hydrocarbon nuclear translocator (ARNT), which subsequently translocates into nucleus and binds to xenobiotic responsive element (XRE), the promoter of *CYP1A1*, and initiates the transcription [288]. Among CSE models, *CYP1A1* genes were the only a significant upregulation that was visible for acute apical and chronic basolateral exposures. Interestingly, that was not the case in 40% CSE 5 min apical exposure, suggesting that 5 min exposure to full intended dose was not sufficient to exhibit any response. It proves *CYP1A1* expression to be a robust indicator of exposure to PAHs, however it is also clear that *CYP1A1* measurements alone are not an accurate measure of the whole CS response. Among 10 SERGs, there were more AhR-induced genes, namely *CYP1B1*, *NQO1*, and *ALDH3A1* [289, 290] (Table

3.2). The increase of their expression was not as drastic as *CYP1A1*, which could be due to its much lower basal expression (Figure 3.16). Therefore it is suggested that *CYP1A1* can cause much higher increase when compared to others, constitutively higher expressed AhR-induced genes. Erythroid 2 related factor 2 (NFE2L2 or Nrf2) is a nuclear factor crucial for activating resistance to oxidative stress [291] by inducing a number of proteins included in SERGs list: AKR1B10 and AKR1C1 [255, 292, 293], ADH7 [294, 295], ALDH3A1 [294], PIR [296], NQO1 [294, 297, 298], possibly also UCHL1 [299]. Marker of the AhR activation and oxidative stress, *CYP1A1*, should in turn activate almost all the SERGs, however that is not the case in almost all exposures. One can assume that the *CYP1A1* upregulation was not sufficient in these exposures, which certainly was not the case in wCS and chronic CSE exposures. In acute submerged basal cell CSE exposure *CYP1A1* induction was lower in comparison, accompanied however by other Nrf2-regulated SERGs, showing *CYP1A1*-activated ROS production in catalytic cycle [300] is not sufficient for Nrf2 signalling activation (Table 3.4).

Interestingly, *MUC5AC*, an important constituent of airway mucus, and *ADH7*, the NAD-dependant oxidation agent and regulator of retinol metabolism [301] were neither upregulated nor yielded their significant downregulation in any of the exposure models, nor Previous reports showed an increased number of *MUC5AC*-positive cells in the chronic basolateral 5% CSE exposure in phBECs, which was, interestingly enough, not accompanied by *MUC5AC* increased expression [118]. Elsewhere, somewhat contradictory *in vitro* results showed A549 CSE-treated cells to have moderate *MUC5AC* transcript increase, but surprisingly also a significant downregulation in the airway cells [302, 303]. Apart from obvious differences in cell material used in experiments, the reported differences might be due to dissimilar media composition [304], which was required for use in accurate and successful differentiation of basal cells into epithelium resembling cell composition seen *in vivo*. It is unclear how this could affect *MUC5AC* expression, yet *ADH7* could be affected by the presence of retinoic acid in the differentiation media [305]. *ADH1C*, another member of dehydrogenase family [306], has been reported to be regulated by the retinoic acid [307, 308]. While whether retinoic acid affects *ADH7* activity or not remains unclear, it is possible that the medium constituents mask effects seen *in vivo*. Furthermore, lack of other cell types present in lungs, such as bronchial macrophages, fibroblasts, neuroendocrine, serous or tuft cells could also lead no effect of CS on the expression of aforementioned genes and hence can account for limitations of investigated *in vitro* models.

As shown in the results section, three very different exposure models, namely acute of basal submerged, and basolateral chronic CSE treatments and acute wCS exposure of differentiated phBECs, were similarly effective in significant upregulation of selected SERGs, specifically six to seven SERGs out of 10 (Figures 3.4, 3.6 and 3.8). Of note, the most drastic upregulations were seen in wCS exposure, possibly dictated by a full range of smoke constituents that wCS contains, as opposed to CSE, which has been identified to contain only its hydrophilic components [309]. The final assessment was performed on the transcript level, just as selection of SERGs was made (Table 3.4). The protein upregulation levels of chosen SERGs were not as pronounced however, in comparison with transcript differences. This was in line with some literature reports, for both CSE [118] and wCS [223]. Among all of the CSE models used in the literature and investigated in Chapter A, submerged CSE exposure of basal cells [190, 282] and chronic basolateral exposure of differentiating phBECs [118] are among the three best *in vitro* models assessed. TEER is a measure of cell adhesion and epithelial cell junctions' integrity [224]. Previously, the epithelial integrity of differentiating cells measured by TEER was affected by 5% CSE basolateral exposure

[118]. Here, this has not been replicated (Figure 3.7). Furthermore, the same goes to changes in cell composition of bronchial epithelium found in the same study, as before mentioned study showed goblet cell hyperplasia. These discrepancies can be explained by a different medium used than in previous study [118], where for expansion Bronchial Epithelial Cell Growth (BEGM) from Lonza was used, instead of PneumaCult™ Ex-Plus (Stemcell). It has recently been reported that different differentiation media can affect bronchial epithelial cells' characteristics [310]. Even though the differentiation medium was the same between both discussed basolateral CSE exposures, the different expansion media could have had persisting effect on later stages of cell culture and exposures to smoke extracts. Additionally, the primary basal cells used in both studies have a different source - samples provided by CPC BioArchive are coming from lung tumor patients, from histologically unchanged regions, from non- or ex-smokers, while two biological replicates used by Schamberger and her colleagues were purchased from Lonza, from healthy, self-reported never-smokers, and performed on them several independent differentiations [118]. Therefore, the current set-up is more relevant due to increased number of biological replicates, but also introduces more variability, which naturally makes it challenging to create more statistically significant outcomes.

Clearly, acute wCS exposure performed on ALICE-Smoke has highest sensitivity, having magnitudes higher upregulations for some SERGs (i.e. *CYP1A1*, *CYP1B1*, *UCHL1*) than other two CSE exposures and differences found in *in vivo* transcriptomic data (Figure 3.8B). That said, both CSE models can be proposed as physiologically relevant models, since the fold changes reasonably well resemble *in vivo* changes (Table 3.4). Considering the wCS models might be less available, due to their sophisticated set-up or high price of commercially available models such as Vitro-Cell®, submerged acute basal cell CSE represent an easy-to-perform and time-efficient test environment, when research question does not necessitate investigating specific response in specific cell types, or alternatively, focuses on main bronchial epithelium progenitor cells. On the other hand, chronic CSE basolateral exposure can additionally be used for addressing changes in cell composition, specific-cell-type responses and cell-to-cell signalling between different cell types.

Interestingly, two models that had the most drastic response among CSE set-ups, had basal cells directly in contact with the CSE. In sharp contrast, acute CSE exposures (Table 3.4) showed barely any differences in expression. Lack of expression in the response to CSE added apically was observed in chronic pilot exposures (data not shown). That led to speculation over basal cells being main drivers of the CSE-related bronchial epithelium response. To address that, selected SERGs, namely *AKR1C1*, *PIRIN*, *NQO1* and *UCHL1* were assessed in immunofluorescence co-stainings with main cell type specific markers after exposing differentiated epithelium to wCS using ALICE-Smoke system, which was shown to be the most sensitive set-up (Figure 3.8D). Colocalisation of p63, a specific basal cell marker, proved involvement of the selected SERGs in a CS response, however much more frequent co-localisations were observed with the other cell-type specific markers. Majority of *NQO1*, *PIR* and *UCHL1* were expressed by ciliated cells, while *AKR1C1* was mainly localised in club cells (Figure 3.13). This is in line with the previous reports, where *NQO1* overexpression in ciliated and basal cells was linked to speculate that it has a protective role for cilia against noxious and carcinogenic agents [311, 312]. In similar fashion, *UCHL1* has been reported to be expressed mostly in the same cell types as *NQO1* [313], where it takes part in ubiquitin hydrolysis homeostasis, proteostasis and apopto-

sis [314, 315]. Surprisingly, this data indicates ciliated cells to be the main drivers of their expression in bronchial epithelium [228]. Club cells, which are thought to be main contributors to biotransformation of noxious agents, by expressing detoxification enzymes, such as CYP2F family [19]. Co-stainings clearly show however, that only AKR1C1 is predominantly co-expressed with CC10, a specific marker for club cells. *AKR1C1* along with *AKR1C2* are aldo-keto reductases, highly upregulated in smokers, converting a range of aldehydes and ketones found in CS into corresponding alcohols [316]. PIR was previously associated with the proapoptotic response in a bronchial epithelium upon CS exposure [266], which implies pirin could be involved in the regulated cell death mechanisms in ciliated cells upon cigarette smoke-related injury. Taken together, these results show more specialized cells than main progenitors of bronchial epithelium to be responsible for CS-related molecular response. Basal cells however do exhibit some potential of xenobiotic metabolism, which could have a decisive role in e.g. acute lung injury, where depletion of luminal cell types may increase basal cells' involvement in xenobiotic metabolism and oxidative stress response.

Overall, this study provides the unique insight into how comparable doses of CSE and wCS differ in triggering responses in bronchial epithelial cells. Surprisingly, changes in different response efficacy varied drastically between models. In the direct comparison, short acute 40% apical exposure failed to upregulate any of the SERGs expression (including highly robust *CYP1A1*), while wCS exposure was among the most efficacious models (Figure 3.8). There could be several reasons for that. Previous reports have shown that CSE constituents are only hydrophilic and correspond to less than 40% of total CS mass [317]. This could explain the much more drastic response with wCS, since AhR-Nrf2 signalling is activated mostly by hydrophobic compounds, which are not retained during CSE generation [318]. Furthermore, CSE toxicants may be scavenged by free thiols and amines present in the cell culture media. Despite previous reports showing that oxidation [190] and cytotoxicity measurements [319] is retained even after using CSE that was stored earlier at -80°C, there is a possibility it affects some of the CSE constituents. PAHs, strong SERGs inducing molecules are also highly hydrophobic, which suggests much lower concentrations of them in CSE. Additionally, it is known that the majority of particles larger than 10 µm deposits in upper airways, while the size of cell-delivered particles in ALICE-Smoke requires further investigation. Taking these arguments into consideration, it is quite remarkable that some CSE-based modalities still could match response robustness of wCS exposure.

Thorough CS exposure validation allowed for investigation into differentially regulated pathways using best exposure models. After performing chronic basolateral CSE exposure, samples underwent proteomic analysis, a robust non-biased approach discovering pathophysiological mechanisms, previously successfully employed in cigarette exposure studies [320, 321]. Statistical analysis revealed significantly upregulated six out of 9 SERGs (*CYP1A1* was not measured in the proteomic analysis), namely *CYP1B1*, *ALDH3A1*, *NQO1*, *AKR1B10*, *AKR1C1* and *PIR*, which were remarkably included the same targets upregulated on the transcript level, including *AKR1C1* (Figure 4.1), which had also upregulation trends in RT-qPCR results (Figure 3.8), which therefore confirmed the expression profile. Again, changes on protein level were not as pronounced as those seen on transcript level, which was shown also in protein expression of selected SERGs in validation study and in previous studies with CSE exposure [118]. Ingenuity Pathway analysis revealed activation of several general xenobiotic metabolizing pathways, including previously discussed AhR pathway, but also to some extent PXR- and CAR-dependent xenobiotic pathways,

also co-regulated by AhR (Figure 4.2A). PXR is a nuclear receptor called master xenobiotic receptor, has a role in xenobiotic sensing, but also in inflammation response, cell proliferation and motility [322], while CAR, also a nuclear receptor, has been linked to xenobiotic and drug metabolism [323]. After activation of both receptors by steroids and xenobiotics present in cigarette smoke [324, 325], and after PXR-PXR or CYR-PXR heterodimerization, nuclear translocation, they bind to promoters of drug and xenobiotic metabolizing enzymes from CYP superfamily and transporters [326]. Sirtuin is involved in another important pathway linked to smoking that has been previously reported to be deactivated upon cigarette smoking in bronchial airways [327] and in *in vivo* mouse models [328]. Notably, these findings further reinforce both basolateral chronic exposure model and the use of CSE as physiologically relevant. IPA gives unique insight into predicting regulatory mechanisms responsible for differentially activated targets. Here, complementary to previous results, regulators of xenobiotic metabolizing enzymes (Nrf2, AKT1 and PI3K) were predicted to be highly activated (Figure 4.2B, Table 4.1). Interestingly, claudin-7, key component of epithelial cells junctions, regulating paracellular permeability and correlated with lung carcinoma was activated [329], therefore reporting for the first time association between smoking and claudin 7 expression in primary cells. Besides, nuclear protein 1 (NUPR1), a transcription factor crucial in the oxidative stress response [330], has not previously been associated with smoking, however here was predicted to be activated by eight differentially expressed proteins upon chronic CSE exposure. NUPR1 has been also recently reported to be the key repressor of ferroptosis, serving as a master regulator of several ferroptosis signaling pathways [3] (Figure 4.2C). Furthermore, Nrf2-regulated components of ferroptotic pathways, such as cysteine ligase catalytic subunit (GCLC) and glucose-6-phosphate dehydrogenase (G6PD) are also up-regulated. Notably, HMOX1, a stress marker responsible for iron metabolism that has dual role in ferroptosis [331], remained stable during exposure. Interestingly, traditional pathway of glutathione (GSH) peroxidase 4 (GPX4) was downregulated in the proteomic dataset (Figure 4.1). Taken together, the proteomic analysis provides further validation of chronic basolateral CSE exposure and novel signaling pathway associated with oxidative stress and ferroptosis, however functional validation is required to further elucidate their contribution to CS response.

While the two first chapters highlighted the CS exposure efficacy, the third chapter reported the investigation focused on integrating *in vivo* BALF proteomic data with *in vitro* results from differentiation of primary bronchial epithelial cells, with patients stratified by smoking history. It is known that some of the *in vivo* changes caused by CS persist even after smoking cessation [270, 332]. Proteomic analysis based on BALF samples revealed several novel proteins abundantly expressed in the bronchial epithelium that were transiently (Figure 5.2A) or persistently changed (Figure 5.2B). After stratifying patients by their smoking status at the time of sample collection, several proteins, namely AKR1B10, ALDH3A1, UCHL1, PIR and AKR1C1, also classified in previous study as SERGs, showed significant differences between active- and never-smokers, thus emphasizing some transient effects of smoking. Since mentioned genes are abundantly expressed in bronchial epithelium *in vivo* (data not shown), an *in vitro* model of differentiated phBECs was used to assess the constitutive transcript levels in samples derived from never-, ex- or active smokers. Surprisingly, RT-qPCR revealed stable if not lower expression of investigated genes in ex-smokers in comparison to never-smokers, and sometimes even lower in current smokers (Figure 5.2B). This can have several explanations. Since the expression was assessed on the transcript level *in vitro*, a negative feedback loop mediated via intron-derived microRNA could explain lower gene expression levels (data not shown) [333]. Secondly, BALF constitutes

also of other cells, such as alveolar macrophages, lymphocytes, granulocytes, squamous epithelial cells, type II pneumocytes or mast cells [334], which can contribute to total mRNA levels, since they are not exclusively expressed by the bronchial epithelial cells. Following on this, monocultures such as differentiated pHBEs lack extracellular triggers and signals present *in vivo* which could be persistently inducing epithelial expression of genes of interest after smoking cessation, implying the CS-derived signaling pathway deregulations are present in other cell types. Lastly, differentiated pHBEs derives from basal cells isolated from patients' bronchi, which may either dilute the signal conferred in basal cells during expansion and differentiation, or implies that basal cells are not the main expressers of these genes. For instance, the immunofluorescence co-stainings of selected SERGs with cell-type specific markers showed ciliated cells express majority of NQO1 present in pHBEs (Figure 3.13).

7. Conclusions

In conclusion, this work presents three distinct investigations, interconnected by CS models validation, which resulted in publishing a paper in American Journal of Physiology – Lung Cellular and Molecular Physiology [197]. This study focused on a validation of six different CS exposure set-ups, based on the direct comparison *in vitro* models by their capacity of inducing expression of a set of genes collectively called SERGs (smoke-expression regulated genes), which were consistently and substantially upregulated in bronchial epithelium of smokers. Of note, the cell-delivered dose quantification allowed for a direct comparison between exposure models, that differed in other characteristics, such as an exposure type (whole CS or CSE), an exposure length (acute or chronic), an administration route (apical, basolateral) or a stage of differentiation (basal cells, differentiating or differentiated pHBEs), and thus permitted further standardization. Three out of six tested models performed the closest with *in vivo* settings: acute submerged CSE exposure and acute whole CS exposure significantly upregulated expression of six out of 10 SERGs, while chronic basolateral CSE exposure induced expression of seven SERGs. Other exposures, namely acute apical or basolateral CSE exposures, failed to upregulate more SERGs than just *CYP1A1*, highlighting the need of assessment beyond concentration or dose, cytotoxicity measurements or *CYP1A1* induction. This study concludes that all three models yield a physiologically relevant response. While wCS provides exposure to the widest range of CS constituents, submerged CSE exposures allows for technologically less complicated and more time-efficient set-ups, which could be successfully used in the investigations of CS effect in bronchial epithelial injury. Chronic basolateral CSE exposure may suit as the best model for considering effects of chronic effects of smoking. Taken together, these results provide guidelines for usage of *in vitro* CS exposure models, particularly when CSE exposures are considered.

These findings helped choosing the right model for proteomic analysis done on chronic basolateral 5% CSE exposure model. The analysis of 186 differentially regulated proteins further validated this model as physiologically relevant, due to the activation xenobiotic metabolism pathways and the deactivation of sirtuin pathway, changes that have been observed previously *in vivo* in smokers. Furthermore, it revealed a novel master regulator activated by CS, nuclear protein 1, which could be involved in oxidative stress response and deregulating ferroptotic pathways.

In the last chapter, the expression levels of persistently upregulated genes by smoking were compared between BALF and differentiated pHBEs *in vitro*. Although more biological replicates are needed to more accurately compare these datasets, transcript levels were surprisingly not increased in samples from either active- or ex-smokers, in some cases suggesting persistent down-regulation upon smoking cessation.

8. Final remarks

8.1 Applications

All studies presented in this thesis give a thorough insight into 2D *in vitro* primary human bronchial epithelial cells exposure models and culture applicability in the translational research, with specific focus on the response to cigarette smoke on molecular level. Validation study of CS exposure models showed which experimental set-ups are able to recapitulate changes observed *in vivo* and discerned which model suits best addressing particular research questions that are focused on the molecular response to CS. One of these models, namely chronic basolateral CSE exposure, was further validated in proteomic analysis, proving their physiological relevance. Last study implies however, that the *in vitro* baseline expression profile differences between cells derived from non-smokers and from patients with smoking history can vary from *in vivo* results. Taken together, physiologically relevant exposure models selected in this study can support translational research in the fields of toxicology and lung injury caused by CS, despite donor-dependent differences that can occur at the baseline expression levels.

8.2 Limitations

Because of the number of variables that are available when designing a CS exposure experiment, validation study in Chapter A could naturally entail even more models, such as chronic wCS exposure or CSC exposures. The main aim was, however, to compare the most frequently used modalities in CS research. In SERGs expression assessment on the transcript level, additionally to RT-qPCR, a comparative transcriptomic analysis could be done to reinforce shown data. Furthermore, it is important to point out that primary cells exhibits *in vitro* high variability in inter-donor gene expression, therefore a higher number biological replicates would be favorable. Lastly, regarding the wCS exposure, ALICE-Smoke device that was kindly shared by Dr Otmar Schmid lab does not meet ISO 20778:2018 for smoking exposure protocols.

Proteomic study in Chapter B partially addressed the lack of unbiased, 'omic' approaches, however it was performed only on one model, namely chronic basolateral CSE exposure. The proteomic results, although having high level of significance, low fold change cut-off was based on IPA recommendations more than proteomic data analysis, which expects significant changes to have a fold change of at least 0.8 [335].

In Chapter C, trends in expression downregulation are quite apparent in *in vitro* results, however, to gain more comprehensive results at least one additional biological replicate for non- and active smokers. Additionally, all BALF patients were diagnosed with interstitial lung disease, which could have introduced confounding bias.

8.3 Follow up studies

State-of-the-art, multiomic expression analyses provide much more comprehensive insight into differentially expressed genes. Transcriptomic validation of the results presented in Chapter A would give more insight into overlaps between exposure systems and *in vivo* results.

Following on this and on results from Chapter B, a functional validation of signaling pathways or using a clinically relevant material, such as precision cut lung slices, for confirming identified aberrantly changed pathways would aid strengthening the validation results.

In Chapter C, analysis of protein expression with western blot would shed more light on basal expression levels or persistently and transiently changed genes, and the use of different model such as submerged 20% CSE from the same samples would help evaluating if basal cells can still hold upregulated signal, and if any 'memory proteins' will be more substantially upregulated by CSE exposure when compared to ex- or never-smokers.

9. Materials and Methods

9.1 Materials

Note: Chapter 9.1.3 was expanded and based on materials and methods described in Mastalerz et al., *AJP Lung*, 2021.

9.1.1 Antibodies list

9.1.1.1 Primary antibodies

Table 9.1. Primary antibodies used in Western Blot (WB) and Immunofluorescence (IF) analysis. This table and the table description has been published in Mastalerz et al., *AJP Lung*, 2021.

Target	Antibody	Ref. number	Manufacturer	Dillutions	
				WB	IF
NQO1	Rabbit, polyclonal	ab34173	Abcam, Berlin, Germany	1:1000	1:1000
AKR1B10	mouse, monoclonal	SAB1405200-100UG	Sigma Aldrich, St. Louis, USA	1:1000	
AKR1C1	rabbit, polyclonal	HPA068265	Atlas Antibodies, Stockholm, Sweden	1:500	1:100
ALDH3A1	sheep, polyclonal	AF6705	Rndsystems, Minneapolis, USA	1:800	
PIR	Rabbit, polyclonal	HPA000697	Atlas Antibodies, Stockholm, Sweden	1:100	1:100
UCHL1	Rabbit, polyclonal	HPA005993	Atlas Antibodies, Stockholm, Sweden		1:100
MUC5AC	Mouse, monoclonal	ab3649	Abcam, Berlin, Germany		1:250
p63	Mouse, monoclonal	Ab735	Abcam, Berlin, Germany		1:100
CC10	Mouse, monoclonal	Sc365992	Santa Cruz, Dallas, USA		1:300
Acetylated tubulin	Mouse, monoclonal	T7461	Sigma Aldrich, St. Louis, USA		1:100

ACTB	HRP-conjugated anti-ACTB antibody, mouse, monoclonal	A3854	Sigma Aldrich, St. Louis, USA	1:40000
-------------	--	-------	-------------------------------	---------

9.1.1.2 Secondary antibodies

Table 9.2. Secondary antibodies used in Western Blot (WB) and Immunofluorescence (IF) analysis. This table and the table description have been published in Mastalerz et al., AJP Lung, 2021.

Antibody, clone	Target	Ref. number	Manufacturer	Dilution	Application
Rabbit Anti-Sheep IgG H&L (HRP), polyclonal	Sheep	Ab6747	Abcam, Berlin, Germany	1:30000	WB
Amersham ECL Rabbit IgG, HRP-linked F(ab')₂ fragment (from donkey), monoclonal	Rabbit	NA934	GE Healthcare Chicago, USA	1:50000	WB
Amersham ECL Mouse IgG, HRP-linked whole Ab (from sheep), monoclonal	Mouse	NA931	GE Healthcare Chicago, USA	1:50000	WB
Donkey anti-ms (red 568), polyclonal	Mouse	A10037	Thermofischer	1:500	IF
Goat anti-rb (green 488), polyclonal	Rabbit	A32731	Thermofischer	1:500	IF

9.1.2 Primers

Table 9.3. Primer list for RT-qPCR. Primers were synthesized by Eurofins. This table and the table description has been published in Mastalerz et al., AJP Lung, 2021.

Target	Forward primer (5'-3')	Reverse primer (5'-3')
AKR1C1	CTGCAGAGGTTTCCTAAAA	CCTGCTCCTCATTATTGTA
PIR	GTAAGGATGGTGTGACAGTT	GTCCACCCTTTAGGGATA

CYP1B1	GCCACTATCACTGACATCT	CAGGATACCTGGTGAAGA
ADH7	GAGTGACTACAGTGAAACCA	CCAGTAATATCGCTCCTAAT
NQO1	AAGGACATCACAGGTAAACT	GAAGTGAATATCACAAGGT
CYP1A1	CTTGGACCTCTTTGGAGCTG	CGAAGGAAGAGTGTCTGGAAG
IL8	CTGGCCGTGGCTCTCTTG	CCTTGGCAAACTGCACCTT
ALDH3A1	CCTGACTACATCCTCTGTG	CCCGTAGAACTCTTTCAGT
MUC5AC	AGCAGGGTCCTCATGAAGGTGGAT	AATGAGGACCCCAGACTGGCTGAA
UCHL1	CTGAAGGGACAAGAAGTTAG	ACTGATCCATCCTCAAATC
AKR1B10	GTGTTGCAATCCTCTCAT	GGACATGAGTGGAGGTAGT
MUC5B	GCTGGAGCTGGATCCCAAAT	CTGGCGTTGTGGGCATAGA
ARPC2	ACATTGGCTACATTACCTTT	GTGAATATAGGCCTTAGAGC
TMSB4X	CAAAGAACTACTGACAACGA	ACTCTAGATTTCACTGTCGTC
PSMB2	CCCGACTATGTTCTTGTC	ACATCTTGTCATGATCGTC
WDR89	AGTACGTTCCATCCCAGCAATCC	AGGCCATCAGATGAACCTGAGACT
GADPH	TGACCTCAACTACATGGTTTACATG	TTGATTTTGGAGGGATCTCG
DHX8	TGACCCAGAGAAGTGGGAGA	ATCTCAAGGTCCTCATCTTCTTCA
HPRT	AAGGACCCCACGAAGTGTTG	GGCTTTGTATTTTGCTTTTCCA

9.1.3 Patient material

Basal primary bronchial epithelial cells (phBECs) were acquired from the CPC-M BioArchive at the Comprehensive Pneumology Center (CPC, six donors) and from Lonza, Basel, Switzerland (three donors). Cells from CPC-M Bio-Archive were collected during tumor resection from patients who had planned lung surgery. Based on self-reported history of smoking, phBECs was derived from patients who were either never smokers or ceased smoking at least 10 years ago (Table 9.4), with similar size of small bronchi across every donor. Upon treatment of bronchi with Pronase E, epithelial cells were carefully scraped with a scalpel, minced and filtered through a 70µm strainer to remove tissue pieces. To remove fibroblasts, cells were plated on uncoated plates for 3 hours. Afterwards, collected supernatant was transferred onto collagen I (C3867, Sigma Aldrich, Germany)-coated plates and then cultured with PneumaCult™ Ex-Plus (Stemcell

Technologies, 05041, Vancouver, Canada) with 1% Penicillin/Streptomycin/Amphotericin. Cells were expanded in passage 1 and then transferred to liquid nitrogen storage until later use.

PhBECs obtained from Lonza had been collected from healthy self-reported non-smokers (2 females, 49 and 52 years old, and one 13 year old male). All samples were tested for Mycoplasma pneumoniae, and those with negative result of the test were later cultured in passage 1 on 100 mm dish. After reaching 100% confluency, samples were collected in the freezing medium, and finally moved to the liquid nitrogen storage at -184°C until later use. Informed consent was obtained from every donor. Furthermore, the study was agreed upon by the local ethics committee (454-12), Ludwig-Maximilians University, Munich, Germany.

Table 9.4. General donor characteristics and information on smoking status. This table and the table description has been published in Mastalerz et al., AJP Lung, 2021.

Donor No.	Age	Gender	Smoking status	Smoking cessation period	Pack years
1	73	M	Ex-smoker	>20 years	21-40
2	80	W	Ex-smoker	>20 years	21-40
3	66	W	Ex-smoker	10-20 years	21-40
4	72	W	Never-smoker	n/a	n/a
5	80	M	Never-smoker	n/a	n/a
6	74	W	Never-smoker	n/a	n/a

9.1.4 Cell culture media

Table 9.5. Cell culture media used in all experimentations.

Cell culture medium	Components	Product number	Manufacturer
PneumaCult ALI	PneumaCult-ALI Basal	05002	Stemcell Technologies
	10X PneumaCult-ALI Supplement	05003	StemCell Technologies
	100X PneumaCult-ALI Supplement	05006	StemCell Technologies
	Heparin	07980	StemCell Technologies
	Hydrocortisone	H2270	StemCell Technologies

	100U Pen/Strep	15140	Sigma Aldrich
PneumaCult Ex-Plus	PneumaCult Ex-Plus Basal	05040	Stemcell Technologies
	50X Supplement	05042	Stemcell Technologies
	100U Pen/Strep	15140	Life Technologies
	Hydrocortisone	H2270	Sigma Aldrich
BEGM	BEBM Clonetics Medium	CC-3170	Lonza
	SingleQuots Supplements and Growth Factors	CC-4175	Lonza
	100U Pen/Strep	15140	Life Technologies
MEM		11095080	Life Technologies

9.1.5 Reagents and chemicals

Table 9.6. Reagent and chemicals.

Reagent/chemicals	Product number	Manufacturer
Reference Cigarette	3R4F	Kentucky Research Cigarettes, USA
HBSS	CC-5024	Lonza, Switzerland
Trypsin + EDTA	CC-5012	Lonza, Switzerland
Trypsin inhibitor TNS	CC-5002	Lonza, Switzerland
HBSS (-) Ca ²⁺ (-) Mg ²⁺	14170138	Life Technologies, USA
Detachment solution (DS)	05426	StemCell Technologies, Canada
Inhibition solution (IS)	05427	StemCell Technologies, Canada
Dimethylsulfoxide (DMSO)	A994.1	Carl Roth, Karlsruhe, Germany
DAKO (Fluorescence Mounting Medium)	S302380-2	Agilent Technologies, USA
Random hexamers	N8080127	Applied Biosystems, USA
Collagen I	C3867	Sigma Aldrich, Germany
Collagen IV	C7521	Sigma Aldrich, Germany
Trypan Blue	T10282	Invitrogen, USA
PCR-Nucleotide Mix	C1145	Promega, USA
MgCl ₂ GeneAmp 10x Buffer II	N8080130	Invitrogen, USA
RNase Inhibitor	N8080119	Applied Biosystems, USA

Reverse Transcriptase	N8080018	Applied Biosystems, USA
DNase/RNase Free Water	10977	Life Technologies, USA
Bovine Serum Albumin	A3059	Sigma Aldrich, Germany
Phosphatase inhibitor	A32957	Thermo Fischer Scientific, USA
SuperSignal West Femto	34095	Thermo Fischer Scientific, USA
Dulbecco's Phosphate Buffer- erd Saline (DPBS)	14190-094	Life Technologies, USA
DTT	A2948	AppliChem, Germany
Pierce ECL Western	32209	Thermo Fischer Scientific, USA
SuperSignal West Dura	34075	Thermo Fischer Scientific, USA
SuperSignal West Pico	34077	Thermo Fischer Scientific, USA

9.1.6 Buffer formulations

Table 9.7. List of buffer formulations.

Product	Reagents
Laemmli buffer	65 mM Tris-HCl pH 6.8
	10% glycerol
	2% SDS
	0.01% bromophenol blue
	100 mM DTT
RIPA buffer	50 mM Tris•HCl
	pH 7.6, 150 mM NaCl
	1% Nonidet P-40
	0.5% sodium deoxycholate
	0.1% SDS
SDS-PAGE Separation Gel (10%)	ddH ₂ O 3.7 ml
	1.5 M Tris/HCl pH 8.8 25 ml
	SDS 20% 45 µl
	Acrylamide 3 ml
	APS 10% 30 µl
	TEMED 6 µl
SDS-PAGE Separation Gel (12%)	ddH ₂ O 3.1 ml

	1.5 M Tris/HCl pH 8.8 2.25 ml
	SDS 20% 45 µl
	Acrylamide 3.6 ml
	APS 10% 30 µl
	TEMED 6 µl
SDS-PAGE Stacking Gel (4%)	ddH ₂ O 1.8 ml
	0.5 M Tris/HCl pH 6.8 750 µl
	SDS 20% 7.5 µl
	Acrylamide 400 µl
	APS 10% 15 µl
	TEMED 3 µl
TBS (Tris-buffered saline) (10x)	Tris/HCl pH 7.4 10 mM
	NaCl 150 mM
TBS-T (TBS with TWEEN®20)	TBS (10x) 10% (v/v)
	Tween®20 0.1% (v/v)
	ddH ₂ O 89.99% (v/v)
1X BSA (Bovine Serum Albumin)	Bovine serum albumin 5 g
	20% Triton X-100 2.5ml
	10X PBS 50ml
5% Milk Blocking Solution	5 mg Skim Milk powder
	100 ml 1X TBS-T
SDS (sodium dodecyl sulphate) solution (20%) (w/v)	SDS 200 g
	ddH ₂ O 1 L
Phosphate Buffer Saline	NaCl 1.37 M
	KCl 27 mM
	Na ₂ HPO ₄ 100 mM
	KH ₂ PO ₄ 20 mM
	NaCl 1.37 M

9.1.7 Consumables

Table 9.8. List of consumables.

Product	Manufacturer
0.2 µm filter	Minisart; Sartorius Stedim Biotech
96-well imaging plates, Falcon®	Corning, Thermo Fisher Scientific, Schwerte, Germany
6-well cell culture plates	Merck, Germany
96-well cel culture plates	Merck, Germany
Chromatography paper	GE Healthcare, Whatman, UK
Combitips advanced® 0.1µl, 0,2µl, 1.5µl, 5µl, 10µl	Eppendorf , Hamburg, Germany
Combitips advanced® sterile 5µl, 10µl, 25µl, 50µl	Eppendorf , Hamburg, Germany
12-well transwells	Corning, New York, USA
Cryovials 1.5 ml	Greiner Bio- One, Frickenhausen, Germany
Falcon 12-well transwells	Corning, New York, USA
Filter System 500 ml	Corning, New York, USA
Falcon Tube (15 ml, 50 ml)	BD Bioscience, Heidelberg, Germany
Filter Tips (10µl, 20µl, 100µl, 200µl, 1000µl)	Biozym Scientific, Hessisch Oldendorf, Germany
Glass Pasteur pipettes	VWR International, Darmstadt, Germany
Greiner 96-well microplate	Sigma-Aldrich, St. Luis, USA
Measuring pipettes, (5 ml, 10 ml, 25 ml, 50 ml)	VWR International, Darmstadt, Germany
Microscope slides	Thermo Fisher Scientific, Darmstadt, Germany
Nitrile Gloves	Meditrade, Ireland
Parafilm	Bemis, USA
PCR plates, 96-well plate	Kisker Biotech, Steinfurt, Germany
Pipette tips, unfiltered (10µl, 20µl, 100µl, 200µl, 1000µl)	Eppendorf, Hamburg, Germany
PVDF Transfer Membrane	Immobilon-P, Millipore, USA
Quartz filters	Merck, Germany
Reaction tubes (0.5 ml, 1.5 ml, 2 ml)	Eppendorf, Hamburg, Germany
Reagent reservoirs, 50 mL	Corning, New York, USA
SafeSeal tube 0.5ml	Sarstedt, Germany

Sealing foils for PCR plates	Kisker Biotech, Steinfurt, Germany
Syringes	Neolab, Heidelberg, Germany

9.1.8 Laboratory equipment

Table 9.9. List of laboratory equipment.

Product	Manufacturer
-20°C freezer MediLine LGex 410	Liebherr, Biberach, Germany
-80°C freezer U570 HEF	New Brunswick, Hamburg, Germany
Air liquid interface cigarette smoke exposure system (ALICE-Smoke)	Built in-house
Analytical scale XS20S Dual Range	Mettler Toledo, Gießen, Germany
Autoclave DX-45	Systec, Wettenberg, Germany
Autoclave VX-120	Systec, Wettenberg, Germany
Axio Imager M2 microscope	Zeiss, Jena, Germany
Axiovert 40C microscope	Zeiss, Jena, Germany
CASY cell counter	OLS-OMNI Life Science, Bremen, Germany
Cell culture work bench Herasafe KS180	Thermo Fisher Scientific, Darmstadt, Germany
Centrifuge Rotina 420R	Hettich, Tuttlingen, Germany
Centrifuge with cooling, Micro200R	Hettich, Tuttlingen, Germany
Cigarette smoke extract generator	Built in-house
CO2 cell Incubator BBD6620	Thermo Fisher Scientific, Darmstadt, Germany
Demineralized water	Thermo Fisher Scientific, Darmstadt, Germany
Dry ice container Forma 8600 Series	Thermo Fisher Scientific, Darmstadt, Germany
Duomax 1030 Shaker	Heidolph Instruments, Germany
Electronic pipet filler	Eppendorf, Hamburg, Germany
Fridge MediLine LKv 3912	Liebherr, Biberach, Germany

Gel image system ChemiDoc XRS+	Biorad, Hercules, USA
Ice machine ZBE 110-35	Ziegra, Hannover, Germany
Liquid nitrogen cell tank BioSafe 420SC	Cryotherm, Kirchen/Sieg, Germany
Heater and magnetic stirrer RSM-10HS	Phönix Instrument, Germany
Manual cell counter	Novolab, Belgium
Nalgene® Freezing Container (Mr. Frosty)	Omnilab, Munich, Germany
NanoDrop 1000	PeqLab, Erlangen, Germany
pH meter InoLab pH 720	WTW, Weilheim, Germany
Plate centrifuge 5430	Eppendorf, Hamburg, Germany
Plate reader Sunrise	Tecan, Crailsheim, Germany
Primo Vert microscope	Zeiss, Jena, Germany
Roll mixer	VWR International, Darmstadt, Germany
Shaker Duomax 1030	Heidolph, Schwabach, Germany
Mini microcentrifuge 230V	Corning, New York, USA
STX01 chopstick electrode	MilliporeSigma, Bioz Stars
TEER Millicell-ERS-2 volt-ohm-meter	MilliporeSigma, Bioz Stars
Thermomixer compact	Eppendorf, Hamburg, Germany
Vortex Mixer	IKA, Staufen, Germany
Water bath Aqua Line AL 12	Lauda, Lauda-Königshofen, Germany

9.1.9 Software

Table 9.10. List of software programs.

Software	Manufacturer
ImageLab 6.0.1	Bio-Rad, USA
Adobe Illustrator 2015	Adobe Systems, San Jose, USA
GraphPad Prism 9	GraphPad Software, La Jolla, USA
Imaris 9.0 software	Bitplane, Zurich, Switzerland
LightCycler® 480 SW 1.5	Roche Diagnostics, Mannheim, Germany

Magelan Software 7.0.5	Tecan, Crailsheim, Germany
Microsoft Office Professional Plus 2010	Microsoft, Redmond, USA
Axio Vision	Zeiss, Jena, Germany
Ingenuity Pathway Analysis	Qiagen, USA
R (programming language)	R Core Team, USA
BioRender	BioRender, USA

9.1.10 Assay kits and standards

Table 9.11. List of assay kits and standards.

Kit and standards	Manufacturer
BCA Protein Assay kit	Pierce Biotechnology, Rockford, USA
LightCycler 480 SYBR Green I Master	Roche Diagnostics, Mannheim, Germany
RNeasy Plus Mini Kit no. 74134 and 74136	Qiagen, Venlo, Netherlands
LDH cytotoxicity kit 11644793001	Roche, Switzerland
PageRuler™ Plus Prestained Protein Ladder, 10 to 250 kDa 26619	Thermo Fisher Scientific, USA

9.2 Methods

Note: Chapters 9.2.1 9.2.3, 9.2.4 and 9.2.5 were expanded and based on methods described in Mastalerz et al., AJP Lung, 2021.

9.2.1 Dose determination by gravimetric analysis

200 µl of media (PneumaCult-ALI or BEGM) used in experiments and media exposed to a cigarette smoke as described above was pipetted on Whatman® quartz filters (Sigma Aldrich) and placed inside a sealed desiccator until completely dry. The weight of the filters was measured before and after medium application. The CS dose was achieved by subtracting 200 µl CSE-free from 200 µl 100% CSE medium, which was then used for dose calculations for all CSE exposures.

9.2.2 Preparation of CSE

The mainstream smoke of six filtered reference cigarettes 3R4F (Kentucky Tobacco Research and Development Center at the University of Kentucky; Lexington, KY) was put through 200 ml PneumaCult ALI-medium (Stemcell Technologies, 05041, Vancouver, Canada) or BEBMTM (Lonza, CC-3170) which were used with supplements. CSE generation was carried out at a flow rate of 0.3 l/min. Once the whole six cigarettes were smoked, the achieved medium was considered as 100% CSE. Next, the mixture was filtered through a 0.2 µm filter (Minisart; Sartorius

Stedim Biotech), and finally aliquoted stored at -80°C. Aliquots were later thawed and used immediately at the indicated concentrations.

9.2.3 Cell culture methods

9.2.3.1 Isolation of primary human bronchial epithelial cells

Bronchial epithelial cells were isolated immediately upon arrival. First, the pictures with bright-field microscope (name) were collected and measured bronchi sizes. Then, lung tissue was dissected in cold Eagle's minimal essential medium+Glutamine+Penicillin/Streptomycin+Amphotericin (MEM+Glut+Pen/Strep+Amph) and remains of connective tissue were removed as much as possible. Next, the bronchi were excised with scalpel and washed three times in MEM+Glut+Pen/Strep+Amph and 20 ml of bronchi was incubated with Pronase E at concentration of 1 mg/ml in MEM+Glut+Pen/Strep+Amph in 4°C overnight with 50-60 cycles/min. Next day, FCS was used to inactivate Pronase E, after which the tissue was placed in 100mm Petri dish and kept moist with 5-10 ml of MEM+Glut+Pen/Strep+Amph. Next, the bronchi size was scraped off the tissue, which was repeated with from 5-10 ml of MEM+Glut+Pen/Strep+Amph. The tissue was then minced into small pieces and transferred all back to the 50 ml Falcon tube and spun down 350 x g for 5 min in 4°C. Supernatant was discarded and tissue resuspended in 10 ml MEM+Glut+Pen/Strep+Amph and filtered through 70µm strainer to remove tissue pieces. Subsequently, tissue was washed again by adding 2 x 5 ml media MEM+Glut+Pen/Strep+Amph to collect cells in Falcon tube, spun down in 350 x g for 5 min in 4°C and resuspended in 10 ml PneumaCult™ Ex-Plus (Stemcell) +Pen/Strep(+Amph). To remove fibroblasts, cells were plated onto 100 mm dish for 3 hours. Afterwards, the supernatant was plated onto Collagen I-coated 100 mm dish. Media was changed every 2 days (10 ml of PneumaCult™ Ex-Plus (Stemcell) +Pen/Strep(+Amph)).

9.2.3.2 Cryopreservation of primary human bronchial epithelial cells

After reaching 80% confluency, media was aspirated and cells were washed with 5 ml of pre-warmed HBSS. 2 ml of Disassociation Solution (DS) (StemCell) was then added to the dish. Cells were then incubated in 37°C for 5-10 min and examined every few minutes under the brightfield microscope to check whether cells were completely detached. Then, 2 ml of Inhibitory Solution (IS) (StemCell) was added and entire mixture was transferred to 50 ml tube. To maximize the cell yield, the dish was rinsed with warm HBSS. Next, the Falcon tube was spun down at 350 x g for 5 min on 4°C. Aspirated supernatant was resuspended in 2 ml PneumaCult™ Ex-Plus+Pen/Strep(+Amph) media and counted with Trypan-Blue (1:1 ratio of cells and Trypan-Blue). In order to freeze the cells (500 000 cells per vial), cells were spun down again, supernatant aspirated and pellet resuspended in freezing media (90%FBS + 10%DMSO) with 1 ml per cryovial. Finally, 1 ml of cell mixture was transferred to cryovials (Greiner Bio-One) and Mister Frosty (Omnilab) overnight at -80°C and then kept in liquid nitrogen at -195°C for long-term storage.

9.2.3.3 Thawing frozen cells

The cells stored in liquid nitrogen were transferred into the water bath set at 37°C until the cell suspension was thawed. Then, cells were immediately transferred to 50 ml Falcon tube with 9 ml

of PneumaCult™ Ex-Plus media supplemented with 50X Supplement (StemCell), 1% penicillin/streptomycin and hydrocortisone. Cells were then carefully mixed and subsequently seeded at a density of 20,000-25,000 cells/cm² on 100 mm plates (Corning, 430167, 58.85cm², New York, USA), pre-coated for 3 hours with collagen I and cultured under standard cell culture conditions of 37°C and 5%CO₂. For acute submerged basal cell exposure, BEGM Bronchial Epithelial Cell Growth Medium BulletKit (Lonza CC-3170, containing: BEBMTM Clonetics Medium (CC-3170) + SingleQuots Supplements and Growth Factors (CC-4175)) + 100U Pen/Strep (Life Technologies, 10,000 U, 15140) was used, in agreement with our previous studies [190, 248].

9.2.3.4 Primary bronchial epithelial cell cultivation and differentiation

For expansion on a collagen I-precoated 100 mm plates, cells were cultured using either BEGM Bronchial Epithelial Cell Growth Medium BulletKit (Lonza CC-3170, containing: BEBM™ Clonetics Medium (CC-3170) + SingleQuots Supplements and Growth Factors (CC-4175)) + 100U Pen/Strep (Life Technologies, 10,000 U, 15140) or PneumaCult™ Ex-Plus (Stemcell Technologies, 05041, Vancouver, Canada) with 1% Pen/Strep. Cells used for all other exposure types, which required pHBECS differentiation, were cultured and expanded in PneumaCult™ Ex-Plus before the differentiation took place in PneumaCult™ ALI. Medium was changed on alternate days. When cell cultures reached approximately 80-90% confluency, cells were trypsinized transferred to a 50 ml Flacon tube, counted and seeded on 12-well transwells (Corning, 3460, 12mm inserts, Polystyrene, 12-well plate, 0.4µm Polyester Membrane, Tissue Culture Treated, 1.12cm²/transwell) or (Falcon® Permeable Support, 12-well Plate, 0.4 µm Transparent PET Membrane) precoated for 3 hours with collagen IV (C7521, Sigma Aldrich, Germany) at 8.9 µg/cm², seeding approximately 100,000 cells per membrane. During the expansion, the differentiation and the exposure incubation times, cells were cultured at 37°C in a humidified cell incubator with 95% air and 5% CO₂.

9.2.3.5 Cigarette smoke exposure models

Exposures performed on each CS treatment model were carried out in every study in at least four biological replicates, using pHBECS originated from independent donors from the CPC BioArchive. Notably, additional experiments made on cells derived from independent donors purchased from Lonza in submerged CSE exposure analysis were performed in three biological replicates. All relevant patient metrics are shown in Table 3.3 and in Table 5.2. Noteworthy, at least three donors overlapped between in all exposure models. Above-mentioned Lonza cells were utilized only as an addition to the submerged acute basal CSE exposure, as it took place in the previous study [190].

Acute submerged exposure of basal cells with CSE

When cultured cells reached 80%-90% confluency on a 100 mm dish cultured in BEGM (not precoated with collagen I), HBSS without Ca²⁺ and Mg²⁺ (Lonza, CC-5024) was added to the dish, swirled several times and replaced Trypsin with EDTA (Lonza, CC-5012) used for cell detachment by incubating 2-3 min in 37°C. Once a vast majority of cells appeared detached under the microscope, 2 ml of Trypsin inhibitor TNS (Lonza, CC-5002) was added, to inactivated Trypsin with EDTA. Next, pHBECS were transferred to a 50 ml Falcon tube, in each they were centrifuged at 400 g for 5 min. After spinning down the cells, the supernatant was carefully removed by a glass aspirator and the dried cell pellet was resuspended in a 2-3 ml of pre-warmed

BEGM medium with supplements. While the volume of added BEGM was known, the cell density was estimated adding 20 µl to a 10 ml CASY container with CASY buffer. In this dilution of 1:400, cell counting was performed on the CASY OLS-OMNI cell counter (Life Science, Bremen, Germany). Once cell density was calculated, wells were diluted accordingly to needed concentrations and finally seeded on 6-well plates (TRP, 92406, 9,6cm²/well) at a cell density of 1.0 x 10⁴ cells/cm². Next, phBECs were cultured in 2-3 days until approximately 90% confluency, and finally exposed to the indicated CSE concentrations for 24 h. Finally, cells were washed twice with ice-cold HBSS and stored at -80°C.

Chronic and acute basolateral exposure with CSE

As for exposures on either phBECs, both differentiated or were differentiating, cells were expanded in PneumaCult Ex-Plus Medium on 100 mm dishes. Next, trypsinized as described previously and seeded on 12-well transwell plates, 100 000 cells per insert. After 1-3 days when the cells reached 100% confluency on the inserts, cells were air-lifted by aspirating apical PneumaCult Ex-Plus Medium, which also indicated Day 0 of differentiation. Subsequently, the basolateral medium was replaced with either PneumaCult™-ALI medium or 5% CSE in bespo-ken medium, as described previously in [118]. Throughout the differentiation period of four weeks, both 5% CSE or PneumaCult™-ALI medium was regularly exchanged at the same days, every second days. Additionally, at the end of every week of differentiation until day 28, inserts were either collected and stored in -80°C for mRNA and protein analyses, or fixed in PFA for IF analysis. Of note, when acute basolateral CSE exposure was performed, cells underwent treatment from basolateral compartment with 5% CSE for 24 h at the end of differentiation. Subsequently, cells were rinsed twice in ice-cold HBSS and stored at -80°C for mRNA and protein analyses.

Acute apical exposure with CSE

Acute apical CSE exposures were performed at the end of every phBECs differentiation, on the day 28. For 24 h the cells were apically exposed to 200µl of 3%, 6% or 12% of CSE. When treatment was finished, apical and basolateral medium was collected for cytotoxicity measurements, which were carried out within next 2-3 days. One additional untreated insert was used for positive LDH control treatment with Triton X. Next, the inserts were rinsed twice in ice-cold HBSS and stored in -80°C for mRNA and protein analysis. One of the modes included pre-treatment 24 starvation, where the cells were starved in PneumaCult™-ALI medium without supplements 24 h prior to the treatment. This was followed by the aforementioned exposure and collection.

In a direct comparison with exposure to the below mentioned whole cigarette smoke exposure, the cells were exposed to 5 min 200µl of 40% CSE, which was administered apically. After 5 min 40% CSE was carefully removed with a glass aspirated and the cells were incubated for 24 h. Subsequently, they were washed twice with an ice-cold HBSS and stored for mRNA and protein analyses at -80°C, along with basolateral medium, again for cytotoxicity measurements.

Air-Liquid Interface Cell Exposure with Whole Cigarette Smoke (ALICE-Smoke)

Whole cigarette smoke exposure were carried out in the Whole Cigarette Smoke (ALICE-Smoke) system, kindly shared by Dr Otmar Schmid. Once fully differentiated after 28 days, the transwell inserts with phBECs were transferred into the pre-warmed 12-well plate in the ALICE-Smoke lower exposure chamber, a 12-well insert adapted version of the continuous flow system, as

described previously [336, 337]. For dosimetric measurements, three to four 1.1 cm² metal plates were placed in inserts without cells. Next, 800 µl of pre-warmed PneumaCult™-ALI medium was added to lower compartment of smoke chamber (Figure 3.9). After tightly and carefully assembling the pre-warmed both lower and upper smoke exposure chamber compartments, ALICE-Smoke was placed in an incubation chamber with a heating pad set at 37°C. After tightly attaching to inlet and outlet connectors, a 3 cm of one filtered research-grade cigarette (Kentucky Tobacco Research and Development Center at the University of Kentucky; Lexington, KY) was installed into cigarette holder. Of note, inside the incubation was placed up-stream from ALICE-Smoke device a smoke humidification bottle, which contained deionized sterile water. Once the cigarette was lit with a lighter, a vacuum piston pump located down-stream from ALICE was started, which resulted in continuous flow of cigarette smoke through the dehumidification bottle (with bubbling through the water) and exposing pHBEs to cigarette smoke inside ALICE-Smoke device. The flow rate of the CS was 0.6 L/min for about 2 min (0.05 L/min per transwell), following by exposing cells to a sterilized air for another 2 min. Conversely, in the sham exposures, cells exposed only to 4 min of air. For dose calculations, the metal plates located during each exposure were washed with 1 ml absolute ethanol in 14 ml falcon bottomround tubes (352059, Corning, USA). Additionally, during every exposure a Quartz filter (WHA1851110, Merck, Germany) located downstream from ALICE-Smoke device. They collect approximately 95% of total CS that has passed through ALICE-Smoke ([336, 338]; Figure 3.9).

9.2.3.6 wCS dose determination by alcohol spectrofluorometry analysis

In order to assess the cell-delivered dose of the CS deposited on inserts containing pHBEs in each exposure, the quartz filters that were located downstream from ALICE-Smoke incubating chamber, after each experiment were carefully transferred in tightly closed plastic containers filled with silica gel, where they stayed for at least 2 h at a room temperature. Next, the weight measured on an analytical scale was compared with the weight measurements of corresponding filter prior to wCS. After simple subtraction the CS particulate weight (M_{tot}) was calculated. After 2 h of incubation on silica gel for drying and gravimetric measurements, the quartz filter was placed in a glass container with 20 ml of absolute ethanol. Once CS particulates were washed away from the filter the solution had a known smoke concentration ($M_{tot}/20$ ml) and was diluted further 1:50 with absolute ethanol. Finally, the total smoke particulate mass was determined by the quantitative fluorescence analysis of all alcohol extracts, both from filters and metal plates (λ_{exc} 355 nm, λ_{em} 460 nm; Safire II Plate reader, Tecan, Männedorf, Switzerland). All measurements were carried out on a Greiner 96-well microplate (Sigma-Aldrich, 655101, St. Luis, USA) in four technical replicates, where as a blank 99 % ethanol was used. Then, based on the known weight and fluorescence measurements, the dose deposited on each metal plate was calculated from the fluorescence intensity of the corresponding alcohol extract from the filter, yielding relative mass and thence the cell-delivered CS dose onto the inserts.

9.2.3.7 Cytotoxicity Assay

The cytotoxicity assay used in the study was lactate dehydrogenase (LDH) assay. After each exposure, supernatants from the apical and basolateral compartments or from the 100 mm were collected and stored in Eppendorf tubes at -80°C. In each exposure an additional mock insert was culture, which was used to establish LDH release level in a positive (high) control with Triton-X. Briefly, 2% Triton-X/PneumaCult™-ALI medium was used for a cell lysis carried out in 15 min,

after which the supernatants were centrifuged at 250 g for 10 min. As a blank, or a negative control, LDH assay was performed on PneumaCult™-ALI without cells. According to the manufacturer instructions, the 30 μ l of the treated supernatants and the corresponding controls were transferred into a Greiner 96-well microplate (Sigma-Aldrich) in technical triplicates, which was followed by adding 70 μ l of PneumaCult™-ALI medium. To start the reaction, 100 μ l of reaction mixture from cytotoxicity detection kit (LDH, 11644793001, Sigma-Aldrich) was added into each well, to quantify levels of lactate dehydrogenase (LDH) release.

9.2.3.8 Transepithelial Electrical Resistance (TEER) Measurements

At the end of each week of differentiation TEER measurement were performed on every donor. Before TEER, in the apical compartment a pre-warmed 500 μ l HBSS (with Mg²⁺ and Ca²⁺, Lonza, CC-5024) was added and then incubated for 5-10 min at 37°C. Afterwards, HBSS in apical compartment was mixed up and down several times with a pipette, then aspirated and new HBSS was added apically again. Next, the pHBECS with HBSS were left to equilibrate at room temperature for at least 10 min. Millicell-ERS-2 volt-ohm-meter (Millipore, Billerica, MA) with a STX01 chopstick electrode (Millipore) is used to make resistance measurements in technical triplicates for each insert and in at least four inserts per transwell plate. In each treatment condition, at least three individual wells per donor were analyzed. After the measurements, the blank value (a similar measurement of a cell-free insert with added HBSS and PneumaCult-ALI) was subtracted and the resulting value was eventually multiplied by the well surface area (1.12 cm² for 12-well transwell inserts from Corning) to give final resistance values in $\Omega \times \text{cm}^2$.

9.2.4 RNA analysis

9.2.4.1 mRNA isolation from differentiated primary human bronchial epithelial cells

In every mRNA isolation, RNeasy Mini Plus Kit (Qiagen, 74136, Venlo, Netherlands) was used, according to the manufacturer's instructions. Before starting the protocol, a fresh 70% ethanol in double-distilled water (ddH₂O), and fresh RLT lysis buffer with thawed dithiothreitol DTT were prepared. Next the inserts were transferred on ice and let for thawing for approximately 5 min. An ice cold HBSS with Mg²⁺ and Ca²⁺ was used for washing the cells twice. Next, by cutting out the insert with a surgical knife, cells were transported to a 12-well plate. Each insert-containing well had 300 μ l RLT+DTT of buffer. Cells were then scraped off the membrane, with the use of reverse side of a 1 ml filtered tip. Alternatively, if a high mRNA yield was expected, inserts were cut in half, one of the halves placed in a well with 150 μ l of RLT buffer, while second half was transferred to another 12-well plate and placed in -80°C for later use (e.g. protein isolation). Next, the cells that were scratched off the membrane were carefully transferred to 1.5 ml Eppendorf tube provided by Qiagen. To maximize mRNA yield, inserts were washed with another 300 μ l of RLA+DTT. After combining the lysates, the tubes were then thoroughly vortexed for 30 seconds. Next the cells pipetted onto blue gDNA removing columns, which were placed in 2 ml collection and centrifuged for 30 sec at 8000 g and added 600 μ l of 70% ethanol to the flow-through left in 2 ml collection tube. Subsequently, the mixture was mixed well pipetting. 700 μ l of the flow-through was transferred to another RNeasy spin column, color-coded red, placed in a 2 ml collection tube. In next step, the lids were closed and tubes centrifuged for 15 sec at 8000 g. The flow-through was discarded and 700 μ l of RW1 buffer was added to the RNeasy spin column,

followed by centrifuged for 15 sec at 8000 g. After discarding flow-through again, 500 µl of RPE buffer was added. Washing step with 500 µl RPE buffer was repeated. In order to maximize the mRNA yield, the RNeasy spin column transferred to a new collection tube and centrifuged at maximum speed for 1 min, followed by drying by opening up the lid for another 1 min. Eventually, the RNeasy spin columns were transferred to a new 1.5 ml RNAase-free Eppendorf tube, and carefully added 30-50 µl of RNase-free water (volume depended on an expected mRNA yield) and centrifuged once more for 1 min at 8000 g to allow mRNA elution and then transferred on ice. The mRNA concentration was assessed by absorbance by using NanoDrop 1000 spectrophotometer (NanoDrop Tech. Inc; Wilmington, Germany), measured from 1.2 µl of the sample, at a wavelength of 260 nm and using of RNase-free water was as a blank.

9.2.4.2 mRNA isolation from primary human basal bronchial epithelial cells

mRNA isolation of basal cells of bronchial epithelium was carried as above, with the exception of using 6-well plates (TRP, 92406, 8.96cm²/well) as cell culture plate, from which cells were scraped off with (DNA/RNA free cell scraper, TRP, 99002).

9.2.4.3 cDNA synthesis by reverse transcription

The mRNA reverse transcription to cDNA was performed with the reverse transcriptase (Applied Biosystems, N8080018, Waltham, USA or Invitrogen, 28025013) and the random hexamer primers (Applied Biosystems). Briefly, the volume of 1 µg RNA for each sample was calculated and topped up to 20 µl with DNase/RNase free water, followed by denaturation process: at 70°C for 10 min finished on 5 min incubation on ice. Later, 20 µl of cDNA synthesis master mix, containing 5 mM MgCl₂, 1x PCR buffer II (10x), 1 mM dGTP, 1 mM dATP, 1 mM dTTP, 1 mM dCTP, 1 U/µl RNase inhibitor, and 2.5 U/µl MuLV reverse transcriptase was created and aliquot-ed into each sample and cDNA synthesis was carried out, according to the program shown below:

- Lid: 85°C (5-10°C higher to avoid lid condensation)
- Block: 37°C for 60min
- 75°C for 10min

Finally, the cDNA was then diluted up to 200 µl with a DNase/RNase-free water for usage in RT-qPCR analysis in -20°C.

9.2.4.4 Real-Time Quantitative Reverse-Transcriptase PCR (RT-qPCR) Analysis

The mRNA transcript levels were quantified using RT-qPCR, which was performed using the 96-well plate (Biozym, 712282, TW-MT-Platte, white) format on a Light Cycler® LC480II instrument (Roche) and LightCycler® 480 DNA SYBR Green I Master (Roche). Firstly, master mixes of primers, cDNA and DNA SYBR Green I, according to the table below:

Table 9.12. RT-qPCR reaction mix per one assay.

Reagent	Stock concentration	Final concentration	Final volume (µl)
---------	---------------------	---------------------	-------------------

Primer mix	10 μ M each	1 μ M each	1
DNase/RNase-free H₂O	N/A	N/A	1.5
SybrGreen	2x	1x	5
cDNA	6.25 ng/ μ l	1.56 ng/ μ l	2.5
		Final volume	10

Next, the final volumes of mastermixes were always calculated for 2 duplicates. Pipetting was performed on ice or on an ice block. Plates were sealed with aluminum foil to protect it from light and transported to the light cycler. Prior to measurements, the 96-well plates were centrifuged for 2 min at 1500 rpm. Detailed RT-qPCR protocol was carried out as shown below:

Table 9.13. RT-qPCR standard protocol.

Action	Temperature [°C]	Time [sec]	Number of cycles
pre-incubation	95	300	1
Amplification	95	5	45
	59	5	
	72	10	
	95	5	
Melting curve	60	60	1
	97	10	
	40	30	
Cooling	40	30	1

Quality and specificity of RT-qPCR was assessed by the melting curve evaluation. Of note, every primer was also tested for specificity by melting curve assessments. Then, fold changes relative to each control were calculated as $2^{-\Delta\Delta Ct}$ with $\Delta\Delta Ct = \Delta Ct (\text{exposure}) - \Delta Ct (\text{mock})$, where $\Delta Ct = Ct (\text{gene of interest}) - Ct (\text{reference})$ for each condition. All primers used are listed in Table 9.1 were used. Additionally, in each cigarette smoke exposure type, several reference genes were tested among DHX8, WDR89, GADPH or HPRT and the most stable gene for every exposure was chosen and later used for the relative mRNA expression standardization. Gene expression changes were always similar for at least two independent internal reference genes. All RT-qPCR reactions were performed in technical duplicates. The fold changes and significant changes were later visualized and calculated using GraphPad 9, respectively.

9.2.5 Protein analysis

9.2.5.1 Protein Isolation from differentiated primary human bronchial epithelial cells

Before every protein isolation, RIPA buffer (50 mM Tris•HCl, pH 7.6, 150 mM NaCl, 1% Nonidet P-40, 0.5% sodium deoxycholate, and 0.1% SDS) was freshly prepared on ice with the 25x Phosphatase protease inhibitor cocktail (05892970001, Roche, Basel, Switzerland) and the 10x PhosSTOP phosphatase inhibitor cocktail (PHOSS-RO, Roche). The inserts with cells were then placed on ice and left for thawing for approximately 5 min, washed twice in ice-cold HBSS and scraped into 80 µl RIPA buffer with a 1 ml pipette tip. To increase the protein yield, the wells or inserts were mixed once more with an equal amount of RIPA buffer and transferred to the same tube, followed by incubation on ice for 30 min. To remove cellular debris, tubes were centrifuged at 4°C for 15 min at 14,000 RPM. Finally supernatants were collected in new Eppendorf tubes and stored at -80°C.

9.2.5.2 Protein Isolation from basal primary human bronchial epithelial cells

Protein isolation of basal cells of bronchial epithelium was carried as above, with the exception of using 6-well plates (TRP, 92406, 8.96cm²/well) as cell culture plate, from which cells were scraped off with (DNA/RNA free cell scraper, TRP, 99002).

9.2.5.3 Bicinchoninic acid (BCA) assay

After protein isolation, total concentration was determined with Pierce™ BCA Protein Assay Kit (23225, Thermo Scientific, Rockford, USA) according to manufacturer's instructions. Briefly, bovine serum albumine (BSA) standards in 1 x RIPA were prepared in duplicates, according to serial dilutions as below:

2mg/ml, 1,5mg/ml, 1mg/ml, 0,75mg/ml, 0,5mg/ml, 0,25mg/ml, 0,125mg/ml, 0,0mg/ml

Samples were next placed on ice, along with previously used 1 x RIPA. The dilution of 1:5 was used, using 1 x RIPA as a diluent and performed in technical triplicates. Next 200 µl of BCA reagent mix (reagent A: reagent B = 50 : 1) was added to diluted proteins and incubated in 37°C for approximately 30-35 min. After 5 min of equilibration in a room temperature. The colorimetric measurements were performed on the Sunrise plate reader (TECAN, Switzerland), analyzed using Magellan 7.2 software (TECAN, Switzerland) and finally visualized GraphPad 9.

9.2.5.4 SDS-Polyacrylamide Gel Electrophoresis (SDS-PAGE)

For SDS-PAGE, samples were denatured with Laemmli buffer (65 mM Tris-HCl pH 6.8, 10% glycerol, 2% SDS, 0.01% bromophenol blue, 100 mM DTT) for 5 min in 95°C and separated on 10% or 12% polyacrylamide gels.

9.2.5.5 Immunoblotting

Proteins were then transferred to polyvinylidene difluoride (PVDF) membranes (Thermo Scientific, 88518, Rockford, USA) using a wet tank blotting system (Mini PROTEAN® Tetra Cell, 552BR, Bio-Rad, Munich, Germany). Blocking was performed for 30 min with 5% skimmed milk

in TBS-T (0.1% Tween 20, TBS), and then blocking repeated three times with approximately ml of TBS-T membranes could be either stored or incubated with accordingly diluted primary antibody (see Table 9.1) overnight at 4°C. On the next day, three washes for 10 min with TBS-T were again carried out. Diluted secondary antibodies were then added and incubated for 1-2 h in the room temperature and finally visualized using with SuperSignal™ West Pico, SuperSignal™ West Dura or SuperSignal™ West Femto Maximum Sensitivity Substrate, according to the intensity of the detected signals (all Thermo Fisher Scientific, 34079, 37071, 34095, respectively) on ChemiDocXRS+. Taken images were then analyzed the ImageLab 6.0.1 imaging system (both Bio-Rad, Munich, Germany). As a reference protein β -actin was used, visualized with Pierce ECL Western (Thermo Fisher Scientific, 32209).

9.2.5.6 Proteomic screening after chronic basolateral CSE exposure on phBECs

Sample preparation

ECM pellets of the individual samples were treated as described previously [317]. After solubilization in 6 M guanidinium-hydrochloride, 100 mM Tris/HCl, pH 8.5 and heating at 100 °C for 10 min, disulfide bridges were reduced by adding dithiothreitol followed by alkylation by iodoacetamide. Precipitation of alkylated ECM proteins was performed with ice-cold ethanol. Then, proteins were resuspended in 50 mM ammonium bicarbonate in pH 7.8. LysC (Wako Chemicals) and trypsin (Promega) was used for proteolytic digestion of ECM proteins. Afterwards, samples were heated at 100 °C, acidified with trifluoroacetic acid and stored at -20 °C. Samples were divided into soluble fractions of 10 μ g each and digested using a modified FASP procedure [318, 319]. Next, after DTT and IAA-induced reduction and alkylation, the proteins underwent centrifugation on a 30 kDa cutoff filter device (Sartorius). Next, each sample was washed each three times with UA buffer (8 M urea in 0.1 M Tris/HCl pH 8.5) and with 50 mM ammonium bicarbonate. Protein digestion was performed for 2 hours at room temperature with 0.5 μ g Lys-C and then for 16 hours at 37°C with 1 μ g trypsin (Promega). Finally, samples were centrifuged for 10 min at 14 000 g and the eluted peptides acidified with 0.5% TFA and stored at -20°C.

After thawing the samples, LC-MS/MS analysis was done on a Q-Exactive HF mass spectrometer (Thermo Scientific), coupled online with an Ultimate 3000 nano-RSLC (Thermo Scientific). Tryptic peptides were automatically loaded on a C18 trap column, at 30 μ l/min flow rate, before C18 reversed phase chromatography on the analytical column (nanoEase MZ HSS T3 Column, Waters) at 250 nl/min flow rate. Non-linear acetonitrile gradient was done from 3 to 40% in 0.1% formic acid for 95 minutes. Precursor spectra profiling from 300 to 1500 m/z was recorded at 60000 resolution and with an automatic gain control (AGC). A maximum precursor injection time was 50 ms. TOP10 fragment spectra of charges 2 to 7 were recorded at 15000 resolution with an AGC target of 1e5, a maximum injection time of 50 ms, with an isolation window of 1.6 m/z, a normalized collision energy of 27 and a dynamic exclusion of 30 seconds. In similar fashion, TOP15 fragment spectra of charges 2 to 7 were recorded at 15000 resolutions with an AGC target of 1e5, a maximum injection time of 50 ms, an isolation window of 1.6 m/z, normalized collision energy of 28 and a dynamic exclusion of 30 seconds.

9.2.6 Immunofluorescence staining

Along with mRNA and protein analyses, cell counting was performed at every time point assessed were also taken for immunofluorescence to assess cell compositions. Additionally, co-localization of chosen SERGs with cell-specific markers was assessed, as described previously [248]. Each performed treatment was followed by washing inserts twice with 1 x HBSS from apical and basolateral compartment, to both was added 3.7% paraformaldehyde (PFA) for 1 h at room temperature. After 1 h, PFA was washed to permeabilized immediately with 0.2% Triton X-100/PBS for 5 min at room temperature. Next, PFA was aspirated and the inserts were washed away in 1 x PBS and put for later storage at 4 °C. Then, 0.2% Triton X-100/PBS for 5 min at room temperature was used for cell permeabilization. Then, inserts were washed again with 1x PBS and blocked with 5% BSA/0.2% Tween/PBS, that lasted 1 h at room temperature. After next washing, the membranes with pHBECs were cut out of the transwells carefully with surgical scalpels into quarters or six pieces. Membrane fragments, were either stored back at 4 °C or transferred into 24-well filled with 150 µl of primary antibody (Table 9.1) dilutions with 5% BSA/0.2% Tween/PBS, were incubated for a duration of 1h at room temperature or overnight at 4°C. Afterwards, after washing in 1 x PBS three times, accordingly diluted, the secondary anti-body conjugated with either Alexa Fluor 488 or Alexa Fluor 568 listed in Table 9.2. As previous-ly for primary antibody dilutions, 5% BSA/0.2% Tween/PBS was used for a duration of 30 min at room temperature, at a volume of 150 µl and protected from light with an aluminum foil cover. 0.5 µg/ml of 4,6-diamidino-2-phenylindole (DAPI) at 1:2000 dilution was used for nuclei staining. After one more three-time washing with 1 x PBS for 5 min each, membranes were finally mounted with a fluorescent mounting medium (Dako, S3023, Hamburg, Germany), labeled and dried overnight. That way prepared slides were then imaged using an upright microscope (Axi-overt II; Carl Zeiss AG; Oberkochen, Germany). Images were processed using ZEN 2010 soft-ware (Carl Zeiss AG) and for cell counting Imaris 7.4.0 software (Bitplane; Zurich, Switzerland) was utilized.

9.2.7 *In silico* analysis

9.2.7.1 Proteomic analysis – Label-free quantification

Juliane Merl-Pham from the PROT Research Unit Protein Science at Helmholtz Zentrum kindly performed non-biased proteomic analysis of inserts collected from basolateral chronic 5% CSE exposure, at time points day 7, day 14, day 21 and day 28, as described in 8.2.3.5. After LC-MS/MS analysis, the acquired spectra were uploaded into the Progenesis Q1 proteomics software (Nonlinear Dynamics, part of Waters), as described previously (Hauck et al. Molecular & Cellular Proteomics. 2010; Merl et al. Proteomics. 2012). Charges' features were aligned and utilized for normalization, after which the corresponding MSMS spectra were saved as mgf file. Mascot search engine was used for peptide search (version 2.6.1) within the Swissprot Human protein database (Release 2017_02, 11,451,954 residues, 20,237 sequences). Search parameters:

- 10 ppm peptide mass tolerance
- 20 mμ fragment mass tolerance
- one missed cleavage allowed
- carbamidomethylation of cysteine was set as fixed modification

- methionine oxidation and asparagine or glutamine deamidation were allowed as variable modifications.
- For extracellular matrix (ECM) samples, oxidation of lysine and proline residues was additionally allowed as variable modification.
- false discovery rate of 0.55% for ECM samples and 0.38% for soluble samples,
- search was performed using Mascot percolator score.

As explained previously, immunofluorescence quantification was carried out in Imaris 7.4.0 software (Bitplane). Z-stack images of stained transwell membranes were obtained by a fluorescent microscopy, pictures sharpness increased with enhanced deep focus function and finally counted 1500 – 4500 cells per image were analyzed for positivity of specific markers or selected SERGs.

9.2.7.2 Immunofluorescence quantification

Immunofluorescence quantification was performed using Imaris 7.4.0 software (Bitplane). Z-stack images of stained transwell membranes were obtained by a fluorescent microscopy, pictures sharpness increased with enhanced deep focus function and finally counted 1500 – 4500 cells per image were analyzed for positivity of specific markers or selected SERGs.

9.2.7.3 Ingenuity pathway analysis (IPA)

Log fold changes and q-values representing differential expression profile of basolateral chronic CSE exposure were fed into the Ingenuity Pathway Analysis (IPA Tool; Ingenuity®Systems, Redwood City, CA, USA; <http://www.ingenuity.com>). There, a cut offs of logFC are used greater than 0.3 or lower than -0.3 and q-value lower than 0.05. 186 proteins were fulfilling these requirements. Then, these proteins along with were mapped onto Ingenuity Pathways Knowledge Base database (IPKB), derived from publicly available in literature of known interactions and proteins, and then ranked, which finally gave the basis to do multiple analyses. IPA was then used to identify and analyze enriched biological pathways, construct networks of interactions between proteins and master regulators as well as downstream functions and diseases. Data generated is based on the number of significantly expressed proteins. IPA generates also significance value of the genes, but also scores genes this target interacts directly or indirectly, including genes interaction predictions, i.e. genes not involved in the proteomic analysis. Networks or master regulations are scored or overlap significance, respectively, based on a number of the significantly expressed targets included. Visualized master regulator interactions (Figure 4.2) are networks of biological relationships between molecules. Interaction is defined as at least one references from the literature, stored in IPKB. Intensity of upregulation is depicted as green or red for downregulation, with shapes indicating various roles, explained in the legends accordingly.

9.2.7.4 Statistical Analysis

Results for each experiment are shown as mean \pm SD and derived from at least four independent experiments (independent donors). To assess normality of data distribution, every data set was tested for Gaussian distribution using the Shapiro-Wilk test. In single comparison experiments (i.e. wCS, acute apical 40% CSE, and basolateral acute 5% CSE exposure) data distribution was normal. Therefore, for these experiments a paired, two tailed student's *t*-test was used. Notably, few data sets from experiments with multiple comparisons (*i. e.* in submerged basal CSE, acute

apical CSE, and basolateral chronic CSE exposure) was not normal. However, due to small sample pool (n=4 or n=5) tests for normal distribution have low sensitivity, nevertheless parametric test methods were used. It is a more suitable option for very small sample sizes, while accepting the risk that normal distribution assumption may not be met in each data set group. Thence, repeated measures ANOVA with Bonferroni correction was used for all multiple comparisons. To address the risk of false positives non-parametric testing for the few data sets, that were not normally distributed a Friedman test with Dunn's correction was used and it did not change the overall results. Finally, statistical significance was reached for the same genes, notably with higher p-values, which predictably emphasizes lower statistical power of the non-parametric test.

In other tests, where the baseline expression of AhR-responsive SERGs was compared (Figure 3.16) a non-parametric Friedman test with Dunn's correction was performed, whereas significance between donors in baseline expression levels of SERGs (Figure 3.15) was tested by using one-way ANOVA with Bonferroni correction. Unpaired two tailed student's *t*-test was used while assessing significance in CSE gravimetric measurements (Figure 3.1). The information which test was used in each experiment is also given in the figure legend and where applicable. All statistical calculations in aforementioned tests were carried out in GraphPad Prism 8 Software (GraphPad Software, San Francisco, CA). Significance levels: * $p < 0.05$, ** $p < 0.01$, *** $p < 0.001$ **** $p < 0.0001$.

9.2.7.5 Bioinformatical analysis

For proteomic data on chronic basolateral CSE exposure, statistical programming software R (Development Core Team) was used by Hannah Marchi and Ronan le Gleut from Core Facility Statistical Consulting at Helmholtz Zentrum, who kindly performed differential expression analysis. List of used packages is enclosed in Appendix A. Analysis was performed on four donors and 4 time points (day 7, day 14, day 21, day 28). In short, variance stabilization and normalization was done with R package vsn. ComBat package was utilized to correct data for the patient (batch) effect. With package blme a Bayesian linear mixed effect regression independently for each protein. Finally, a Wald test with Storey correction was implemented to find differentially expressed proteins. Significance level: $q < 0.05$.

References

- [1] J. Domagala-Kulawik, "Effects of cigarette smoke on the lung and systemic immunity," (in eng), *J. Physiol. Pharmacol.*, vol. 59 Suppl 6, pp. 19-34, Dec 2008.
- [2] D. P. Jones, D. I. Walker, K. Uppal, P. Rohrbeck, C. T. Mallon, and Y. M. Go, "Metabolic Pathways and Networks Associated With Tobacco Use in Military Personnel," (in eng), *J. Occup. Environ. Med.*, vol. 58, no. 8 Suppl 1, pp. S111-6, Aug 2016, doi: 10.1097/jom.0000000000000763.
- [3] J. Liu *et al.*, "NUPR1 is a critical repressor of ferroptosis," *Nature Communications*, vol. 12, no. 1, p. 647, 2021/01/28 2021, doi: 10.1038/s41467-021-20904-2.
- [4] M. Ball, M. Hossain, and D. Padalia, "Anatomy, Airway," in *StatPearls*. Treasure Island (FL), 2021.
- [5] I. R. Morris, "Functional anatomy of the upper airway," (in eng), *Emerg. Med. Clin. North Am.*, vol. 6, no. 4, pp. 639-69, Nov 1988.
- [6] A. Tam, S. Wadsworth, D. Dorscheid, S. F. Man, and D. D. Sin, "The airway epithelium: more than just a structural barrier," *Ther. Adv. Respir. Dis.*, vol. 5, no. 4, pp. 255-73, Aug 2011, doi: 10.1177/1753465810396539.
- [7] E. R. Weibel, B. Sapoval, and M. Filoche, "Design of peripheral airways for efficient gas exchange," *Respir. Physiol. Neurobiol.*, vol. 148, no. 1, pp. 3-21, 2005/08/25/ 2005, doi: <https://doi.org/10.1016/j.resp.2005.03.005>.
- [8] A. M. Vignola and J. Bousquet, "The aging lung: A challenging entity in respiratory medicine," *Curr. Allergy Asthma Rep.*, vol. 1, no. 1, pp. 1-2, 2001/01/01 2001, doi: 10.1007/s11882-001-0086-3.
- [9] M. Ochs *et al.*, "The number of alveoli in the human lung," (in eng), *Am J Respir Crit Care Med*, vol. 169, no. 1, pp. 120-4, Jan 1 2004, doi: 10.1164/rccm.200308-1107OC.
- [10] P. Gehr, M. Bachofen, and E. R. Weibel, "The normal human lung: ultrastructure and morphometric estimation of diffusion capacity," (in eng), *Respir. Physiol.*, vol. 32, no. 2, pp. 121-40, Feb 1978, doi: 10.1016/0034-5687(78)90104-4.
- [11] P. B. Dominelli *et al.*, "Sex differences in large conducting airway anatomy," (in eng), *J Appl Physiol (1985)*, vol. 125, no. 3, pp. 960-965, Sep 1 2018, doi: 10.1152/jappphysiol.00440.2018.
- [12] A. S. Verkman, Y. Song, and J. R. Thiagarajah, "Role of airway surface liquid and submucosal glands in cystic fibrosis lung disease," (in eng), *Am. J. Physiol. Cell Physiol.*, vol. 284, no. 1, pp. C2-15, Jan 2003, doi: 10.1152/ajpcell.00417.2002.
- [13] R. G. Crystal, S. H. Randell, J. F. Engelhardt, J. Voynow, and M. E. Sunday, "Airway epithelial cells: current concepts and challenges," (in eng), *Proc. Am. Thorac. Soc.*, vol. 5, no. 7, pp. 772-7, Sep 15 2008, doi: 10.1513/pats.200805-041HR.
- [14] H. Yoshisue *et al.*, "Characterization of Ciliated Bronchial Epithelium 1, a Ciliated Cell-Associated Gene Induced During Mucociliary Differentiation," *Am. J. Respir. Cell Mol. Biol.*, vol. 31, no. 5, pp. 491-500, 2004, doi: 10.1165/rcmb.2004-0050OC.
- [15] P. S. Hiemstra, P. B. McCray, Jr., and R. Bals, "The innate immune function of airway epithelial cells in inflammatory lung disease," (in eng), *The European respiratory journal*, vol. 45, no. 4, pp. 1150-1162, 2015, doi: 10.1183/09031936.00141514.
- [16] I. Salwig *et al.*, "Bronchioalveolar stem cells are a main source for regeneration of distal lung epithelia in vivo," *The EMBO Journal*, vol. 38, no. 12, p. e102099, 2019, doi: <https://doi.org/10.15252/embj.2019102099>.
- [17] J. D. Davis and T. P. Wypych, "Cellular and functional heterogeneity of the airway epithelium," *Mucosal Immunol.*, vol. 14, no. 5, pp. 978-990, 2021/09/01 2021, doi: 10.1038/s41385-020-00370-7.
- [18] D.-P. Dao, "Histology, Goblet Cells," *StatPearls*, 2021 2021.

- [19] W. Rokicki, M. Rokicki, J. Wojtacha, and A. Dželjijli, "The role and importance of club cells (Clara cells) in the pathogenesis of some respiratory diseases," (in eng), *Kardiochirurgia Pol.*, vol. 13, no. 1, pp. 26-30, Mar 2016, doi: 10.5114/kitp.2016.58961.
- [20] D. T. Montoro *et al.*, "A revised airway epithelial hierarchy includes CFTR-expressing ionocytes," *Nature*, vol. 560, no. 7718, pp. 319-324, 2018/08/01 2018, doi: 10.1038/s41586-018-0393-7.
- [21] J. D. Davis and T. P. Wypych, "Cellular and functional heterogeneity of the airway epithelium," *Mucosal Immunol.*, 2021/02/19 2021, doi: 10.1038/s41385-020-00370-7.
- [22] X. M. Bustamante-Marin and L. E. Ostrowski, "Cilia and Mucociliary Clearance," (in eng), *Cold Spring Harb. Perspect. Biol.*, vol. 9, no. 4, Apr 3 2017, doi: 10.1101/cshperspect.a028241.
- [23] A. E. Tilley, M. S. Walters, R. Shaykhiev, and R. G. Crystal, "Cilia dysfunction in lung disease," (in eng), *Annu. Rev. Physiol.*, vol. 77, pp. 379-406, 2015, doi: 10.1146/annurev-physiol-021014-071931.
- [24] G. Matute-Bello, "The Pulmonary Epithelium in Health and Disease," *Respir. Care*, vol. 54, no. 9, p. 1272, 2009. [Online]. Available: <http://rc.rcjournal.com/content/54/9/1272.abstract>.
- [25] T. Raman *et al.*, "Quality control in microarray assessment of gene expression in human airway epithelium," (in eng), *BMC Genomics*, vol. 10, p. 493, Oct 24 2009, doi: 10.1186/1471-2164-10-493.
- [26] R. Hajj, T. Baranek, R. Le Naour, P. Lesimple, E. Puchelle, and C. Coraux, "Basal cells of the human adult airway surface epithelium retain transit-amplifying cell properties," (in eng), *Stem Cells*, vol. 25, no. 1, pp. 139-48, Jan 2007, doi: 10.1634/stemcells.2006-0288.
- [27] J. E. Boers, A. W. Amberg, and F. B. Thunnissen, "Number and proliferation of basal and parabasal cells in normal human airway epithelium," *Am J Respir Crit Care Med*, vol. 157, no. 6 Pt 1, pp. 2000-6, Jun 1998, doi: 10.1164/ajrccm.157.6.9707011.
- [28] H. Mou *et al.*, "Airway basal stem cells generate distinct subpopulations of PNECs," (in eng), *Cell Rep*, vol. 35, no. 3, p. 109011, Apr 20 2021, doi: 10.1016/j.celrep.2021.109011.
- [29] H. A. Ting and J. von Moltke, "The Immune Function of Tuft Cells at Gut Mucosal Surfaces and Beyond," (in eng), *J Immunol*, vol. 202, no. 5, pp. 1321-1329, Mar 1 2019, doi: 10.4049/jimmunol.1801069.
- [30] J. Pan, L. Zhang, X. Shao, and J. Huang, "Acetylcholine From Tuft Cells: The Updated Insights Beyond Its Immune and Chemosensory Functions," (in eng), *Front Cell Dev Biol*, vol. 8, p. 606, 2020, doi: 10.3389/fcell.2020.00606.
- [31] T. E. Billipp, M. S. Nadjisombati, and J. von Moltke, "Tuning tuft cells: new ligands and effector functions reveal tissue-specific function," (in eng), *Curr. Opin. Immunol.*, vol. 68, pp. 98-106, Feb 2021, doi: 10.1016/j.coi.2020.09.006.
- [32] J. V. Wu, M. E. Krouse, and J. J. Wine, "Acinar origin of CFTR-dependent airway submucosal gland fluid secretion," *American Journal of Physiology-Lung Cellular and Molecular Physiology*, vol. 292, no. 1, pp. L304-L311, 2007, doi: 10.1152/ajplung.00286.2006.
- [33] D.-Y. Kim *et al.*, "The Airway Antigen Sampling System: Respiratory M Cells as an Alternative Gateway for Inhaled Antigens," *The Journal of Immunology*, vol. 186, no. 7, pp. 4253-4262, 2011, doi: 10.4049/jimmunol.0903794.
- [34] S. Kimura *et al.*, "Airway M Cells Arise in the Lower Airway Due to RANKL Signaling and Reside in the Bronchiolar Epithelium Associated With iBALT in Murine Models of Respiratory Disease," (in eng), *Front Immunol*, vol. 10, p. 1323, 2019, doi: 10.3389/fimmu.2019.01323.
- [35] L. W. Plasschaert *et al.*, "A single-cell atlas of the airway epithelium reveals the CFTR-rich pulmonary ionocyte," (in eng), *Nature*, vol. 560, no. 7718, pp. 377-381, Aug 2018, doi: 10.1038/s41586-018-0394-6.

- [36] D. Duke, E. Wohlgemuth, K. R. Adams, A. Armstrong-Ingram, S. K. Rice, and D. C. Young, "Earliest evidence for human use of tobacco in the Pleistocene Americas," *Nature Human Behaviour*, 2021/10/11 2021, doi: 10.1038/s41562-021-01202-9.
- [37] A. W. MUSK and N. H. DE KLERK, "History of tobacco and health," *Respirology*, vol. 8, no. 3, pp. 286-290, 2003, doi: <https://doi.org/10.1046/j.1440-1843.2003.00483.x>.
- [38] E. Boliwerk, *Perspectives on the archaeology of pipes, tobacco and other smoke plants in the ancient Americas*. New York, NY: Springer Science+Business Media, 2015.
- [39] R. N. Proctor, "The Global Smoking Epidemic: A History and Status Report," *Clin. Lung Cancer*, vol. 5, no. 6, pp. 371-376, 2004/05/01/ 2004, doi: <https://doi.org/10.3816/CLC.2004.n.016>.
- [40] M. Ng *et al.*, "Smoking prevalence and cigarette consumption in 187 countries, 1980-2012," (in eng), *JAMA*, vol. 311, no. 2, pp. 183-92, Jan 8 2014, doi: 10.1001/jama.2013.284692.
- [41] R. Doll, "Uncovering the effects of smoking: historical perspective," *Stat. Methods Med. Res.*, vol. 7, no. 2, pp. 87-117, 1998, doi: 10.1177/096228029800700202.
- [42] P. Jha *et al.*, "Global Hazards of Tobacco and the Benefits of Smoking Cessation and Tobacco Taxes," in *Cancer: Disease Control Priorities, Third Edition (Volume 3)*, H. Gelband, P. Jha, R. Sankaranarayanan, and S. Horton Eds. Washington (DC), 2015.
- [43] X. Wang, J. Xu, L. Wang, C. Liu, and H. Wang, "The role of cigarette smoking and alcohol consumption in the differentiation of oral squamous cell carcinoma for the males in China," (in eng), *J Cancer Res Ther*, vol. 11, no. 1, pp. 141-5, Jan-Mar 2015, doi: 10.4103/0973-1482.137981.
- [44] X. Jiang, J. Wu, J. Wang, and R. Huang, "Tobacco and oral squamous cell carcinoma: A review of carcinogenic pathways," (in eng), *Tob. Induc. Dis.*, vol. 17, p. 29, 2019, doi: 10.18332/tid/105844.
- [45] S. D. Stellman, J. E. Muscat, S. Thompson, D. Hoffmann, and E. L. Wynder, "Risk of squamous cell carcinoma and adenocarcinoma of the lung in relation to lifetime filter cigarette smoking," (in eng), *Cancer*, vol. 80, no. 3, pp. 382-8, Aug 1 1997, doi: 10.1002/(sici)1097-0142(19970801)80:3<382::aid-cnrcr5>3.0.co;2-u.
- [46] P. M. Bracci *et al.*, "Cigarette smoking associated with lung adenocarcinoma in situ in a large case-control study (SFBALCS)," (in eng), *J. Thorac. Oncol.*, vol. 7, no. 9, pp. 1352-60, Sep 2012, doi: 10.1097/JTO.0b013e31825aba47.
- [47] K. E. Osann, J. T. Lowery, and M. J. Schell, "Small cell lung cancer in women: risk associated with smoking, prior respiratory disease, and occupation," (in eng), *Lung Cancer*, vol. 28, no. 1, pp. 1-10, Apr 2000, doi: 10.1016/s0169-5002(99)00106-3.
- [48] B. Secretan *et al.*, "A review of human carcinogens—Part E: tobacco, areca nut, alcohol, coal smoke, and salted fish," (in en), *The Lancet Oncology*, vol. 10, no. 11, pp. 1033-1034, 2009/11// 2009, doi: 10.1016/S1470-2045(09)70326-2.
- [49] M. Bartal, "COPD and tobacco smoke," (in eng), *Monaldi Arch. Chest Dis.*, vol. 63, no. 4, pp. 213-25, Dec 2005, doi: 10.4081/monaldi.2005.623.
- [50] J. M. Sethi and C. L. Rochester, "Smoking and chronic obstructive pulmonary disease," (in eng), *Clin Chest Med*, vol. 21, no. 1, pp. 67-86, viii, Mar 2000, doi: 10.1016/s0272-5231(05)70008-3.
- [51] N. Terzikhan, K. M. Verhamme, A. Hofman, B. H. Stricker, G. G. Brusselle, and L. Lahousse, "Prevalence and incidence of COPD in smokers and non-smokers: the Rotterdam Study," (in eng), *Eur. J. Epidemiol.*, vol. 31, no. 8, pp. 785-92, Aug 2016, doi: 10.1007/s10654-016-0132-z.
- [52] A. G. Wheaton *et al.*, "Chronic Obstructive Pulmonary Disease and Smoking Status - United States, 2017," (in eng), *MMWR Morb. Mortal. Wkly. Rep.*, vol. 68, no. 24, pp. 533-538, Jun 21 2019, doi: 10.15585/mmwr.mm6824a1.

- [53] D. P. Tashkin and R. P. Murray, "Smoking cessation in chronic obstructive pulmonary disease," (in eng), *Respir. Med.*, vol. 103, no. 7, pp. 963-74, Jul 2009, doi: 10.1016/j.rmed.2009.02.013.
- [54] J. L. Townsend and T. W. Meade, "Ischaemic heart disease mortality risks for smokers and non-smokers," (in eng), *J. Epidemiol. Community Health*, vol. 33, no. 4, pp. 243-7, Dec 1979, doi: 10.1136/jech.33.4.243.
- [55] J. Barry *et al.*, "Effect of smoking on the activity of ischemic heart disease," (in eng), *JAMA*, vol. 261, no. 3, pp. 398-402, Jan 20 1989.
- [56] K. Hbejan, "Smoking effect on ischemic heart disease in young patients," (in eng), *Heart Views*, vol. 12, no. 1, pp. 1-6, Jan 2011, doi: 10.4103/1995-705x.81547.
- [57] R. S. Shah and J. W. Cole, "Smoking and stroke: the more you smoke the more you stroke," (in eng), *Expert Rev. Cardiovasc. Ther.*, vol. 8, no. 7, pp. 917-32, Jul 2010, doi: 10.1586/erc.10.56.
- [58] B. Pan, X. Jin, L. Jun, S. Qiu, Q. Zheng, and M. Pan, "The relationship between smoking and stroke: A meta-analysis," (in eng), *Medicine (Baltimore)*, vol. 98, no. 12, p. e14872, Mar 2019, doi: 10.1097/md.00000000000014872.
- [59] M. A. Venditto, "Therapeutic considerations: lower respiratory tract infections in smokers," (in eng), *J. Am. Osteopath. Assoc.*, vol. 92, no. 7, pp. 897-900, 903-5, Jul 1992.
- [60] T. W. Marcy and W. W. Merrill, "Cigarette smoking and respiratory tract infection," (in eng), *Clin Chest Med*, vol. 8, no. 3, pp. 381-91, Sep 1987.
- [61] B. Eliasson, "Cigarette smoking and diabetes," (in eng), *Prog. Cardiovasc. Dis.*, vol. 45, no. 5, pp. 405-13, Mar-Apr 2003, doi: 10.1053/pcad.2003.00103.
- [62] J. Maddatu, E. Anderson-Baucum, and C. Evans-Molina, "Smoking and the risk of type 2 diabetes," (in eng), *Transl. Res.*, vol. 184, pp. 101-107, Jun 2017, doi: 10.1016/j.trsl.2017.02.004.
- [63] D. Campagna *et al.*, "Smoking and diabetes: dangerous liaisons and confusing relationships," (in eng), *Diabetol. Metab. Syndr.*, vol. 11, p. 85, 2019, doi: 10.1186/s13098-019-0482-2.
- [64] J. Xia *et al.*, "Cigarette smoking and chronic kidney disease in the general population: a systematic review and meta-analysis of prospective cohort studies," (in eng), *Nephrol. Dial. Transplant.*, vol. 32, no. 3, pp. 475-487, Mar 1 2017, doi: 10.1093/ndt/gfw452.
- [65] C. Jones-Burton *et al.*, "Cigarette smoking and incident chronic kidney disease: a systematic review," (in eng), *Am. J. Nephrol.*, vol. 27, no. 4, pp. 342-51, 2007, doi: 10.1159/000103382.
- [66] T. C. Durazzo, N. Mattsson, M. W. Weiner, and I. Alzheimer's Disease Neuroimaging, "Smoking and increased Alzheimer's disease risk: a review of potential mechanisms," *Alzheimers Dement*, vol. 10, no. 3 Suppl, pp. S122-45, Jun 2014, doi: 10.1016/j.jalz.2014.04.009.
- [67] J. K. Cataldo, J. J. Prochaska, and S. A. Glantz, "Cigarette smoking is a risk factor for Alzheimer's Disease: an analysis controlling for tobacco industry affiliation," (in eng), *J. Alzheimers Dis.*, vol. 19, no. 2, pp. 465-80, 2010, doi: 10.3233/jad-2010-1240.
- [68] P. M. Joseph, M. L. Witten, C. H. Burke, and C. A. Hales, "The Effects of Chronic Sidestream Cigarette Smoke Exposure on Eicosanoid Production by Tracheal Epithelium," *Exp. Lung Res.*, vol. 22, no. 3, pp. 317-335, 1996/01/01 1996, doi: 10.3109/01902149609031778.
- [69] M. R. Law, J. K. Morris, and N. J. Wald, "Environmental tobacco smoke exposure and ischaemic heart disease: an evaluation of the evidence," (in eng), *BMJ*, vol. 315, no. 7114, pp. 973-80, Oct 18 1997, doi: 10.1136/bmj.315.7114.973.

- [70] S. P. Doherty, J. Grabowski, C. Hoffman, S. P. Ng, and J. T. Zelikoff, "Early life insult from cigarette smoke may be predictive of chronic diseases later in life," *Biomarkers*, vol. 14, no. sup1, pp. 97-101, 2009/07/01 2009, doi: 10.1080/13547500902965898.
- [71] D. Hoffmann, I. Hoffmann, and K. El-Bayoumy, "The less harmful cigarette: a controversial issue. a tribute to Ernst L. Wynder," (in eng), *Chem. Res. Toxicol.*, vol. 14, no. 7, pp. 767-90, Jul 2001, doi: 10.1021/tx000260u.
- [72] S. S. Hecht, "Lung carcinogenesis by tobacco smoke," *Int. J. Cancer*, vol. 131, no. 12, pp. 2724-2732, 2012, doi: <https://doi.org/10.1002/ijc.27816>.
- [73] M. E. Counts, F. S. Hsu, S. W. Laffoon, R. W. Dwyer, and R. H. Cox, "Mainstream smoke constituent yields and predicting relationships from a worldwide market sample of cigarette brands: ISO smoking conditions," (in eng), *Regul. Toxicol. Pharmacol.*, vol. 39, no. 2, pp. 111-34, Apr 2004, doi: 10.1016/j.yrtph.2003.12.005.
- [74] J. C. Morgan, M. J. Byron, S. A. Baig, I. Stepanov, and N. T. Brewer, "How people think about the chemicals in cigarette smoke: a systematic review," (in eng), *J. Behav. Med.*, vol. 40, no. 4, pp. 553-564, Aug 2017, doi: 10.1007/s10865-017-9823-5.
- [75] "Wood dust and formaldehyde: IARC Monographs on the Evaluation of Carcinogenic Risks to Humans. Volume 62. International Agency for Research on Cancer, Lyon, France, 1995; 406 pp. Sw. Fr. 80, ISBN 92 832 1262 2," (in en), *Cancer Causes Control*, vol. 6, no. 6, pp. 574-575, 1995/11// 1995, doi: 10.1007/BF00054167.
- [76] N. Moretto, G. Volpi, F. Pastore, and F. Facchinetti, "Acrolein effects in pulmonary cells: relevance to chronic obstructive pulmonary disease," (in eng), *Ann. N. Y. Acad. Sci.*, vol. 1259, pp. 39-46, Jul 2012, doi: 10.1111/j.1749-6632.2012.06531.x.
- [77] "Acetaldehyde," ed: International Agency for Research on Cancer (IARC), 1999.
- [78] C. R. Gilbert, M. Baram, and N. C. Cavarocchi, "'Smoking wet': respiratory failure related to smoking tainted marijuana cigarettes," (in eng), *Tex. Heart Inst. J.*, vol. 40, no. 1, pp. 64-7, 2013.
- [79] R. H. Demling, "Smoke inhalation lung injury: an update," (in eng), *Eplasty*, vol. 8, p. e27, May 16 2008.
- [80] N. L. Benowitz, "Cigarette smoking and cardiovascular disease: pathophysiology and implications for treatment," (in eng), *Prog. Cardiovasc. Dis.*, vol. 46, no. 1, pp. 91-111, Jul-Aug 2003, doi: 10.1016/s0033-0620(03)00087-2.
- [81] S. Zevin, S. Saunders, S. G. Gourlay, P. Jacob, and N. L. Benowitz, "Cardiovascular effects of carbon monoxide and cigarette smoking," (in eng), *J. Am. Coll. Cardiol.*, vol. 38, no. 6, pp. 1633-8, Nov 15 2001, doi: 10.1016/s0735-1097(01)01616-3.
- [82] A. Rodgman, C. J. Smith, and T. A. Perfetti, "The composition of cigarette smoke: a retrospective, with emphasis on polycyclic components," *Hum. Exp. Toxicol.*, vol. 19, no. 10, pp. 573-595, 2000/10/01 2000, doi: 10.1191/096032700701546514.
- [83] S. S. Hecht, "Tobacco Smoke Carcinogens and Lung Cancer," *JNCI: Journal of the National Cancer Institute*, vol. 91, no. 14, pp. 1194-1210, 1999, doi: 10.1093/jnci/91.14.1194.
- [84] B. Prokopczyk *et al.*, "Improved Methodology for the Quantitative Assessment of Tobacco-Specific N-Nitrosamines in Tobacco by Supercritical Fluid Extraction," (in en), *J. Agric. Food. Chem.*, vol. 43, no. 4, pp. 916-922, 1995/04// 1995, doi: 10.1021/jf00052a013.
- [85] I. Stepanov, E. Sebero, R. Wang, Y. T. Gao, S. S. Hecht, and J. M. Yuan, "Tobacco-specific N-nitrosamine exposures and cancer risk in the Shanghai Cohort Study: remarkable coherence with rat tumor sites," (in eng), *Int. J. Cancer*, vol. 134, no. 10, pp. 2278-83, May 15 2014, doi: 10.1002/ijc.28575.
- [86] I. Stepanov, S. S. Hecht, S. Ramakrishnan, and P. C. Gupta, "Tobacco-specific nitrosamines in smokeless tobacco products marketed in India," (in eng), *Int. J. Cancer*, vol. 116, no. 1, pp. 16-9, Aug 10 2005, doi: 10.1002/ijc.20966.

- [87] R. Goldman *et al.*, "Smoking increases carcinogenic polycyclic aromatic hydrocarbons in human lung tissue," (in eng), *Cancer Res*, vol. 61, no. 17, pp. 6367-71, Sep 1 2001.
- [88] B. G. Armstrong and G. Gibbs, "Exposure-response relationship between lung cancer and polycyclic aromatic hydrocarbons (PAHs)," (in eng), *Occup. Environ. Med.*, vol. 66, no. 11, pp. 740-6, Nov 2009, doi: 10.1136/oem.2008.043711.
- [89] Y. S. Ding, D. L. Ashley, and C. H. Watson, "Determination of 10 carcinogenic polycyclic aromatic hydrocarbons in mainstream cigarette smoke," (in eng), *J Agric Food Chem*, vol. 55, no. 15, pp. 5966-73, Jul 25 2007, doi: 10.1021/jf070649o.
- [90] *IARC Monographs on the Identification of Carcinogenic Hazards to Humans*. International Agency for Research on Cancer, 1987.
- [91] R. Khlifi and A. Hamza-Chaffai, "Head and neck cancer due to heavy metal exposure via tobacco smoking and professional exposure: a review," (in eng), *Toxicol. Appl. Pharmacol.*, vol. 248, no. 2, pp. 71-88, Oct 15 2010, doi: 10.1016/j.taap.2010.08.003.
- [92] M. G. Cumberbatch, M. Rota, J. W. Catto, and C. La Vecchia, "The Role of Tobacco Smoke in Bladder and Kidney Carcinogenesis: A Comparison of Exposures and Meta-analysis of Incidence and Mortality Risks," (in eng), *Eur. Urol.*, vol. 70, no. 3, pp. 458-66, Sep 2016, doi: 10.1016/j.eururo.2015.06.042.
- [93] C. J. Brown and J. M. Cheng, "Electronic cigarettes: product characterisation and design considerations," (in eng), *Tob. Control*, vol. 23 Suppl 2, no. Suppl 2, pp. ii4-10, May 2014, doi: 10.1136/tobaccocontrol-2013-051476.
- [94] D. B. Abrams, A. M. Glasser, J. L. Pearson, A. C. Villanti, L. K. Collins, and R. S. Niaura, "Harm Minimization and Tobacco Control: Reframing Societal Views of Nicotine Use to Rapidly Save Lives," *Annu. Rev. Public Health*, vol. 39, no. 1, pp. 193-213, 2018, doi: 10.1146/annurev-publhealth-040617-013849.
- [95] D. J. K. Balfour *et al.*, "Balancing Consideration of the Risks and Benefits of E-Cigarettes," *Am. J. Public Health*, vol. 111, no. 9, pp. 1661-1672, 2021, doi: 10.2105/ajph.2021.306416.
- [96] W. G. Kuschner, A. D'Alessandro, H. Wong, and P. D. Blanc, "Dose-dependent cigarette smoking-related inflammatory responses in healthy adults," (in eng), *Eur Respir J*, vol. 9, no. 10, pp. 1989-94, Oct 1996, doi: 10.1183/09031936.96.09101989.
- [97] W. J. Muller, G. D. Hess, and P. W. Scherer, "A model of cigarette smoke particle deposition," (in eng), *Am. Ind. Hyg. Assoc. J.*, vol. 51, no. 5, pp. 245-56, May 1990, doi: 10.1080/15298669091369600.
- [98] "Regional Lung Deposition: In Vivo Data," *J. Aerosol Med. Pulm. Drug Deliv.*, vol. 33, no. 6, pp. 291-299, 2020, doi: 10.1089/jamp.2020.29032.sh.
- [99] M. V. Djordjevic, S. D. Stellman, and E. Zang, "Doses of nicotine and lung carcinogens delivered to cigarette smokers," (in eng), *J. Natl. Cancer Inst.*, vol. 92, no. 2, pp. 106-11, Jan 19 2000, doi: 10.1093/jnci/92.2.106.
- [100] W. Hinds, M. W. First, G. L. Huber, and J. W. Shea, "A method for measuring respiratory deposition of cigarette smoke during smoking," (in eng), *Am. Ind. Hyg. Assoc. J.*, vol. 44, no. 2, pp. 113-8, Feb 1983, doi: 10.1080/15298668391404473.
- [101] A. R. Paul, F. Khan, A. Jain, and S. C. Saha, "Deposition of Smoke Particles in Human Airways with Realistic Waveform," *Atmosphere*, vol. 12, no. 7, p. 912, 2021. [Online]. Available: <https://www.mdpi.com/2073-4433/12/7/912>.
- [102] G. A. Giotopoulou and G. T. Stathopoulos, "Effects of Inhaled Tobacco Smoke on the Pulmonary Tumor Microenvironment," (in eng), *Adv. Exp. Med. Biol.*, vol. 1225, pp. 53-69, 2020, doi: 10.1007/978-3-030-35727-6_4.
- [103] "Tobacco smoke and involuntary smoking," (in eng), *IARC Monogr. Eval. Carcinog. Risks Hum.*, vol. 83, pp. 1-1438, 2004.

- [104] C. M. Dresler, M. E. León, K. Straif, R. Baan, and B. Secretan, "Reversal of risk upon quitting smoking," *The Lancet*, vol. 368, no. 9533, pp. 348-349, 2006/07/29/ 2006, doi: [https://doi.org/10.1016/S0140-6736\(06\)69086-7](https://doi.org/10.1016/S0140-6736(06)69086-7).
- [105] P. G. Shields, "Molecular epidemiology of smoking and lung cancer," (in eng), *Oncogene*, vol. 21, no. 45, pp. 6870-6, Oct 7 2002, doi: 10.1038/sj.onc.1205832.
- [106] L. Garfinkel and S. D. Stellman, "Smoking and lung cancer in women: findings in a prospective study," (in eng), *Cancer Res*, vol. 48, no. 23, pp. 6951-5, Dec 1 1988.
- [107] R. Peto, S. Darby, H. Deo, P. Silcocks, E. Whitley, and R. Doll, "Smoking, smoking cessation, and lung cancer in the UK since 1950: combination of national statistics with two case-control studies," (in eng), *BMJ*, vol. 321, no. 7257, pp. 323-9, Aug 5 2000, doi: 10.1136/bmj.321.7257.323.
- [108] J. O. Ebbert *et al.*, "Lung cancer risk reduction after smoking cessation: observations from a prospective cohort of women," (in eng), *J. Clin. Oncol.*, vol. 21, no. 5, pp. 921-6, Mar 1 2003, doi: 10.1200/jco.2003.05.085.
- [109] K. Yoshida *et al.*, "Tobacco smoking and somatic mutations in human bronchial epithelium," (in eng), *Nature*, vol. 578, no. 7794, pp. 266-272, Feb 2020, doi: 10.1038/s41586-020-1961-1.
- [110] A. C. Gower, K. Steiling, J. F. Brothers, 2nd, M. E. Lenburg, and A. Spira, "Transcriptomic studies of the airway field of injury associated with smoking-related lung disease," (in eng), *Proc. Am. Thorac. Soc.*, vol. 8, no. 2, pp. 173-9, May 2011, doi: 10.1513/pats.201011-066MS.
- [111] J. C. Willey *et al.*, "Quantitative RT-PCR measurement of cytochromes p450 1A1, 1B1, and 2B7, microsomal epoxide hydrolase, and NADPH oxidoreductase expression in lung cells of smokers and nonsmokers," (in eng), *Am J Respir Cell Mol Biol*, vol. 17, no. 1, pp. 114-24, Jul 1997, doi: 10.1165/ajrcmb.17.1.2783.
- [112] M. C. Boelens *et al.*, "Current smoking-specific gene expression signature in normal bronchial epithelium is enhanced in squamous cell lung cancer," (in eng), *J Pathol*, vol. 218, no. 2, pp. 182-91, Jun 2009, doi: 10.1002/path.2520.
- [113] M. Woenckhaus *et al.*, "Smoking and cancer-related gene expression in bronchial epithelium and non-small-cell lung cancers," (in eng), *J Pathol*, vol. 210, no. 2, pp. 192-204, Oct 2006, doi: 10.1002/path.2039.
- [114] A. Spira *et al.*, "Effects of cigarette smoke on the human airway epithelial cell transcriptome," *Proc Natl Acad Sci U S A*, vol. 101, no. 27, pp. 10143-8, Jul 6 2004, doi: 10.1073/pnas.0401422101.
- [115] "The top 10 causes of death." World Health Organisation. <https://www.who.int/news-room/fact-sheets/detail/the-top-10-causes-of-death> (accessed 20 Oct, 2020).
- [116] A. D. Lopez *et al.*, "Chronic obstructive pulmonary disease: current burden and future projections," *Eur. Respir. J.*, vol. 27, no. 2, pp. 397-412, 2006, doi: 10.1183/09031936.06.00025805.
- [117] D. Adeloye *et al.*, "Global and regional estimates of COPD prevalence: Systematic review and meta-analysis," (in eng), *J Glob Health*, vol. 5, no. 2, p. 020415, Dec 2015, doi: 10.7189/jogh.05-020415.
- [118] A. C. Schamberger, C. A. Staab-Weijnitz, N. Mise-Racek, and O. Eickelberg, "Cigarette smoke alters primary human bronchial epithelial cell differentiation at the air-liquid interface," *Sci Rep*, vol. 5, p. 8163, Feb 2 2015, doi: 10.1038/srep08163.
- [119] S. M. Cloonan, H. C. Lam, S. W. Ryter, and A. M. Choi, "'Ciliophagy': The consumption of cilia components by autophagy," (in eng), *Autophagy*, vol. 10, no. 3, pp. 532-4, Mar 2014, doi: 10.4161/auto.27641.
- [120] R. Shaykhiev, "Emerging biology of persistent mucous cell hyperplasia in COPD," (in eng), *Thorax*, vol. 74, no. 1, pp. 4-6, Jan 2019, doi: 10.1136/thoraxjnl-2018-212271.

- [121] V. Kim and G. J. Criner, "Chronic bronchitis and chronic obstructive pulmonary disease," (in eng), *Am J Respir Crit Care Med*, vol. 187, no. 3, pp. 228-37, Feb 1 2013, doi: 10.1164/rccm.201210-1843CI.
- [122] I. H. Heijink, S. M. Brandenburg, D. S. Postma, and A. J. van Oosterhout, "Cigarette smoke impairs airway epithelial barrier function and cell-cell contact recovery," *Eur Respir J*, vol. 39, no. 2, pp. 419-28, Feb 2012, doi: 10.1183/09031936.00193810.
- [123] R. M. Forteza, S. M. Casalino-Matsuda, N. S. Falcon, M. Valencia Gattas, and M. E. Monzon, "Hyaluronan and layilin mediate loss of airway epithelial barrier function induced by cigarette smoke by decreasing E-cadherin," (in eng), *J Biol Chem*, vol. 287, no. 50, pp. 42288-98, Dec 7 2012, doi: 10.1074/jbc.M112.387795.
- [124] N. Mercado, K. Ito, and P. J. Barnes, "Accelerated ageing of the lung in COPD: new concepts," (in eng), *Thorax*, vol. 70, no. 5, pp. 482-9, May 2015, doi: 10.1136/thoraxjnl-2014-206084.
- [125] K. Mizumura *et al.*, "Autophagy: Friend or Foe in Lung Disease?," (in eng), *Ann Am Thorac Soc*, vol. 13 Suppl 1, no. Suppl 1, pp. S40-7, Mar 2016, doi: 10.1513/AnnalsATS.201507-450MG.
- [126] S. Ito *et al.*, "PARK2-mediated mitophagy is involved in regulation of HBEC senescence in COPD pathogenesis," (in eng), *Autophagy*, vol. 11, no. 3, pp. 547-59, 2015, doi: 10.1080/15548627.2015.1017190.
- [127] Y. Wang *et al.*, "Endoplasmic reticulum chaperone GRP78 mediates cigarette smoke-induced necroptosis and injury in bronchial epithelium," (in eng), *Int J Chron Obstruct Pulmon Dis*, vol. 13, pp. 571-581, 2018, doi: 10.2147/copd.S150633.
- [128] J. D. Mancias, X. Wang, S. P. Gygi, J. W. Harper, and A. C. Kimmelman, "Quantitative proteomics identifies NCOA4 as the cargo receptor mediating ferritinophagy," *Nature*, vol. 509, no. 7498, pp. 105-109, 2014/05/01 2014, doi: 10.1038/nature13148.
- [129] M. Yoshida *et al.*, "Involvement of cigarette smoke-induced epithelial cell ferroptosis in COPD pathogenesis," *Nature Communications*, vol. 10, no. 1, p. 3145, 2019/07/17 2019, doi: 10.1038/s41467-019-10991-7.
- [130] M. Chilosi, A. Carloni, A. Rossi, and V. Poletti, "Premature lung aging and cellular senescence in the pathogenesis of idiopathic pulmonary fibrosis and COPD/emphysema," (in eng), *Transl. Res.*, vol. 162, no. 3, pp. 156-73, Sep 2013, doi: 10.1016/j.trsl.2013.06.004.
- [131] T. Rangasamy *et al.*, "Genetic ablation of Nrf2 enhances susceptibility to cigarette smoke-induced emphysema in mice," (in eng), *J Clin Invest*, vol. 114, no. 9, pp. 1248-59, Nov 2004, doi: 10.1172/jci21146.
- [132] S. D. Pouwels *et al.*, "Susceptibility for cigarette smoke-induced DAMP release and DAMP-induced inflammation in COPD," (in eng), *Am J Physiol Lung Cell Mol Physiol*, vol. 311, no. 5, pp. L881-L892, Nov 1 2016, doi: 10.1152/ajplung.00135.2016.
- [133] C. Brightling and N. Greening, "Airway inflammation in COPD: progress to precision medicine," (in eng), *Eur Respir J*, vol. 54, no. 2, Aug 2019, doi: 10.1183/13993003.00651-2019.
- [134] T. Scambler, J. Holbrook, S. Savic, M. F. McDermott, and D. Peckham, "Autoinflammatory disease in the lung," (in eng), *Immunology*, vol. 154, no. 4, pp. 563-73, Apr 19 2018, doi: 10.1111/imm.12937.
- [135] K. B. Baumgartner, J. M. Samet, C. A. Stidley, T. V. Colby, and J. A. Waldron, "Cigarette smoking: a risk factor for idiopathic pulmonary fibrosis," (in eng), *Am J Respir Crit Care Med*, vol. 155, no. 1, pp. 242-8, Jan 1997, doi: 10.1164/ajrccm.155.1.9001319.
- [136] G. Raghu *et al.*, "An Official ATS/ERS/JRS/ALAT Clinical Practice Guideline: Treatment of Idiopathic Pulmonary Fibrosis. An Update of the 2011 Clinical Practice Guideline," *Am. J. Respir. Crit. Care Med.*, vol. 192, no. 2, pp. e3-e19, 2015/07/15 2015, doi: 10.1164/rccm.201506-1063ST.

- [137] M. Selman, T. E. King, and A. Pardo, "Idiopathic pulmonary fibrosis: prevailing and evolving hypotheses about its pathogenesis and implications for therapy," (in eng), *Ann. Intern. Med.*, vol. 134, no. 2, pp. 136-51, Jan 16 2001, doi: 10.7326/0003-4819-134-2-200101160-00015.
- [138] J. A. Bjoraker *et al.*, "Prognostic significance of histopathologic subsets in idiopathic pulmonary fibrosis," (in eng), *Am J Respir Crit Care Med*, vol. 157, no. 1, pp. 199-203, Jan 1998, doi: 10.1164/ajrccm.157.1.9704130.
- [139] G. Raghu *et al.*, "Idiopathic pulmonary fibrosis in US Medicare beneficiaries aged 65 years and older: incidence, prevalence, and survival, 2001-11," (in eng), *Lancet Respir Med*, vol. 2, no. 7, pp. 566-72, Jul 2014, doi: 10.1016/s2213-2600(14)70101-8.
- [140] A. Kaur, S. K. Mathai, and D. A. Schwartz, "Genetics in Idiopathic Pulmonary Fibrosis Pathogenesis, Prognosis, and Treatment," (in eng), *Front Med (Lausanne)*, vol. 4, p. 154, 2017, doi: 10.3389/fmed.2017.00154.
- [141] T. E. Fingerlin *et al.*, "Genome-wide association study identifies multiple susceptibility loci for pulmonary fibrosis," *Nat. Genet.*, vol. 45, no. 6, pp. 613-620, 2013/06/01 2013, doi: 10.1038/ng.2609.
- [142] I. Noth *et al.*, "Genetic variants associated with idiopathic pulmonary fibrosis susceptibility and mortality: a genome-wide association study," *The Lancet Respiratory Medicine*, vol. 1, no. 4, pp. 309-317, 2013/06/01/ 2013, doi: [https://doi.org/10.1016/S2213-2600\(13\)70045-6](https://doi.org/10.1016/S2213-2600(13)70045-6).
- [143] M. A. Seibold *et al.*, "A Common MUC5B Promoter Polymorphism and Pulmonary Fibrosis," *N. Engl. J. Med.*, vol. 364, no. 16, pp. 1503-1512, 2011/04/21 2011, doi: 10.1056/NEJMoa1013660.
- [144] C. M. Evans *et al.*, "Idiopathic Pulmonary Fibrosis: A Genetic Disease That Involves Mucociliary Dysfunction of the Peripheral Airways," (in eng), *Physiol. Rev.*, vol. 96, no. 4, pp. 1567-1591, 2016, doi: 10.1152/physrev.00004.2016.
- [145] Y. Xu *et al.*, "Single-cell RNA sequencing identifies diverse roles of epithelial cells in idiopathic pulmonary fibrosis," *JCI Insight*, vol. 1, no. 20, 03/16/ 2017, doi: 10.1172/jci.insight.90558.
- [146] X. Li *et al.*, "Toll interacting protein protects bronchial epithelial cells from bleomycin-induced apoptosis," (in eng), *FASEB journal : official publication of the Federation of American Societies for Experimental Biology*, vol. 34, no. 8, pp. 9884-9898, 2020, doi: 10.1096/fj.201902636RR.
- [147] X. Li *et al.*, "Toll interacting protein protects bronchial epithelial cells from bleomycin-induced apoptosis," *The FASEB Journal*, vol. 34, no. 8, pp. 9884-9898, 2020, doi: <https://doi.org/10.1096/fj.201902636RR>.
- [148] G. Zhang and S. Ghosh, "Negative regulation of toll-like receptor-mediated signaling by Tollip," (in eng), *J Biol Chem*, vol. 277, no. 9, pp. 7059-65, Mar 1 2002, doi: 10.1074/jbc.M109537200.
- [149] T. Adams *et al.*, *Single Cell RNA-seq reveals ectopic and aberrant lung resident cell populations in Idiopathic Pulmonary Fibrosis*. 2019.
- [150] S. K. Mathai *et al.*, "Desmoplakin Variants Are Associated with Idiopathic Pulmonary Fibrosis," (in eng), *Am J Respir Crit Care Med*, vol. 193, no. 10, pp. 1151-60, May 15 2016, doi: 10.1164/rccm.201509-1863OC.
- [151] A. Asimaki and J. E. Saffitz, "Remodeling of cell-cell junctions in arrhythmogenic cardiomyopathy," (in eng), *Cell Commun Adhes*, vol. 21, no. 1, pp. 13-23, Feb 2014, doi: 10.3109/15419061.2013.876016.
- [152] Y. Hao *et al.*, "GWAS Functional Variant rs2076295 Regulates Desmoplakin (DSP) Expression in Airway Epithelial Cells," (in eng), *Am. J. Respir. Crit. Care Med.*, 2020. [Online]. Available: <https://doi-org.ezp-prod1.hul.harvard.edu/10.1164/rccm.201910-1958OC>.

- [153] M. Doubkova *et al.*, "DSP rs2076295 variants influence nintedanib and pirfenidone outcomes in idiopathic pulmonary fibrosis: a pilot study," (in eng), *Ther. Adv. Respir. Dis.*, vol. 15, p. 17534666211042529, Jan-Dec 2021, doi: 10.1177/17534666211042529.
- [154] J. Qu *et al.*, "AKR1B10 promotes breast cancer cell proliferation and migration via the PI3K/AKT/NF- κ B signaling pathway," *Cell & Bioscience*, vol. 11, no. 1, p. 163, 2021/08/21 2021, doi: 10.1186/s13578-021-00677-3.
- [155] C. Hirano *et al.*, "FAM13A polymorphism as a prognostic factor in patients with idiopathic pulmonary fibrosis," *Respir. Med.*, vol. 123, pp. 105-109, 2017, doi: 10.1016/j.rmed.2016.12.007.
- [156] E. P. Rahardini, K. Ikeda, D. B. Nugroho, K. I. Hirata, and N. Emoto, "Loss of Family with Sequence Similarity 13, Member A Exacerbates Pulmonary Fibrosis Potentially by Promoting Epithelial to Mesenchymal Transition," (in eng), *Kobe J. Med. Sci.*, vol. 65, no. 3, pp. E100-e109, Jan 20 2020.
- [157] R. J. Allen *et al.*, "Genetic variants associated with susceptibility to idiopathic pulmonary fibrosis in people of European ancestry: a genome-wide association study," (in eng), *Lancet Respir Med*, vol. 5, no. 11, pp. 869-880, Nov 2017, doi: 10.1016/s2213-2600(17)30387-9.
- [158] D. Diviani, J. Soderling, and J. D. Scott, "AKAP-Lbc Anchors Protein Kinase A and Nucleates G α 12-selective Rho-mediated Stress Fiber Formation *," *J. Biol. Chem.*, vol. 276, no. 47, pp. 44247-44257, 2001, doi: 10.1074/jbc.M106629200.
- [159] A. Prasse *et al.*, "BAL Cell Gene Expression Is Indicative of Outcome and Airway Basal Cell Involvement in Idiopathic Pulmonary Fibrosis," (in eng), *Am J Respir Crit Care Med*, vol. 199, no. 5, pp. 622-630, Mar 1 2019, doi: 10.1164/rccm.201712-2551OC.
- [160] M. Plataki, A. V. Koutsopoulos, K. Darivianaki, G. Delides, N. M. Siafakas, and D. Bouros, "Expression of apoptotic and antiapoptotic markers in epithelial cells in idiopathic pulmonary fibrosis," (in eng), *Chest*, vol. 127, no. 1, pp. 266-74, Jan 2005, doi: 10.1378/chest.127.1.266.
- [161] K. Kuwano *et al.*, "P21Waf1/Cip1/Sdi1 and p53 expression in association with DNA strand breaks in idiopathic pulmonary fibrosis," (in eng), *Am J Respir Crit Care Med*, vol. 154, no. 2 Pt 1, pp. 477-83, Aug 1996, doi: 10.1164/ajrccm.154.2.8756825.
- [162] M. R. Hadjicharalambous and M. A. Lindsay, "Idiopathic Pulmonary Fibrosis: Pathogenesis and the Emerging Role of Long Non-Coding RNAs," *Int. J. Mol. Sci.*, vol. 21, no. 2, p. 524, 2020. [Online]. Available: <https://www.mdpi.com/1422-0067/21/2/524>.
- [163] N. Omote *et al.*, "Long noncoding RNA TINCR is a novel regulator of human bronchial epithelial cell differentiation state," *Physiological Reports*, vol. 9, no. 3, p. e14727, 2021, doi: <https://doi.org/10.14814/phy2.14727>.
- [164] S. Minagawa *et al.*, "Accelerated epithelial cell senescence in IPF and the inhibitory role of SIRT6 in TGF- β -induced senescence of human bronchial epithelial cells," (in eng), *Am J Physiol Lung Cell Mol Physiol*, vol. 300, no. 3, pp. L391-401, Mar 2011, doi: 10.1152/ajplung.00097.2010.
- [165] A. L. Bolaños *et al.*, "Role of Sonic Hedgehog in idiopathic pulmonary fibrosis," (in eng), *Am J Physiol Lung Cell Mol Physiol*, vol. 303, no. 11, pp. L978-90, Dec 1 2012, doi: 10.1152/ajplung.00184.2012.
- [166] M. Königshoff *et al.*, "Functional Wnt signaling is increased in idiopathic pulmonary fibrosis," (in eng), *PLoS One*, vol. 3, no. 5, p. e2142, May 14 2008, doi: 10.1371/journal.pone.0002142.
- [167] M. Antoine and M. Mlika. (2021). Interstitial Lung Disease. Available: <https://www.ncbi.nlm.nih.gov/books/NBK541084/>
- [168] J. Moon, R. M. du Bois, T. V. Colby, D. M. Hansell, and A. G. Nicholson, "Clinical significance of respiratory bronchiolitis on open lung biopsy and its relationship to smoking related interstitial lung disease," (in eng), *Thorax*, vol. 54, no. 11, pp. 1009-14, Nov 1999, doi: 10.1136/thx.54.11.1009.

- [169] R. R. Patel, J. H. Ryu, and R. Vassallo, "Cigarette Smoking and Diffuse Lung Disease," *Drugs*, vol. 68, no. 11, pp. 1511-1527, 2008/08/01 2008, doi: 10.2165/00003495-200868110-00004.
- [170] V. Cottin *et al.*, "Combined pulmonary fibrosis and emphysema: a distinct underrecognised entity," *Eur. Respir. J.*, vol. 26, no. 4, pp. 586-593, 2005, doi: 10.1183/09031936.05.00021005.
- [171] N. Kwak *et al.*, "Lung cancer risk among patients with combined pulmonary fibrosis and emphysema," *Respir. Med.*, vol. 108, no. 3, pp. 524-530, 2014/03/01/ 2014, doi: <https://doi.org/10.1016/j.rmed.2013.11.013>.
- [172] C. S. Ulrik and P. Lange, "Cigarette smoking and asthma," (in eng), *Monaldi Arch. Chest Dis.*, vol. 56, no. 4, pp. 349-53, Aug 2001.
- [173] M. Stapleton, A. Howard-Thompson, C. George, R. M. Hoover, and T. H. Self, "Smoking and asthma," (in eng), *J. Am. Board Fam. Med.*, vol. 24, no. 3, pp. 313-22, May-Jun 2011, doi: 10.3122/jabfm.2011.03.100180.
- [174] F. Archer, A. Bobet-Erny, and M. Gomes, "State of the art on lung organoids in mammals," (in eng), *Vet. Res.*, vol. 52, no. 1, p. 77, Jun 2 2021, doi: 10.1186/s13567-021-00946-6.
- [175] R. Nossa, J. Costa, L. Cacopardo, and A. Ahluwalia, "Breathing in vitro: Designs and applications of engineered lung models," *Journal of Tissue Engineering*, vol. 12, p. 20417314211008696, 2021/01/01 2021, doi: 10.1177/20417314211008696.
- [176] T. J. Bennet, A. Randhawa, J. Hua, and K. C. Cheung, "Airway-On-A-Chip: Designs and Applications for Lung Repair and Disease," (in eng), *Cells*, vol. 10, no. 7, Jun 26 2021, doi: 10.3390/cells10071602.
- [177] G. Matute-Bello, C. W. Frevert, and T. R. Martin, "Animal models of acute lung injury," (in eng), *Am J Physiol Lung Cell Mol Physiol*, vol. 295, no. 3, pp. L379-99, Sep 2008, doi: 10.1152/ajplung.00010.2008.
- [178] J. L. Wright, M. Cosio, and A. Churg, "Animal models of chronic obstructive pulmonary disease," (in eng), *Am J Physiol Lung Cell Mol Physiol*, vol. 295, no. 1, pp. L1-15, Jul 2008, doi: 10.1152/ajplung.90200.2008.
- [179] J. L. Wright and A. Churg, "Animal models of cigarette smoke-induced chronic obstructive pulmonary disease," (in eng), *Expert Rev Respir Med*, vol. 4, no. 6, pp. 723-34, Dec 2010, doi: 10.1586/ers.10.68.
- [180] C. R. Coggins, "An updated review of inhalation studies with cigarette smoke in laboratory animals," (in eng), *Int. J. Toxicol.*, vol. 26, no. 4, pp. 331-8, Jul-Aug 2007, doi: 10.1080/10915810701490190.
- [181] M. K. Elliott, J. H. Sisson, W. W. West, and T. A. Wyatt, "Differential in vivo effects of whole cigarette smoke exposure versus cigarette smoke extract on mouse ciliated tracheal epithelium," (in eng), *Exp Lung Res*, vol. 32, no. 3-4, pp. 99-118, Mar-Apr 2006, doi: 10.1080/01902140600710546.
- [182] S. Kispert, S. Crawford, G. Kolar, and J. McHowat, "In Vivo Effects of Long-Term Cigarette Smoke Exposure on Mammary Tissue in Mice," *The American Journal of Pathology*, vol. 187, no. 6, pp. 1238-1244, 2017/06/01/ 2017, doi: <https://doi.org/10.1016/j.ajpath.2017.02.004>.
- [183] S. M. Simet *et al.*, "Long-term cigarette smoke exposure in a mouse model of ciliated epithelial cell function," (in eng), *Am J Respir Cell Mol Biol*, vol. 43, no. 6, pp. 635-40, Dec 2010, doi: 10.1165/rcmb.2009-0297OC.
- [184] P. Sakhatskyy *et al.*, "Double-hit mouse model of cigarette smoke priming for acute lung injury," *American Journal of Physiology-Lung Cellular and Molecular Physiology*, vol. 312, no. 1, pp. L56-L67, 2017, doi: 10.1152/ajplung.00436.2016.

- [185] R. W. Vandivier and M. Ghosh, "Understanding the Relevance of the Mouse Cigarette Smoke Model of COPD: Peering through the Smoke," (in eng), *Am J Respir Cell Mol Biol*, vol. 57, no. 1, pp. 3-4, Jul 2017, doi: 10.1165/rcmb.2017-0110ED.
- [186] B. J. Canning and J. L. Wright, "Animal models of asthma and chronic obstructive pulmonary disease," (in eng), *Pulm Pharmacol Ther*, vol. 21, no. 5, p. 695, Oct 2008, doi: 10.1016/j.pupt.2008.04.007.
- [187] S. D. Pouwels *et al.*, "Cigarette smoke-induced necroptosis and DAMP release trigger neutrophilic airway inflammation in mice," *Am J Physiol Lung Cell Mol Physiol*, vol. 310, no. 4, pp. L377-86, Feb 15 2016, doi: 10.1152/ajplung.00174.2015.
- [188] S. Yanagisawa *et al.*, "The dynamic shuttling of SIRT1 between cytoplasm and nuclei in bronchial epithelial cells by single and repeated cigarette smoke exposure," *PLoS One*, vol. 13, no. 3, p. e0193921, 2018, doi: 10.1371/journal.pone.0193921.
- [189] F. H. Wong *et al.*, "Cigarette smoke activates CFTR through ROS-stimulated cAMP signaling in human bronchial epithelial cells," *Am. J. Physiol. Cell Physiol.*, vol. 314, no. 1, pp. C118-C134, Jan 1 2018, doi: 10.1152/ajpcell.00099.2017.
- [190] P. M. Andrault *et al.*, "Cigarette smoke induces overexpression of active human cathepsin S in lungs from current smokers with or without COPD," vol. 317, no. 5, pp. L625-L638, Nov 1 2019, doi: 10.1152/ajplung.00061.2019.
- [191] J. Phillips, B. Kluss, A. Richter, and E. Massey, "Exposure of bronchial epithelial cells to whole cigarette smoke: assessment of cellular responses," *Altern Lab Anim*, vol. 33, no. 3, pp. 239-48, Jun 2005, doi: 10.1177/026119290503300310.
- [192] R. M. Starke *et al.*, "Cigarette smoke modulates vascular smooth muscle phenotype: implications for carotid and cerebrovascular disease," *PLoS One*, vol. 8, no. 8, p. e71954, 2013, doi: 10.1371/journal.pone.0071954.
- [193] Y. P. Wu *et al.*, "Activating transcription factor 3 represses cigarette smoke-induced IL6 and IL8 expression via suppressing NF-kappaB activation," *Toxicol. Lett.*, vol. 270, pp. 17-24, Mar 15 2017, doi: 10.1016/j.toxlet.2017.02.002.
- [194] J. V. Thaikootathil, R. J. Martin, J. Zdunek, A. Weinberger, J. G. Rino, and H. W. Chu, "Cigarette smoke extract reduces VEGF in primary human airway epithelial cells," *Eur Respir J*, vol. 33, no. 4, pp. 835-43, Apr 2009, doi: 10.1183/09031936.00080708.
- [195] J. Jukosky, B. J. Gosselin, L. Foley, T. Dechen, S. Fiering, and M. A. Crane-Godreau, "In vivo Cigarette Smoke Exposure Decreases CCL20, SLPI, and BD-1 Secretion by Human Primary Nasal Epithelial Cells," *Front Psychiatry*, vol. 6, p. 185, 2015, doi: 10.3389/fpsy.2015.00185.
- [196] S. Ito, K. Ishimori, and S. Ishikawa, "Effects of repeated cigarette smoke extract exposure over one month on human bronchial epithelial organotypic culture," *Toxicol Rep*, vol. 5, pp. 864-870, 2018, doi: 10.1016/j.toxrep.2018.08.015.
- [197] M. Mastalerz *et al.*, "Validation of in vitro models for smoke exposure of primary human bronchial epithelial cells," *American Journal of Physiology-Lung Cellular and Molecular Physiology*, vol. 0, no. 0, p. null, doi: 10.1152/ajplung.00091.2021.
- [198] D. M. Comer, J. S. Elborn, and M. Ennis, "Comparison of nasal and bronchial epithelial cells obtained from patients with COPD," *PLoS One*, vol. 7, no. 3, p. e32924, 2012, doi: 10.1371/journal.pone.0032924.
- [199] C. A. Carter, "Multiplexed High Content Screening Reveals That Cigarette Smoke Condensate-Altered Cell Signaling Pathways Are Accentuated Through FAK Inhibition in Human Bronchial Cells," *Int. J. Toxicol.*, vol. 31, no. 3, pp. 257-266, 2012/06/01 2012, doi: 10.1177/1091581812440890.
- [200] G. R. Hellermann, S. B. Nagy, X. Kong, R. F. Lockey, and S. S. Mohapatra, "Mechanism of cigarette smoke condensate-induced acute inflammatory response in human bronchial epithelial cells," (in eng), *Respir Res*, vol. 3, no. 1, p. 22, 2002, doi: 10.1186/rr172.

- [201] C. Mathis *et al.*, "Human bronchial epithelial cells exposed in vitro to cigarette smoke at the air-liquid interface resemble bronchial epithelium from human smokers," *American Journal of Physiology-Lung Cellular and Molecular Physiology*, vol. 304, no. 7, pp. L489-L503, 2013, doi: 10.1152/ajplung.00181.2012.
- [202] J. M. Park *et al.*, "Differential Effects between Cigarette Total Particulate Matter and Cigarette Smoke Extract on Blood and Blood Vessel," (in eng), *Toxicol Res*, vol. 32, no. 4, pp. 353-358, Oct 2016, doi: 10.5487/tr.2016.32.4.353.
- [203] M. van der Toorn *et al.*, "The biological effects of long-term exposure of human bronchial epithelial cells to total particulate matter from a candidate modified-risk tobacco product," *Toxicol In Vitro*, vol. 50, pp. 95-108, Aug 2018, doi: 10.1016/j.tiv.2018.02.019.
- [204] J. A. Gindele *et al.*, "Intermittent exposure to whole cigarette smoke alters the differentiation of primary small airway epithelial cells in the air-liquid interface culture," *Sci Rep*, vol. 10, no. 1, p. 6257, Apr 10 2020, doi: 10.1038/s41598-020-63345-5.
- [205] S. Ishikawa and S. Ito, "Repeated whole cigarette smoke exposure alters cell differentiation and augments secretion of inflammatory mediators in air-liquid interface three-dimensional co-culture model of human bronchial tissue," (in eng), *Toxicol In Vitro*, vol. 38, pp. 170-178, Feb 2017, doi: 10.1016/j.tiv.2016.09.004.
- [206] J. St-Laurent, L.-I. Proulx, L.-P. Boulet, and E. Bissonnette, "Comparison of two in vitro models of cigarette smoke exposure," *Inhal. Toxicol.*, vol. 21, no. 13, pp. 1148-1153, 2009/11/01 2009, doi: 10.3109/08958370902926692.
- [207] C. A. Gellner, D. D. Reynaga, and F. M. Leslie, "Cigarette Smoke Extract: A Preclinical Model of Tobacco Dependence," (in eng), *Curr. Protoc. Neurosci.*, vol. 77, pp. 9.54.1-9.54.10, Oct 3 2016, doi: 10.1002/cpns.14.
- [208] D. F. Church and W. A. Pryor, "Free-radical chemistry of cigarette smoke and its toxicological implications," (in eng), *Environ. Health Perspect.*, vol. 64, pp. 111-26, Dec 1985, doi: 10.1289/ehp.8564111.
- [209] S. Majeed *et al.*, "Characterization of the Vitrocell® 24/48 in vitro aerosol exposure system using mainstream cigarette smoke," (in eng), *Chem. Cent. J.*, vol. 8, no. 1, p. 62, 2014, doi: 10.1186/s13065-014-0062-3.
- [210] S. Zhang, X. Li, F. Xie, K. Liu, H. Liu, and J. Xie, "Evaluation of whole cigarette smoke induced oxidative stress in A549 and BEAS-2B cells," *Environ Toxicol Pharmacol*, vol. 54, pp. 40-47, Sep 2017, doi: 10.1016/j.etap.2017.06.023.
- [211] C. Long, Y. Lai, T. Li, T. Nyunoya, and C. Zou, "Cigarette smoke extract modulates *Pseudomonas aeruginosa* bacterial load via USP25/HDAC11 axis in lung epithelial cells," *Am J Physiol Lung Cell Mol Physiol*, vol. 318, no. 2, pp. L252-L263, Feb 1 2020, doi: 10.1152/ajplung.00142.2019.
- [212] K. Nishida *et al.*, "Cigarette smoke disrupts monolayer integrity by altering epithelial cell-cell adhesion and cortical tension," *Am J Physiol Lung Cell Mol Physiol*, vol. 313, no. 3, pp. L581-L591, Sep 1 2017, doi: 10.1152/ajplung.00074.2017.
- [213] M. I. Hermanns, R. E. Unger, K. Kehe, K. Peters, and C. J. Kirkpatrick, "Lung epithelial cell lines in coculture with human pulmonary microvascular endothelial cells: development of an alveolo-capillary barrier in vitro," *Lab. Invest.*, vol. 84, no. 6, pp. 736-752, 2004/06/01 2004, doi: 10.1038/labinvest.3700081.
- [214] J. Ji *et al.*, "Multi-cellular human bronchial models exposed to diesel exhaust particles: assessment of inflammation, oxidative stress and macrophage polarization," *Part. Fibre Toxicol.*, vol. 15, no. 1, p. 19, 2018/05/02 2018, doi: 10.1186/s12989-018-0256-2.
- [215] C. E. Barkauskas, M. I. Chung, B. Fioret, X. Gao, H. Katsura, and B. L. Hogan, "Lung organoids: current uses and future promise," (in eng), *Development*, vol. 144, no. 6, pp. 986-997, Mar 15 2017, doi: 10.1242/dev.140103.
- [216] A. I. Vazquez-Armendariz and S. Herold, "From Clones to Buds and Branches: The Use of Lung Organoids to Model Branching Morphogenesis Ex Vivo," (in English), *Frontiers*

- in Cell and Developmental Biology*, Mini Review vol. 9, no. 448, 2021-March-04 2021, doi: 10.3389/fcell.2021.631579.
- [217] J. Kong *et al.*, "Lung organoids, useful tools for investigating epithelial repair after lung injury," *Stem Cell. Res. Ther.*, vol. 12, no. 1, p. 95, 2021/01/30 2021, doi: 10.1186/s13287-021-02172-5.
- [218] M. A. Lancaster and J. A. Knoblich, "Organogenesis in a dish: modeling development and disease using organoid technologies," (in eng), *Science*, vol. 345, no. 6194, p. 1247125, Jul 18 2014, doi: 10.1126/science.1247125.
- [219] X. Wu, S. Bos, M. Schmidt, L. Kistemaker, and R. Gosens, "Cigarette smoke and diesel particles repress functional responses in lung epithelial progenitors," *Eur. Respir. J.*, vol. 54, no. suppl 63, p. PA2437, 2019, doi: 10.1183/13993003.congress-2019.PA2437.
- [220] S. Konishi *et al.*, "Directed Induction of Functional Multi-ciliated Cells in Proximal Airway Epithelial Spheroids from Human Pluripotent Stem Cells," *Stem Cell Reports*, vol. 6, no. 1, pp. 18-25, 2016/01/12/ 2016, doi: <https://doi.org/10.1016/j.stemcr.2015.11.010>.
- [221] J. Shrestha *et al.*, "Lung-on-a-chip: the future of respiratory disease models and pharmacological studies," *Crit. Rev. Biotechnol.*, vol. 40, no. 2, pp. 213-230, 2020/02/17 2020, doi: 10.1080/07388551.2019.1710458.
- [222] G. D. Amatngalim *et al.*, "Basal cells contribute to innate immunity of the airway epithelium through production of the antimicrobial protein RNase 7," *J Immunol*, vol. 194, no. 7, pp. 3340-50, Apr 1 2015, doi: 10.4049/jimmunol.1402169.
- [223] K. H. Benam *et al.*, "Matched-Comparative Modeling of Normal and Diseased Human Airway Responses Using a Microengineered Breathing Lung Chip," *Cell Syst*, vol. 3, no. 5, pp. 456-466 e4, Nov 23 2016, doi: 10.1016/j.cels.2016.10.003.
- [224] B. Srinivasan, A. R. Kolli, M. B. Esch, H. E. Abaci, M. L. Shuler, and J. J. Hickman, "TEER measurement techniques for in vitro barrier model systems," *J Lab Autom*, vol. 20, no. 2, pp. 107-26, Apr 2015, doi: 10.1177/2211068214561025.
- [225] D. Thorne *et al.*, "Characterisation of a Vitrocell(R) VC 10 in vitro smoke exposure system using dose tools and biological analysis," *Chem. Cent. J.*, vol. 7, no. 1, p. 146, Sep 3 2013, doi: 10.1186/1752-153X-7-146.
- [226] E. Billatos *et al.*, "Impact of acute exposure to cigarette smoke on airway gene expression," *Physiol Genomics*, vol. 50, no. 9, pp. 705-713, Sep 1 2018, doi: 10.1152/physiolgenomics.00092.2017.
- [227] C. Mathis *et al.*, "Human bronchial epithelial cells exposed in vitro to cigarette smoke at the air-liquid interface resemble bronchial epithelium from human smokers," *Am J Physiol Lung Cell Mol Physiol*, vol. 304, no. 7, pp. L489-503, Apr 1 2013, doi: 10.1152/ajplung.00181.2012.
- [228] G. E. Duclos *et al.*, "Characterizing smoking-induced transcriptional heterogeneity in the human bronchial epithelium at single-cell resolution," *Sci Adv*, vol. 5, no. 12, p. eaaw3413, Dec 2019, doi: 10.1126/sciadv.aaw3413.
- [229] R. Wang *et al.*, "Smoking-induced upregulation of AKR1B10 expression in the airway epithelium of healthy individuals," (in eng), *Chest*, vol. 138, no. 6, pp. 1402-10, Dec 2010, doi: 10.1378/chest.09-2634.
- [230] R. Chari, K. M. Lonergan, R. T. Ng, C. MacAulay, W. L. Lam, and S. Lam, "Effect of active smoking on the human bronchial epithelium transcriptome," *BMC Genomics*, vol. 8, p. 297, Aug 29 2007, doi: 10.1186/1471-2164-8-297.
- [231] B. G. Harvey, A. Heguy, P. L. Leopold, B. J. Carolan, B. Ferris, and R. G. Crystal, "Modification of gene expression of the small airway epithelium in response to cigarette smoking," (in eng), *J. Mol. Med. (Berl.)*, vol. 85, no. 1, pp. 39-53, Jan 2007, doi: 10.1007/s00109-006-0103-z.

- [232] R. Shaykhiev *et al.*, "Cigarette smoking reprograms apical junctional complex molecular architecture in the human airway epithelium in vivo," *Cell. Mol. Life Sci.*, vol. 68, no. 5, pp. 877-92, Mar 2011, doi: 10.1007/s00018-010-0500-x.
- [233] M. S. Walters *et al.*, "Smoking accelerates aging of the small airway epithelium," *Respiratory Research*, vol. 15, no. 1, p. 94, 2014/09/24 2014, doi: 10.1186/s12931-014-0094-1.
- [234] M. T. Landi *et al.*, "Gene expression signature of cigarette smoking and its role in lung adenocarcinoma development and survival," (in eng), *PLoS One*, vol. 3, no. 2, p. e1651, Feb 20 2008, doi: 10.1371/journal.pone.0001651.
- [235] G. Pintarelli *et al.*, "Cigarette smoke alters the transcriptome of non-involved lung tissue in lung adenocarcinoma patients," *Sci. Rep.*, vol. 9, no. 1, p. 13039, 2019/09/10 2019, doi: 10.1038/s41598-019-49648-2.
- [236] K. M. Bakulski, J. Dou, N. Lin, S. J. London, and J. A. Colacino, "DNA methylation signature of smoking in lung cancer is enriched for exposure signatures in newborn and adult blood," *Sci. Rep.*, vol. 9, no. 1, p. 4576, 2019/03/14 2019, doi: 10.1038/s41598-019-40963-2.
- [237] J. Wang *et al.*, "Identification and validation of smoking-related genes in lung adenocarcinoma using an in vitro carcinogenesis model and bioinformatics analysis," *J. Transl. Med.*, vol. 18, no. 1, p. 313, 2020/08/14 2020, doi: 10.1186/s12967-020-02474-x.
- [238] Y. Bossé *et al.*, "Molecular Signature of Smoking in Human Lung Tissues," *Cancer Res.*, vol. 72, no. 15, p. 3753, 2012, doi: 10.1158/0008-5472.CAN-12-1160.
- [239] L. A. Murray *et al.*, "Acute cigarette smoke exposure activates apoptotic and inflammatory programs but a second stimulus is required to induce epithelial to mesenchymal transition in COPD epithelium," *Respir Res*, vol. 18, no. 1, p. 82, May 3 2017, doi: 10.1186/s12931-017-0565-2.
- [240] H. Voic *et al.*, "RNA sequencing identifies common pathways between cigarette smoke exposure and replicative senescence in human airway epithelia," *BMC Genomics*, vol. 20, no. 1, p. 22, 2019/01/09 2019, doi: 10.1186/s12864-018-5409-z.
- [241] A. Higham, D. Bostock, G. Booth, J. V. Dungwa, and D. Singh, "The effect of electronic cigarette and tobacco smoke exposure on COPD bronchial epithelial cell inflammatory responses," (in eng), *Int. J. Chron. Obstruct. Pulmon. Dis.*, vol. 13, pp. 989-1000, 2018, doi: 10.2147/COPD.S157728.
- [242] F. Bucchieri *et al.*, "Cigarette smoke causes caspase-independent apoptosis of bronchial epithelial cells from asthmatic donors," *PLoS One*, vol. 10, no. 3, p. e0120510, 2015, doi: 10.1371/journal.pone.0120510.
- [243] Y. Liang, L. Tian, K.-F. Ho, M. S.-M. Ip, and J. C.-W. Mak, "Comparisons on mitochondrial function following exposure of cigarette smoke extract and fine particulate matter in human bronchial epithelial cells," *Eur. Respir. J.*, vol. 54, no. suppl 63, p. PA2436, 2019, doi: 10.1183/13993003.congress-2019.PA2436.
- [244] J. E. Boers, A. W. Ambergen, and F. B. Thunnissen, "Number and proliferation of clara cells in normal human airway epithelium," *Am J Respir Crit Care Med*, vol. 159, no. 5 Pt 1, pp. 1585-91, May 1999, doi: 10.1164/ajrccm.159.5.9806044.
- [245] D. F. Rogers, "The airway goblet cell," *The International Journal of Biochemistry & Cell Biology*, vol. 35, no. 1, pp. 1-6, 2003/01/01/ 2003, doi: [https://doi.org/10.1016/S1357-2725\(02\)00083-3](https://doi.org/10.1016/S1357-2725(02)00083-3).
- [246] A. Farhana and S. L. Lappin, "Biochemistry, Lactate Dehydrogenase," in *StatPearls*. Treasure Island (FL): StatPearls Publishing, 2021.
- [247] B. Srinivasan, A. R. Kolli, M. B. Esch, H. E. Abaci, M. L. Shuler, and J. J. Hickman, "TEER measurement techniques for in vitro barrier model systems," (in eng), *Journal of laboratory automation*, vol. 20, no. 2, pp. 107-126, 2015, doi: 10.1177/2211068214561025.

- [248] A. C. Schamberger *et al.*, "Cigarette smoke-induced disruption of bronchial epithelial tight junctions is prevented by transforming growth factor-beta," *Am J Respir Cell Mol Biol*, vol. 50, no. 6, pp. 1040-52, Jun 2014, doi: 10.1165/rcmb.2013-0090OC.
- [249] C. H. Kim, K. S. Song, S. S. Kim, H. U. Kim, J. K. Seong, and J. H. Yoon, "Expression of MUC5AC mRNA in the goblet cells of human nasal mucosa," (in eng), *Laryngoscope*, vol. 110, no. 12, pp. 2110-3, Dec 2000, doi: 10.1097/00005537-200012000-00026.
- [250] B. Aslam, M. Basit, M. A. Nisar, M. Khurshid, and M. H. Rasool, "Proteomics: Technologies and Their Applications," *J. Chromatogr. Sci.*, vol. 55, no. 2, pp. 182-196, 2017, doi: 10.1093/chromsci/bmw167.
- [251] A. Krämer, J. Green, J. Pollard, Jr., and S. Tugendreich, "Causal analysis approaches in Ingenuity Pathway Analysis," (in eng), *Bioinformatics*, vol. 30, no. 4, pp. 523-30, Feb 15 2014, doi: 10.1093/bioinformatics/btt703.
- [252] S. Booth *et al.*, "Identification of central nervous system genes involved in the host response to the scrapie agent during preclinical and clinical infection," *J. Gen. Virol.*, vol. 85, no. 11, pp. 3459-3471, 2004, doi: <https://doi.org/10.1099/vir.0.80110-0>.
- [253] E. Ruiz-Ballesteros *et al.*, "Splenic marginal zone lymphoma: proposal of new diagnostic and prognostic markers identified after tissue and cDNA microarray analysis," (in eng), *Blood*, vol. 106, no. 5, pp. 1831-8, Sep 1 2005, doi: 10.1182/blood-2004-10-3898.
- [254] T. Han, J. Wang, W. Tong, M. M. Moore, J. C. Fuscoe, and T. Chen, "Microarray analysis distinguishes differential gene expression patterns from large and small colony Thymidine kinase mutants of L5178Y mouse lymphoma cells," (in eng), *BMC Bioinformatics*, vol. 7 Suppl 2, no. Suppl 2, p. S9, Sep 6 2006, doi: 10.1186/1471-2105-7-s2-s9.
- [255] T. M. Penning, "Aldo-Keto Reductase Regulation by the Nrf2 System: Implications for Stress Response, Chemotherapy Drug Resistance, and Carcinogenesis," (in eng), *Chem. Res. Toxicol.*, vol. 30, no. 1, pp. 162-176, Jan 17 2017, doi: 10.1021/acs.chemrestox.6b00319.
- [256] S. Shin *et al.*, "NRF2 modulates aryl hydrocarbon receptor signaling: influence on adipogenesis," (in eng), *Mol. Cell. Biol.*, vol. 27, no. 20, pp. 7188-97, Oct 2007, doi: 10.1128/mcb.00915-07.
- [257] W. Miao, L. Hu, P. J. Scrivens, and G. Batist, "Transcriptional regulation of NF-E2 p45-related factor (NRF2) expression by the aryl hydrocarbon receptor-xenobiotic response element signaling pathway: direct cross-talk between phase I and II drug-metabolizing enzymes," (in eng), *J Biol Chem*, vol. 280, no. 21, pp. 20340-8, May 27 2005, doi: 10.1074/jbc.M412081200.
- [258] X. Wei, Z. Wei, Y. Li, Z. Tan, and C. Lin, "AKR1C1 Contributes to Cervical Cancer Progression via Regulating TWIST1 Expression," (in eng), *Biochem. Genet.*, vol. 59, no. 2, pp. 516-530, Apr 2021, doi: 10.1007/s10528-020-10014-x.
- [259] S. Luo *et al.*, "Akt Phosphorylates NQO1 and Triggers its Degradation, Abolishing Its Antioxidative Activities in Parkinson's Disease," (in eng), *J. Neurosci.*, vol. 39, no. 37, pp. 7291-7305, Sep 11 2019, doi: 10.1523/jneurosci.0625-19.2019.
- [260] W. Jiang *et al.*, "Wentilactone A induces cell apoptosis by targeting AKR1C1 gene via the IGF-1R/IRS1/PI3K/AKT/Nrf2/FLIP/Caspase-3 signaling pathway in small cell lung cancer," *Oncol Lett*, vol. 16, no. 5, pp. 6445-6457, 2018/11/01 2018, doi: 10.3892/ol.2018.9486.
- [261] D. G. Yanbaeva, M. A. Dentener, E. C. Creutzberg, G. Wesseling, and E. F. Wouters, "Systemic effects of smoking," (in eng), *Chest*, vol. 131, no. 5, pp. 1557-66, May 2007, doi: 10.1378/chest.06-2179.
- [262] Z. Chen *et al.*, "From tobacco smoking to cancer mutational signature: a mediation analysis strategy to explore the role of epigenetic changes," *BMC Cancer*, vol. 20, no. 1, p. 880, 2020/09/14 2020, doi: 10.1186/s12885-020-07368-1.
- [263] F. Martin, M. Talikka, J. Hoeng, and M. C. Peitsch, "Identification of gene expression signature for cigarette smoke exposure response—from man to mouse," *Hum. Exp.*

- Toxicol.*, vol. 34, no. 12, pp. 1200-1211, 2015/12/01 2015, doi: 10.1177/0960327115600364.
- [264] S. Sridhar *et al.*, "Smoking-induced gene expression changes in the bronchial airway are reflected in nasal and buccal epithelium," *BMC Genomics*, vol. 9, no. 1, p. 259, 2008/05/30 2008, doi: 10.1186/1471-2164-9-259.
- [265] M. C. Boelens *et al.*, "Current smoking-specific gene expression signature in normal bronchial epithelium is enhanced in squamous cell lung cancer," *The Journal of Pathology*, vol. 218, no. 2, pp. 182-191, 2009, doi: <https://doi.org/10.1002/path.2520>.
- [266] B. D. Gelbman, A. Heguy, T. P. O'Connor, J. Zabner, and R. G. Crystal, "Upregulation of pirin expression by chronic cigarette smoking is associated with bronchial epithelial cell apoptosis," *Respiratory Research*, vol. 8, no. 1, p. 10, 2007/02/08 2007, doi: 10.1186/1465-9921-8-10.
- [267] E. Van Dyck *et al.*, "Bronchial airway gene expression in smokers with lung or head and neck cancer," *Cancer Medicine*, vol. 3, no. 2, pp. 322-336, 2014, doi: <https://doi.org/10.1002/cam4.190>.
- [268] C. X. Yang *et al.*, "Widespread Sexual Dimorphism in the Transcriptome of Human Airway Epithelium in Response to Smoking," (in eng), *Sci Rep*, vol. 9, no. 1, p. 17600, Nov 26 2019, doi: 10.1038/s41598-019-54051-y.
- [269] "WHO Report on the Global Tobacco Epidemic," 2019 2019. [Online]. Available: <https://www.who.int/publications/i/item/9789241516204>.
- [270] J. Beane, P. Sebastiani, G. Liu, J. S. Brody, M. E. Lenburg, and A. Spira, "Reversible and permanent effects of tobacco smoke exposure on airway epithelial gene expression," *Genome Biol.*, vol. 8, no. 9, p. R201, 2007/09/25 2007, doi: 10.1186/gb-2007-8-9-r201.
- [271] M. Chen, T. Yang, X. Meng, and T. Sun, "Azithromycin attenuates cigarette smoke extract-induced oxidative stress injury in human alveolar epithelial cells," *Mol Med Rep*, vol. 11, no. 5, pp. 3414-22, May 2015, doi: 10.3892/mmr.2015.3226.
- [272] M. Ferraro, M. Gjomarkaj, L. Siena, S. Di Vincenzo, and E. Pace, "Formoterol and fluticasone propionate combination improves histone deacetylation and anti-inflammatory activities in bronchial epithelial cells exposed to cigarette smoke," *Biochim Biophys Acta Mol Basis Dis*, vol. 1863, no. 7, pp. 1718-1727, Jul 2017, doi: 10.1016/j.bbadis.2017.05.003.
- [273] H. Qin *et al.*, "Nur77 promotes cigarette smoke-induced autophagic cell death by increasing the dissociation of Bcl2 from Beclin-1," *Int J Mol Med*, vol. 44, no. 1, pp. 25-36, Jul 2019, doi: 10.3892/ijmm.2019.4184.
- [274] M. E. Parrish, J. L. Lyons-Hart, and K. H. Shafer, "Puff-by-puff and intrapuff analysis of cigarette smoke using infrared spectroscopy," (in English), *Vib. Spectrosc*, vol. 27, no. 1, pp. 29-42, Nov 29 2001, doi: 10.1016/S0924-2031(01)00118-7.
- [275] R. J. Robinson and C. P. Yu, "Deposition of cigarette smoke particles in the human respiratory tract," (in English), *Aerosol Sci. Technol.*, vol. 34, no. 2, pp. 202-215, Feb 2001, doi: Doi 10.1080/027868201300034844.
- [276] H. R. Paur *et al.*, "In-vitro cell exposure studies for the assessment of nanoparticle toxicity in the lung-A dialog between aerosol science and biology," (in English), *J. Aerosol Sci*, vol. 42, no. 10, pp. 668-692, Oct 2011, doi: 10.1016/j.jaerosci.2011.06.005.
- [277] I. Balashazy, W. Hofmann, and T. Heistracher, "Local particle deposition patterns may play a key role in the development of lung cancer," *J Appl Physiol (1985)*, vol. 94, no. 5, pp. 1719-25, May 2003, doi: 10.1152/japplphysiol.00527.2002.
- [278] J. Heyder, "Deposition of inhaled particles in the human respiratory tract and consequences for regional targeting in respiratory drug delivery," *Proc. Am. Thorac. Soc.*, vol. 1, no. 4, pp. 315-20, 2004, doi: 10.1513/pats.200409-046TA.
- [279] J. S. Brody, "Transcriptome alterations induced by cigarette smoke," *Int. J. Cancer*, vol. 131, no. 12, pp. 2754-62, Dec 15 2012, doi: 10.1002/ijc.27829.

- [280] I. Balásházy, W. Hofmann, and T. Heistracher, "Computation of local enhancement factors for the quantification of particle deposition patterns in airway bifurcations," *J. Aerosol Sci*, vol. 30, pp. 185-203, 1999, doi: [https://doi.org/10.1016/S0021-8502\(98\)00040-8](https://doi.org/10.1016/S0021-8502(98)00040-8).
- [281] D. Wilson, M. Wakefield, N. Owen, and L. Roberts, "Characteristics of heavy smokers," (in eng), *Prev. Med.*, vol. 21, no. 3, pp. 311-9, May 1992, doi: 10.1016/0091-7435(92)90030-l.
- [282] A. Mossina *et al.*, "Cigarette smoke alters the secretome of lung epithelial cells," *Proteomics*, vol. 17, no. 1-2, Jan 2017, doi: 10.1002/pmic.201600243.
- [283] M. Tatsuta *et al.*, "Effects of cigarette smoke on barrier function and tight junction proteins in the bronchial epithelium: protective role of cathelicidin LL-37," *Respir Res*, vol. 20, no. 1, p. 251, Nov 9 2019, doi: 10.1186/s12931-019-1226-4.
- [284] A. Faiz *et al.*, "Cigarette smoke exposure decreases CFLAR expression in the bronchial epithelium, augmenting susceptibility for lung epithelial cell death and DAMP release," *Sci Rep*, vol. 8, no. 1, p. 12426, Aug 20 2018, doi: 10.1038/s41598-018-30602-7.
- [285] S. M. Simet *et al.*, "Long-term cigarette smoke exposure in a mouse model of ciliated epithelial cell function," (in eng), *Am. J. Respir. Cell Mol. Biol.*, vol. 43, no. 6, pp. 635-640, 2010, doi: 10.1165/rcmb.2009-0297OC.
- [286] G. Pickett, J. Seagrave, S. Boggs, G. Polzin, P. Richter, and Y. Tesfaigzi, "Effects of 10 cigarette smoke condensates on primary human airway epithelial cells by comparative gene and cytokine expression studies," *Toxicol. Sci.*, vol. 114, no. 1, pp. 79-89, Mar 2010, doi: 10.1093/toxsci/kfp298.
- [287] S. Zevin and N. L. Benowitz, "Drug Interactions with Tobacco Smoking," *Clin. Pharmacokinet.*, vol. 36, no. 6, pp. 425-438, 1999/06/01 1999, doi: 10.2165/00003088-199936060-00004.
- [288] N. Guerrina, H. Traboulsi, D. H. Eidelman, and C. J. Baglole, "The Aryl Hydrocarbon Receptor and the Maintenance of Lung Health," *Int J Mol Sci*, vol. 19, no. 12, Dec 5 2018, doi: 10.3390/ijms19123882.
- [289] D. W. Nebert, A. L. Roe, M. Z. Dieter, W. A. Solis, Y. Yang, and T. P. Dalton, "Role of the aromatic hydrocarbon receptor and [Ah] gene battery in the oxidative stress response, cell cycle control, and apoptosis," (in eng), *Biochem. Pharmacol.*, vol. 59, no. 1, pp. 65-85, Jan 1 2000, doi: 10.1016/s0006-2952(99)00310-x.
- [290] G. I. Murray, W. T. Melvin, W. F. Greenlee, and M. D. Burke, "Regulation, Function, and Tissue-Specific Expression of Cytochrome P450 CYP1B1," *Annu. Rev. Pharmacol. Toxicol.*, vol. 41, no. 1, pp. 297-316, 2001, doi: 10.1146/annurev.pharmtox.41.1.297.
- [291] Q. Ma, "Role of nrf2 in oxidative stress and toxicity," (in eng), *Annu. Rev. Pharmacol. Toxicol.*, vol. 53, pp. 401-26, 2013, doi: 10.1146/annurev-pharmtox-011112-140320.
- [292] T. Nishinaka, T. Miura, M. Okumura, F. Nakao, H. Nakamura, and T. Terada, "Regulation of aldo-keto reductase AKR1B10 gene expression: Involvement of transcription factor Nrf2," *Chem. Biol. Interact.*, vol. 191, no. 1, pp. 185-191, 2011/05/30/ 2011, doi: <https://doi.org/10.1016/j.cbi.2011.01.026>.
- [293] H. Lou, S. Du, Q. Ji, and A. Stolz, "Induction of *AKR1C2* by Phase II Inducers: Identification of a Distal Consensus Antioxidant Response Element Regulated by NRF2," *Mol. Pharmacol.*, vol. 69, no. 5, pp. 1662-1672, 2006, doi: 10.1124/mol.105.019794.
- [294] T. Rangasamy *et al.*, "Genetic ablation of Nrf2 enhances susceptibility to cigarette smoke-induced emphysema in mice," *The Journal of Clinical Investigation*, vol. 114, no. 9, pp. 1248-1259, 11/01/ 2004, doi: 10.1172/JCI21146.
- [295] H. Y. Cho, S. P. Reddy, A. Debiase, M. Yamamoto, and S. R. Kleeberger, "Gene expression profiling of NRF2-mediated protection against oxidative injury," (in eng), *Free Radic Biol Med*, vol. 38, no. 3, pp. 325-43, Feb 1 2005, doi: 10.1016/j.freeradbiomed.2004.10.013.

- [296] K. Brzóska, T. M. Stępkowski, and M. Kruszewski, "Basal PIR expression in HeLa cells is driven by NRF2 via evolutionary conserved antioxidant response element," *Mol. Cell. Biochem.*, vol. 389, no. 1, pp. 99-111, 2014/04/01 2014, doi: 10.1007/s11010-013-1931-0.
- [297] R. K. Thimmulappa, K. H. Mai, S. Srisuma, T. W. Kensler, M. Yamamoto, and S. Biswal, "Identification of Nrf2-regulated genes induced by the chemopreventive agent sulforaphane by oligonucleotide microarray," (in eng), *Cancer Res*, vol. 62, no. 18, pp. 5196-203, Sep 15 2002, doi: <https://cancerres.aacrjournals.org/content/canres/62/18/5196.full.pdf>.
- [298] K. Chan and Y. W. Kan, "Nrf2 is essential for protection against acute pulmonary injury in mice," (in eng), *Proc. Natl. Acad. Sci. U. S. A.*, vol. 96, no. 22, pp. 12731-12736, 1999, doi: 10.1073/pnas.96.22.12731.
- [299] A. Namani, M. Matiur Rahaman, M. Chen, and X. Tang, "Gene-expression signature regulated by the KEAP1-NRF2-CUL3 axis is associated with a poor prognosis in head and neck squamous cell cancer," (in eng), *BMC Cancer*, vol. 18, no. 1, p. 46, Jan 6 2018, doi: 10.1186/s12885-017-3907-z.
- [300] Y. Morel, N. Mermod, and R. Barouki, "An autoregulatory loop controlling CYP1A1 gene expression: role of H(2)O(2) and NFI," (in eng), *Mol. Cell. Biol.*, vol. 19, no. 10, pp. 6825-6832, 1999, doi: 10.1128/mcb.19.10.6825.
- [301] S. Jairam and H. J. Edenberg, "Single-nucleotide polymorphisms interact to affect ADH7 transcription," (in eng), *Alcohol. Clin. Exp. Res.*, vol. 38, no. 4, pp. 921-9, Apr 2014, doi: 10.1111/acer.12340.
- [302] C. Di Sano, C. D'Anna, M. Ferraro, G. Chiappara, and E. Pace, "Notch-1 expression is increased by cigarette smoke exposure and its activation up-regulates ki67, PCNA proliferative markers and actin polymerizations in bronchial epithelial cells," *Eur. Respir. J.*, vol. 54, no. suppl 63, p. PA2399, 2019, doi: 10.1183/13993003.congress-2019.PA2399.
- [303] H. F. Ou-Yang, C. G. Wu, S. Y. Qu, and Z. K. Li, "Notch signaling downregulates MUC5AC expression in airway epithelial cells through Hes1-dependent mechanisms," *Respiration*, vol. 86, no. 4, pp. 341-6, 2013, doi: 10.1159/000350647.
- [304] R. E. Rayner, P. Makena, G. L. Prasad, and E. Cormet-Boyaka, "Optimization of Normal Human Bronchial Epithelial (NHBE) Cell 3D Cultures for in vitro Lung Model Studies," *Sci Rep*, vol. 9, no. 1, p. 500, Jan 24 2019, doi: 10.1038/s41598-018-36735-z.
- [305] M. L. Fulcher, S. Gabriel, K. A. Burns, J. R. Yankaskas, and S. H. Randell, "Well-Differentiated Human Airway Epithelial Cell Cultures," in *Human Cell Culture Protocols*, J. Picot Ed. Totowa, NJ: Humana Press, 2005, pp. 183-206.
- [306] S. Ebrahim *et al.*, "Alcohol dehydrogenase type 1C (ADH1C) variants, alcohol consumption traits, HDL-cholesterol and risk of coronary heart disease in women and men: British Women's Heart and Health Study and Caerphilly cohorts," (in eng), *Atherosclerosis*, vol. 196, no. 2, pp. 871-8, Feb 2008, doi: 10.1016/j.atherosclerosis.2007.02.002.
- [307] G. Duester, M. L. Shean, M. S. McBride, and M. J. Stewart, "Retinoic acid response element in the human alcohol dehydrogenase gene ADH3: implications for regulation of retinoic acid synthesis," (in eng), *Mol. Cell. Biol.*, vol. 11, no. 3, pp. 1638-46, Mar 1991, doi: 10.1128/mcb.11.3.1638.
- [308] J. E. Balmer and R. Blomhoff, "Gene expression regulation by retinoic acid," (in eng), *J Lipid Res*, vol. 43, no. 11, pp. 1773-808, Nov 2002, doi: 10.1194/jlr.r100015-jlr200.
- [309] E. J. Park, Y. J. Park, S. J. Lee, C. Yoon, and K. Lee, "Cigarette smoke extract may induce lysosomal storage disease-like adverse health effects," (in eng), *J. Appl. Toxicol.*, vol. 39, no. 3, pp. 510-524, Mar 2019, doi: 10.1002/jat.3744.

- [310] J. M. Leung *et al.*, "ACE-2 Expression in the Small Airway Epithelia of Smokers and COPD Patients: Implications for COVID-19," *Eur. Respir. J.*, p. 2000688, 2020, doi: 10.1183/13993003.00688-2020.
- [311] D. Ross and D. Siegel, "NAD(P)H:quinone oxidoreductase 1 (NQO1, DT-diaphorase), functions and pharmacogenetics," *Methods Enzymol.*, vol. 382, pp. 115-44, 2004, doi: 10.1016/S0076-6879(04)82008-1.
- [312] D. Siegel, W. A. Franklin, and D. Ross, "Immunohistochemical detection of NAD(P)H:quinone oxidoreductase in human lung and lung tumors," *Clin Cancer Res*, vol. 4, no. 9, pp. 2065-70, Sep 1998, doi: <https://clincancerres.aacrjournals.org/content/clincanres/4/9/2065.full.pdf>.
- [313] B. J. Carolan, A. Heguy, B. G. Harvey, P. L. Leopold, B. Ferris, and R. G. Crystal, "Up-regulation of expression of the ubiquitin carboxyl-terminal hydrolase L1 gene in human airway epithelium of cigarette smokers," *Cancer Res*, vol. 66, no. 22, pp. 10729-40, Nov 15 2006, doi: 10.1158/0008-5472.CAN-06-2224.
- [314] H. Osaka *et al.*, "Ubiquitin carboxy-terminal hydrolase L1 binds to and stabilizes monoubiquitin in neuron," *Hum. Mol. Genet.*, vol. 12, no. 16, pp. 1945-58, Aug 15 2003, doi: 10.1093/hmg/ddg211.
- [315] K. Brinkmann *et al.*, "Ubiquitin C-terminal hydrolase-L1 potentiates cancer chemosensitivity by stabilizing NOXA," *Cell Rep*, vol. 3, no. 3, pp. 881-91, Mar 28 2013, doi: 10.1016/j.celrep.2013.02.014.
- [316] S. Woo *et al.*, "AKR1C1 as a Biomarker for Differentiating the Biological Effects of Combustible from Non-Combustible Tobacco Products," (in eng), *Genes (Basel)*, vol. 8, no. 5, May 3 2017, doi: 10.3390/genes8050132.
- [317] J. N. Schumacher, C. R. Green, F. W. Best, and M. P. Newell, "Smoke composition. An extensive investigation of the water-soluble portion of cigarette smoke," *J Agric Food Chem*, vol. 25, no. 2, pp. 310-20, Mar-Apr 1977, doi: 10.1021/jf60210a003.
- [318] L. Larigot, L. Juricek, J. Dairou, and X. Coumoul, "AhR signaling pathways and regulatory functions," (in eng), *Biochim Open*, vol. 7, pp. 1-9, Dec 2018, doi: 10.1016/j.biopen.2018.05.001.
- [319] J. S. Bourgeois, J. Jacob, A. Garewal, R. Ndahayo, and J. Paxson, "The Bioavailability of Soluble Cigarette Smoke Extract Is Reduced through Interactions with Cells and Affects the Cellular Response to CSE Exposure," *PLOS ONE*, vol. 11, no. 9, p. e0163182, 2016, doi: 10.1371/journal.pone.0163182.
- [320] E. J. Lee *et al.*, "Proteomic Analysis in Lung Tissue of Smokers and COPD Patients," *Chest*, vol. 135, no. 2, pp. 344-352, 2009/02/01/ 2009, doi: <https://doi.org/10.1378/chest.08-1583>.
- [321] G. Colombo *et al.*, "Protein carbonylation in human bronchial epithelial cells exposed to cigarette smoke extract," *Cell Biol. Toxicol.*, vol. 35, no. 4, pp. 345-360, 2019/08/01 2019, doi: 10.1007/s10565-019-09460-0.
- [322] P. O. Oladimeji and T. Chen, "PXR: More Than Just a Master Xenobiotic Receptor," (in eng), *Mol. Pharmacol.*, vol. 93, no. 2, pp. 119-127, Feb 2018, doi: 10.1124/mol.117.110155.
- [323] R. D. Patel, B. D. Hollingshead, C. J. Omiecinski, and G. H. Perdew, "Aryl-hydrocarbon receptor activation regulates constitutive androstane receptor levels in murine and human liver," (in eng), *Hepatology*, vol. 46, no. 1, pp. 209-18, Jul 2007, doi: 10.1002/hep.21671.
- [324] B. Blumberg *et al.*, "SXR, a novel steroid and xenobioticsensing nuclear receptor," *Genes Dev.*, vol. 12, no. 20, pp. 3195-3205, October 15, 1998 1998, doi: 10.1101/gad.12.20.3195.
- [325] I. Washio *et al.*, "Cigarette smoke extract induces CYP2B6 through constitutive androstane receptor in hepatocytes," (in eng), *Drug Metab. Dispos.*, vol. 39, no. 1, pp. 1-3, Jan 2011, doi: 10.1124/dmd.110.034504.

- [326] J. Yan and W. Xie, "A brief history of the discovery of PXR and CAR as xenobiotic receptors," *Acta Pharmaceutica Sinica B*, vol. 6, no. 5, pp. 450-452, 2016/09/01/ 2016, doi: <https://doi.org/10.1016/j.apsb.2016.06.011>.
- [327] J. Beane *et al.*, "SIRT1 pathway dysregulation in the smoke-exposed airway epithelium and lung tumor tissue," (in eng), *Cancer Res*, vol. 72, no. 22, pp. 5702-11, Nov 15 2012, doi: 10.1158/0008-5472.Can-12-1043.
- [328] W. J. Ting *et al.*, "Environmental tobacco smoke increases autophagic effects but decreases longevity associated with Sirt-1 protein expression in young C57BL mice hearts," (in eng), *Oncotarget*, vol. 7, no. 26, pp. 39017-39025, Jun 28 2016, doi: 10.18632/oncotarget.9176.
- [329] H. Merikallio *et al.*, "Impact of smoking on the expression of claudins in lung carcinoma," (in eng), *Eur J Cancer*, vol. 47, no. 4, pp. 620-30, Mar 2011, doi: 10.1016/j.ejca.2010.10.017.
- [330] C. Huang, P. Santofimia-Castaño, and J. Iovanna, "NUPR1: A Critical Regulator of the Antioxidant System," (in eng), *Cancers (Basel)*, vol. 13, no. 15, Jul 22 2021, doi: 10.3390/cancers13153670.
- [331] B. Hassannia *et al.*, "Nano-targeted induction of dual ferroptotic mechanisms eradicates high-risk neuroblastoma," (in eng), *J Clin Invest*, vol. 128, no. 8, pp. 3341-3355, Aug 1 2018, doi: 10.1172/jci99032.
- [332] K. Hijazi *et al.*, "Tobacco-Related Alterations in Airway Gene Expression are Rapidly Reversed Within Weeks Following Smoking-Cessation," *Sci. Rep.*, vol. 9, no. 1, p. 6978, 2019/05/06 2019, doi: 10.1038/s41598-019-43295-3.
- [333] A. Singh, "Negative feedback through mRNA provides the best control of gene-expression noise," (in eng), *IEEE Trans Nanobioscience*, vol. 10, no. 3, pp. 194-200, Sep 2011, doi: 10.1109/tnb.2011.2168826.
- [334] R. Wattiez and P. Falmagne, "Proteomics of bronchoalveolar lavage fluid," (in eng), *J. Chromatogr. B Analyt. Technol. Biomed. Life Sci.*, vol. 815, no. 1-2, pp. 169-78, Feb 5 2005, doi: 10.1016/j.jchromb.2004.10.029.
- [335] J. Gregori, L. Villarreal, A. Sánchez, J. Baselga, and J. Villanueva, "An effect size filter improves the reproducibility in spectral counting-based comparative proteomics," (in eng), *J. Proteomics*, vol. 95, pp. 55-65, Dec 16 2013, doi: 10.1016/j.jprot.2013.05.030.

Appendix A:

List of used packages in programming environment R:

vsn	openxlsx	ggplot2	cAIC4
sva	blme	umap	knitr
qvalue	parameters	patchwork	Enhancedvolcano

List of abbreviations

ACTB	β -actin	HPRT	Hypoxanthine-guanine phosphoribosyltransferase
acTub	Acetylated tubulin	ILDs	Interstitial lung diseases
AEP	Acute eosinophilic pneumonia	IPF	Idiopathic pulmonary fibrosis
AGC	Automatic gain control	HMBS	Hydroxymethylbilane synthase transcript
AhR	Arylhydrocarbon receptor	LFQ	Label-free quantitation
AKAP13	A kinase anchor protein 13	MUC5AC	Mucin 5AC
ALICE-Smoke	Air Liquid Interface Cigarette smoke Exposure	MUC5B	Mucin 5B
ARNT	Aryl hydrocarbon nuclear translocator	NFE2L2	Nuclear Factor, Erythroid 2 Like 2
BADJ	Bronchoalveolar duct junctions	NNK	4-(methylnitrosamino)-1-(3-pyridyl)-1-butanone
BALF	Bronchoalveolar lavage	NNN	N-nitrosornicotine
BSA	Bovine Serum Albumin	NSCLC	non-small cell lung cancers
CAR	Constitutive androstane receptor	NUPR1	Nuclear protein 1
CF	Cystic fibrosis	PAH	Polycyclic arylhydrocarbons
CFTR	Cystic fibrosis transmembrane conductance regulator	PBS	Phosphate Buffer Saline
COPD	Chronic obstructive pulmonary disease	phBECs	Primary human bronchial epithelial cells
CPFE	Combined pulmonary fibrosis and emphysema	PLCH	Pulmonary Langerhans' cell histiocytosis
CS	Cigarette smoke	PNECs	Pulmonary Neuroendocrine Cells
CSC	Cigarette smoke condensate	PXR	Pregnane-X-Receptor
CSE	Cigarette smoke extract	RB-ILD	Bronchiolitis-Interstitial Lung Disease
ddH ₂ O	double-distilled water	ROS	Reactive Oxygen Species
DEA	Downstream effect analysis	SDS	Sodium Dodecyl Sulphate
DHX8	DEAH-Box Helicase 8	SERGs	Smoke-exposure regulated genes
DIP	Desquamative Interstitial Pneumonitis	SSLCs	Small Cell Lung Carcinomas
DMSO	Dimethyl Sulfoxide	TEER	Transepithelial Electrical Resistance

DTT	Dithiothreitol	TGF- β 1	transforming growth factor β 1
ECM	extracellular matrix	TOLLIP	toll interactive protein
G6PD	glucose-6-phosphate dehydrogenase	UBC	Polyubiquitin-C
GCLC	cysteine ligase catalytic subunit	wCS	Whole cigarette smoke
GPX4	glutathione peroxidase 4	WDR89	WD repeat-containing protein 89
GSH	glutathione	XRE	xenobiotic responsive element

List of figures

Figure 1.1. Cell types residing in bronchial epithelium. Modified from [17]	6
Figure 1.2. Main characteristics of lung microenvironments required in ideal physiologically relevant <i>in vitro</i> models. Modified from [175].	17
Figure 3.1. Dose of CSE was successfully determined by gravimetric measurement of cigarette smoke particulates in cigarette smoke extract (CSE).	21
Figure 3.2. Differentiation analyses proved the differentiations of primary bronchial epithelial cells were successful.	27
Figure 3.3. TEER and LDH assessments show no non-toxic doses were used in CS exposures.....	29
Figure 3.4. Acute submerged basal cell exposure to various concentrations of cigarette smoke extract (CSE) resulted in upregulation of six out of nine smoke exposure regulated genes (SERGs).....	34
Figure 3.5. Acute submerged exposure with cigarette smoke extract (CSE) of primary human bronchial epithelial basal cells.....	35
Figure 3.6. Chronic basolateral exposure to 5% cigarette smoke extract (CSE) of primary human bronchial epithelial cells during the complete course of differentiation revealed CSE significantly upregulates seven out of 10 smoke exposure regulated genes (SERGs).	37
Figure 3.7. Quantitative immunofluorescence of major cell types and transepithelial electrical resistance (TEER) during chronic basolateral treatment with cigarette smoke extract (CSE) during differentiation shows no cytotoxicity incurred by CSE, relative to mock.	38
Figure 3.8. Short acute apical exposure of differentiated primary human bronchial epithelial cells with whole cigarette smoke (wCS) and cigarette smoke extract (CSE) using comparable CS particulate doses resulted in significant upregulation of six out of 10 smoke exposure regulated genes (SERGs) for wCS, but none for CSE.	40
Figure 3.9. Air-Liquid Interface Cigarette Smoke Exposure (ALICE-Smoke) system allows for continuous exposure to cigarette smoke.	41
Figure 3.10. Acute apical exposure of differentiated primary human epithelial cells with various concentrations of cigarette smoke extract (CSE) revealed only one significant upregulation at highest used CSE concentration.	43
Figure 3.11. Acute apical exposure to various concentrations of cigarette smoke extract (CSE) including prior starvation reveals another treatment upregulating only in SERG.....	44
Figure 3.12. Acute basolateral exposure of fully differentiated primary human bronchial epithelial cells to 5% cigarette smoke extract (CSE) resulted in significant upregulation of 1 smoke exposure regulated gene (SERGs).	45
Figure 3.13. Analysis of immunofluorescent stainings revealed ciliated cells as strongest expressers of NQO1, PIR and UCHL1.....	47
Figure 3.14. Immunofluorescent stainings club cell protein (CC10) revealed no co-expression with NQO1, PIR and UCHL1, while mucin 5AC (MUC5AC) did not co-expressed with all 4 assessed proteins.	49
Figure 3.15. Threshold Cycles (Ct) comparison of basal expression of smoke exposure regulated genes (SERGs) between never-smokers and ex-smokers.....	49
Figure 3.16. Threshold Cycles (Ct) comparison between AhR-responsive SERGs....	50
Figure 4.1. Overview of differentially altered proteins expressions in BALF proteomic data. $P < 0.05$, $\log_2FC > 0.3$	52
Figure 4.2. Ingenuity Pathway Analysis identified significantly altered pathways and predicted upstream regulators.	54
Figure 4.3. Overview of predicted upstream regulators activity.	55

Figure 5.1. Transcriptomic molecular signature comparison between never smokers, former smokers and active smokers.....	57
Figure 5.2. <i>In vitro</i> experiments indicate neither transience nor persistence reported in <i>in vivo</i> bronchoalveolar lavage (BALF) dataset.....	60

List of tables

Table 1.1. Abbreviated list of CS constituents considered as harmful by the Food and Drug Administration (FDA).	8
Table 1.2. Reviewed factors influencing smoking behavior, modified from [99]	10
Table 1.3. Genes associated with risk variants, which are predominantly expressed in bronchial epithelial cells.	13
Table 3.1. List of evaluated cigarette smoke extract (CSE) and whole cigarette smoke (wCS) models. For details on the respective models, please refer to the relevant figures and text passages in the Material and Methods section. Note: This table and table description have been published in Mastalerz et al., AJP Lung, 2021.	1
Table 3.2. List of smoke exposure regulated genes (SERGs).	30
Table 3.3. Basic metrics and smoking status of donors used in cigarette smoke exposures. Note: This table and table description have been published in Mastalerz et al., AJP Lung, 2021.	31
Table 3.4. Overview of smoke exposure-regulated genes (SERGs) mRNA fold changes in the evaluated models, in comparison to upregulation by CS in current smokers (top row).	1
Table 4.1. Upstream regulators. Z-score>1, p-value<0.05.	56
Table 5.1. Basic metrics of patients from smoking BALF cohort. FVC – Forced vital capacity, DLCO – diffusing capacity of the lungs for carbon monoxide . Data provided by Herbert Schiller.	58
Table 5.2. Basic metrics and smoking status of donors of phBECs. Note: Parts of this table and table description have been published in Mastalerz et al., AJP Lung, 2021.	58
Table 9.1. Primary antibodies used in Western Blot (WB) and Immunofluorescence (IF) analysis. This table and the table description has been published in Mastalerz et al., AJP Lung, 2021.	71
Table 9.2. Secondary antibodies used in Western Blot (WB) and Immunofluorescence (IF) analysis. This table and the table description have been published in Mastalerz et al., AJP Lung, 2021.	72
Table 9.3. Primer list for RT-qPCR. Primers were synthesized by Eurofins. This table and the table description has been published in Mastalerz et al., AJP Lung, 2021.	72
Table 9.4. General donor characteristics and information on smoking status. This table and the table description has been published in Mastalerz et al., AJP Lung, 2021.	74
Table 9.5. Cell culture media used in all experimentations.	74
Table 9.6. Reagent and chemicals.	75
Table 9.7. List of buffer formulations.	76
Table 9.8. List of consumables.	77
Table 9.9. List of laboratory equipment.	79
Table 9.10. List of software programs.	80
Table 9.11. List of assay kits and standards.	81
Table 9.12. RT-qPCR reaction mix per one assay.	87
Table 9.13. RT-qPCR standard protocol.	88

List of publications

[Validation of in vitro models for smoke exposure of primary human bronchial epithelial cells](#)

Michal Mastalerz, Elisabeth Dick, Ashesh Anjankumar Chakraborty, Elisabeth Hennen, Andrea C Schamberger, Andreas Schröppel, Michael Lindner, Rudolf Hatz, Jürgen Behr, Anne Hilgendorff, Otmar Schmid, and Claudia A Staab-Weijnitz

American Journal of Physiology-Lung Cellular and Molecular Physiology 0 0:0

Acknowledgements

I would like to gratefully acknowledge my supervisor and mentor, Principal Investigator PD Dr Claudia Staab-Weijnitz, for this unique opportunity of working in Comprehensive Pneumology Center. Her professionalism, insightful approach to science, exemplary work ethics and undying optimism, patience and motivation allowed me to gain priceless scientific and academia experience, which will greatly impact the future of my career. Overall, her supervision, insightful ideas, inspiration and were extremely helpful in completion of my PhD in just over three years, during challenging times of the SARS-Cov-2 pandemics, publishing the paper on CS exposure models validation and conclusion of my work with successful submission of this thesis, among many other accomplishments that would not be possible without her.

I am very grateful for collaboration opportunity with Dr. Otmar Schmid, who kindly provided ALICE-Smoke, which had a pivotal role in methods and dose comparison in Chapter A, proving wCS is one of the most important experimental set-ups available. Additionally, Dr. Schmid's vast expertise in particles flow and deposition provided crucial points of discussion.

I want to thank to all the collaborators involved in cigarette smoke validation study, whose contribution resulted in publishing the data presented in Chapter A: Elisabeth Dick, Ashesh Chakraborty, Elisabeth Hennen, Dr. Andrea Schamberger, Andreas Schröppel, Prof. Michael Lindner, Prof. Rudolf Hatz, Prof. Jürgen Behr, Dr. Anne Hilgendorff, Dr. Otmar Schmid, and Dr. Claudia A Staab-Weijnitz

I am thankful to my thesis advisory committee members: Prof. Dr. Thomas Gudermann, Prof. Dr. Robert Bals, Dr. Claudia Staab-Weijnitz and Dr. Otmar Schmid, for all their expertise, advice and guidance. I consider myself lucky to have had the training received from the CPC research school "Lung Biology and Disease", where special thanks go again to Dr. Claudia Staab-Weijnitz for the CPC research school leadership, and to Dr. Doreen Franke and Dr Karin Herbert for their constant involvement and support.

I want to express my honest thanks to all current and previous members of Dr Staab Weijnitz lab: Elizabeth Dick, Ashesh Chakraborty, Elizabeth Hennen, Ceylan Onursal, Karolina Pijadina, Natalia Christina Cabeza-Boeddinghaus, Emilia Berthold and Nathaniel Chukwuebuka Okpala, for their insight, support, professionalism and positive attitude lightening up laboratory meetings and working together.

Special thanks go to CPC BioArchive Team, especially Dr Annika Frank, for her kind support in providing pHBECS samples, as well as for and everyone involved in isolating and preparing samples for culturing.

I gratefully acknowledge Dr Hannah Marchi and Dr Ronan de Gleut, for their help in statistical analysis, but also for insightful discussions on best statistical model fitted for the study, and for being extremely informative on the matter. Also involved in the study was Dr Juliane Merl-Pham, who I am very grateful for performing the proteomics analysis for the study investigated in the Chapter B.

I am thankful to Dr Herbert Schiller, Dr Claudia Staab-Weijnitz and Dr Christopher Mayr and everyone else involved in performing proteomic analysis of BALF patient cohort, which laid foundation for investigations reported in Chapter C.

I feel honored to have all members of CPC and ILBD as my work colleagues and want thank everyone in CPC/ILBD for making the time of PhD fellowship a truly memorable experience. Apart from already mentioned PhD, Masters and MD students, Postdoctoral fellows, I would like to thank in particular Georgia Giotopoulou, Sabine Behrend, Dr. Caroline Hackl, Dr. Johannes Nowak, Dr. Mario Pepe, Juliana Giraldo, Dr. Valeria Viteri Alvarez, Anna Semenova, Jeanine Chantal Pestoni, Andrea Schneider, Andy Qarri, Aydan Sardogan, Haifeng Ye, Dr. Shruthi Kalgudde, Vijay Rajendran, Dr. Jie Jia, Dr. Erika Gonzalez, Armando-Marco Dworsky, Severine Cranz Somlo, Dr. Mahesh Gouda, Michael Gerckens, Dr. Pushkar Ramesh, Dr. Arunima Sengupta, Yves Haufe, Suhasini Rajan, Florian Schelter, Dr. Anna Stefanska, Dr. Tankut Gurney, Miriam Kastlmeier, Dr. Sezer Orak, Dr. Lin Yang, and many, many more.

Special thanks go to also to all coordinators, administrators and technicians, especially Julia Brandt, Steffi Resenberger, Silke Lauer, Kaori Sumikawa, Daniela Dietel, Marissa Neumann and Daniela Vogt.

Finally, I want to thank my family and closest friends for undying and unconditional support, belief, motivation and inspiration without which this task would be much more challenging undertaking.